UNIVERSIDAD
DE LA REPÚBLICA
URUGUAY

Universidad de la República
Facultad de Química
Centro de Bioinformática Estructural

Tamizaje reverso de p-naftoquinonas tripanocidas: una estrategia bioinformática para el descubrimiento de nuevos antichagasicos

Tesis para optar por el grado de Magíster en Bioinformática

P R E S E N T A

QBP. Brenda Vera Meléndez

Dirigido por la

Dra. Margot Paulino Zunini

Dr. Fabio Polticelli

Octubre 2018

Tribunal

- Dr. Cristian Salas - Pontificia Universidad Católica de Chile. Facultad de Química, Departamento de Química Orgánica.
- Dr. Federico Iribarne - Universidad de la República. Uruguay, Facultad de Química, Departamento DETEMA.
- Dr. Marcelo Comini- Instituto Pasteur de Montevideo. Laboratorio de Biología Redox de Tripanosomátidos.

FACULTAD DE CIENCIAS

UNIVERSIDAD DE LA REPUBLICA URUGUAY

ACTA DE EXAMEN

Fecha: 31/10/2018
10:00

Carrera: PEDECIBA BIOINFORMATICA

Materia: P600- TESIS DE MAESTRÍA - BIOINFORMÁTICA

Tribunal: CRISTIAN SALAS
MARCELO COMINI
FEDERICO IRIBARNE

Estudiante	Nombre	Calificación	Literal
6101872-5	VERA, BRENDA	Con mención	—

Estudiantes aprobados	Estudiantes aplazados	Total
1	0	

Federico Iribarne

Marcelo A. Comini

CRISTIAN SALAS S.

Iguá 4225 • Montevideo • Uruguay • Tel. 2525.8618 al 23-int.101, directos 25258534 - 25251958 • Fax. 2525.8617 • C.P. 11400 • E-Mail: bedelia@fcien.edu.uy

Resumen

La presente Tesis está estructurada como se muestra en el esquema de la Figura I. Dentro de cada capítulo se encuentra detallada la metodología, los resultados y las consideraciones finales.

En el capítulo 1, que defino personalmente como mi entrada al tema, es una revisión realizada en colaboración con investigadores uruguayos, mexicanos y chilenos. En este capítulo se describen algunos inhibidores de la enzima tripanotión reductasa y la importancia de esta enzima como blanco para el desarrollo de antichagásicos. Si bien, en este trabajo no soy la primer autora, es un trabajo que no podía dejar de mencionar en esta Tesis, ya que fue parte importante en mi conocimiento del Estado del Arte en este tema.

En el segundo capítulo, utilizó como base los resultados obtenidos en la Tesis Doctoral de Karina Vazquez, realizada bajo tutoría del Dr. Cristian Salas en la Facultad de Química de la Pontificia Universidad Católica de Chile. En este capítulo se realiza un estudio de anclajes moleculares en tripanotión y glutatión reductasas (TR y GR) de un set de moléculas (quinonas) que fueron probadas como inhibidores del crecimiento en epimastigotes de *T. cruzi*. Como resultado de este capítulo, queda demostrado que las naftoquinonas son las moléculas del set que presentan mejor actividad inhibidora, siendo la Nq-h y Nq-b (Figura II) las que tienen mejor actividad tripanocida y selectiva en TR y epimastigotes de *T. cruzi*, respectivamente. Además, se concluyó que la enzima TR no sería la única enzima responsable de la inhibición del crecimiento de la fase parasitaria, dando lugar a la necesidad de conocer otros posibles blancos que pudieran dar respuesta al efecto biológico observado.

En el capítulo 3 se utiliza una estrategia de tamizaje reverso para predecir -a partir de moléculas con actividad conocida– los blancos en los cuales estas moléculas podrían generar un efecto biológico. Esta estrategia es conocida como "*target fishing*". En el desarrollo de este capítulo se usaron dos métodos: uno basado en similitud estructural y otro basado en un mapeo farmacofórico. Se seleccionaron las naftoquinonas Nq-h y Nq-b para alimentar estos algoritmos de búsqueda. Como resultado, obtuvimos un listado de blancos putativos para tales naftoquinonas. Entre ellos, algunos blancos claves en el metabolismo de *T.cruzi* y humanos. Estos blancos predichos por los algoritmos antes mencionados, fueron mapeados en la base de datos KEGG y analizados usando la base de datos STRING para enriquecer las asociaciones

funcionales de estas proteínas. Los blancos que tienen relación con alguna enfermedad fueron priorizados para ser presentados en esta tesis. Si bien los resultados de este capítulo nos ayudan a conocer otros posibles blancos para ser estudiados en *T.cruzi,* también amplía la investigación hacia la polifarmacología de las naftoquinonas y su uso no solo como potentes antichagasicos sino para el tratamiento de otras patologías. Lo anterior dicho, es una perspectiva que está considerada para ser desarrollada en mi tesis doctoral.

Con estos tres capítulos concluyo mi Tesis de Maestría, con la satisfacción de haber contribuido con conocimiento al llamado de ayuda de la población mundial desatendida que padece el Mal de Chagas.

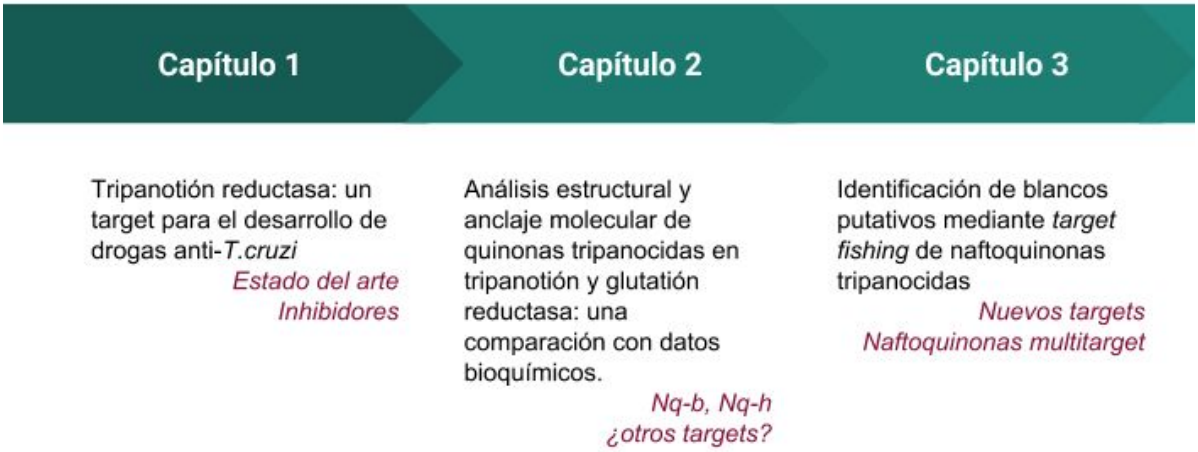

Figura i. Estructura y secuencia de los capítulos de la presente tesis

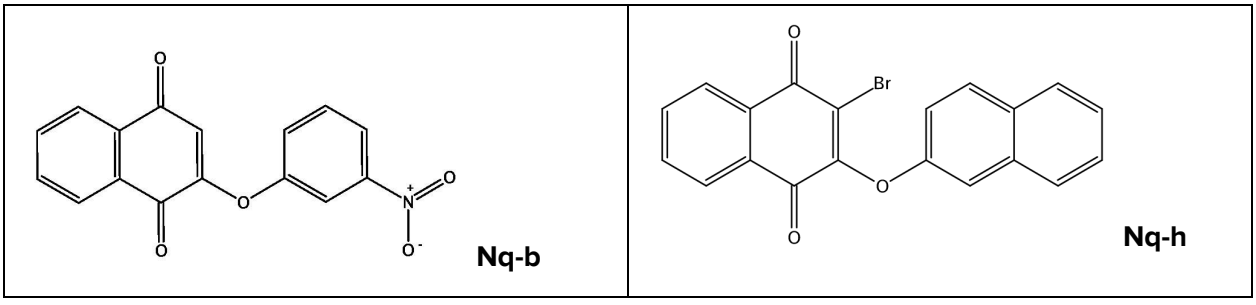

Figura ii. Estructura química de las naftoquinonas Nq-b y Nq-h

Índice General

Tabla de contenidos

1.Introducción

La enfermedad de Chagas presenta un escenario en el que se estima que entre 7 y 8 millones de personas se encuentran infectadas (“Website,” n.d.). Esta enfermedad, también llamada tripanosomiasis americana, es causada por el parásito *Trypanosoma cruzi* (Hotez et al., 2012) (Senior, 2007)(Hotez et al., 2012), se encuentra sobre todo en zonas endémicas de 21 países de América Latina, pero en la actualidad se ha propagado a otros continentes (Schmunis & Yadon, 2010) Figura 1.

Las dos drogas clásicas usadas en el tratamiento antichagásico desde hace más de 30 años son el Nirfurtimox® y el Benznidazol® (Cerecetto & Gonzalez, 2002). Ambos fármacos tienen una significativa actividad tripanocida en la fase aguda de la enfermedad, pero en la fase crónica esta actividad disminuye considerablemente, además de presentar importantes efectos adversos (Castro, de Mecca, & Bartel, 2006); (Jannin & Villa, 2007); (Marin-Neto et al., 2008).

Por otro lado, pese a los esfuerzos realizados, ninguno de los blancos farmacológicos identificados hasta ahora y usados en el diseño de nuevos antichagásicos, han logrado proveer de una solución para la quimioterapia de la Enfermedad de Chagas.

Los blancos farmacológicos o dianas terapéuticas (*targets*) se definen como aquellas entidades biomoleculares capaces de reconocer una molécula y producir una respuesta celular, formando parte del conjunto de biomoléculas responsables de un mecanismo de acción determinado (Imming, Sinning, & Meyer, 2006) . Buena parte de las enzimas relacionadas al metabolito tripanotiona se han considerado como blancos terapéuticos interesantes debido a que están presentes solamente en los tripanosomatídeos, en particular *T. cruzi*, lo cual le podría dar selectividad para el desarrollo de nuevos fármacos en la quimioterapia de la Enfermedad de Chagas, aprovechando además que estos parásitos son sensibles contra el estrés oxidativo. Sin embargo, el hecho de que las quinonas ensayadas en esta Tesis no tiene un efecto tripanocida asociado a la inhibición de la TR, sugiere que el efecto tripanocida producido por las quinonas, sería el resultado de la interacción de estos compuestos con distintos blancos celulares.

Por todo esto consideramos tan importante la búsqueda e identificación de nuevos blancos farmacológicos (tanto para acciones deseadas como no) que podrá aportar conocimiento con el objetivo final que es el diseño de nuevas sustancias con capacidad tripanocida.

1.1 Prevalencia de la Enfermedad de Chagas

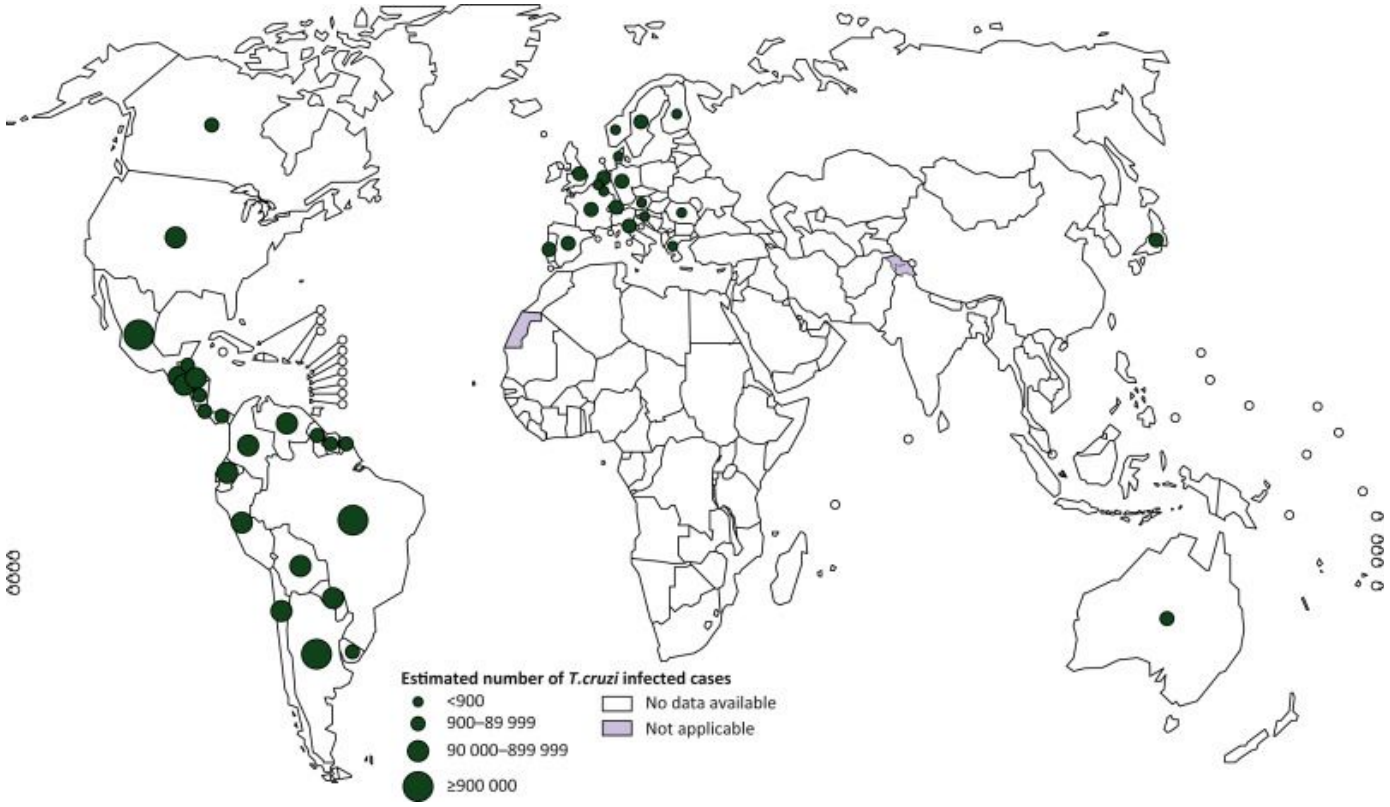

Figura 1. Distribución mundial de la Enfermedad de Chagas

La enfermedad se transmite por insectos vectores Hemípteros de la subfamilia Triatominae, de alimentación hematófaga, popularmente conocidos como chinches y en Uruguay como 'vinchucas'. En Uruguay, son dos las más importantes especies de triatominos presentes: *Triatoma infestans*, responsable de la endemia en Uruguay, y *Triatoma rubrovaria*, especie autóctona responsable de la enzootia silvestre, que puede causar accidentalmente la transmisión efectiva de *T.cruzi* a seres humanos (Salvatella & Rosa, 2007). En Uruguay se alcanzaron los valores endémicos más altos en las décadas de los 40 y 50 y en 1997, fue el primer país que controló al *Triatoma infestans* mediante programas de control de vectores en los domicilios infestados (Salvatella et al., 1999).

1.2 Transmisión

La principal vía de transmisión de la enfermedad es vectorial: insectos hematofagos de la familia Triatominae (Hemiptera, Reduviidae) transmiten mediante las heces al parásito *T.cruzi* el cual penetra a través de la piel o las mucosas y alcanza los tejidos, donde finalmente se establece (Figura 2). A nivel celular, tras varias etapas evolutivas del parásito se producen de nuevo tripomastigotes infectivos que invaden nuevas células, estableciéndose el ciclo biológico del parásito (CDC-Centers for Disease Control & Prevention, 2009).

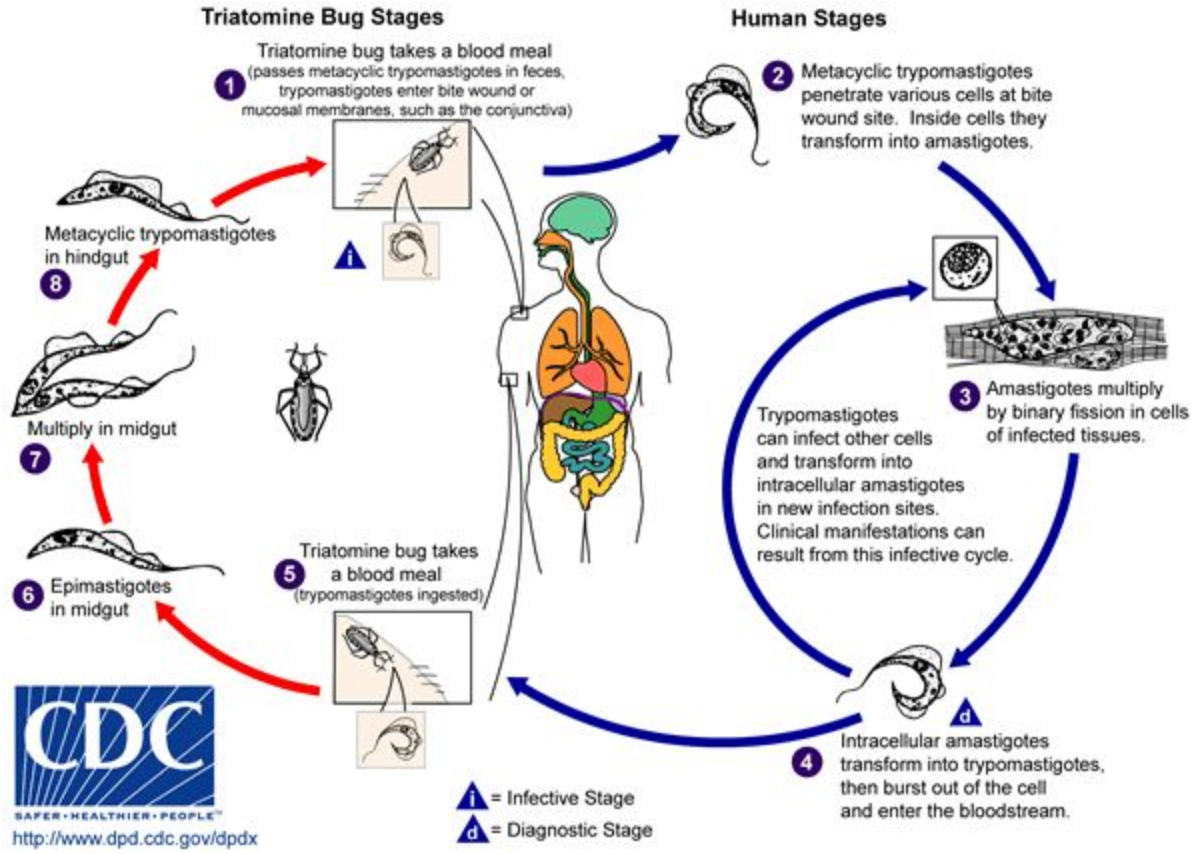

Figura 2. Ciclo vital de *T.cruzi*

1.3 Fármacos para el tratamiento del mal del Chagas

Los medicamentos utilizados en la terapia contra la enfermedad de Chagas se descubrieron hace más de cuatro décadas (Cerecetto & Gonzalez, 2002). Estos medicamentos están compuestos por fármacos derivados de nitrocompuestos: Nifurtimox® y Benznidazol® Figura 3.

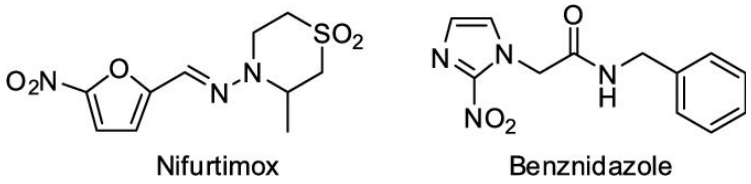

Figura 3. Estructura química de los fármacos empleados en la enfermedad de Chagas

Estos compuestos presentan importantes efectos secundarios, donde destacan pérdida de peso, náuseas, vómito, prurito, neuropatía periférica, leucopenia y neurotoxicidad, entre otras. El uso de estos medicamentos en la fase aguda de la enfermedad está aceptado y ha demostrado ser exitoso; sin embargo, son poco efectivos en la fase crónica de la enfermedad.

Además de la cuestionada eficacia en las distintas fases de la enfermedad, también se han descrito diferentes eficacias según el área endémica y la cepa de *T.cruzi* (Murta, Gazzinelli, Brener, & Romanha, 1998). Sin embargo, el problema más relevante, aunado a los efectos adversos mencionados anteriormente, es la genotoxicidad de estos compuestos convirtiéndolos en medicamentos inadecuados para el tratamientos de cualquier tipo de enfermedad (Bartel et al., 2007; Castro et al., 2006; Nagel, 1987).

En el proceso de investigación de nuevos medicamentos se han desarrollado candidatos para la inhibición de proteínas del metabolismo de este parásito, entre las que se encuentran inhibidores de cruzipaina, inhibidores de la biosíntesis de ergosterol e inhibidores de tripanotión reductasa, por mencionar algunos .

Por lo anterior dicho, resulta importante aportar en la búsqueda de nuevas moléculas con capacidad de inhibir blancos del *T. cruzi* mediante un diseño racional de fármacos tripanocidas.

1.4 Diseño de fármacos

El diseño de nuevos fármacos para la enfermedad de Chagas puede abordarse mediante algunas estrategias generales. Una de ellas consiste en el aislamiento y estudio de productos naturales procedentes de la medicina tradicional o de otras fuentes y otra, se refiere al desarrollo de nuevos compuestos de síntesis química o de procedencia biotecnológica (Goodman, Hardman, Limbird, & Gilman, 2001; Wermuth, 2003). Una estrategia más reciente utilizada en la búsqueda de nuevos *hits* es la que se refiere al diseño de fármacos asistido por computadoras.

1.5 Diseño de fármacos asistido por computadora

El diseño de fármacos asistido por computadora (DIFAC) consiste en aplicar algún procedimiento realizado por una computadora para relacionar la actividad de un compuesto con su estructura química (Hopfinger, 1985). Los objetivos principales del DiFAC son tres: descubrir moléculas activas, optimizar moléculas activas ya conocidas y seleccionar, a partir de un grupo dado de estructuras, a los candidatos que tengan mayor o menor probabilidad de convertirse en fármacos exitosos. De esta manera, el uso de la computadora puede ayudar a descubrir y diseñar estructuras químicas que tengan las propiedades adecuadas para entrar en el proceso de desarrollo de un fármaco (Cortés-Ruiz, Palomino-Hernández, Rodríguez-Hernández, Espinoza, & Medina-Franco, 2018; Naveja, Oviedo-Osornio, & Medina-Franco, 2018).

1.5.1 Estrategias generales para el DIFAC

Muchos fármacos ejercen su acción debido a su interacción con una macromolécula presente en el organismo. Tomando este principio, las estrategias del DiFAC se podrían clasificar (Tropsha & Zheng, 2001).

a) Diseño basado en la estructura del ligando.

b) Diseño basado en la estructura del receptor.

c) Combinación de métodos.

1.5.2 Diseño basado en la estructura del ligando

Cuando no se conoce la estructura del receptor se utilizan los métodos basados en el ligando. Los métodos que se agrupan en esta área se centran en el estudio de la estructura química de la molécula con actividad biológica. A esta última nos referimos como ligando. Estos métodos dependen de la información experimental disponible para una serie de estructuras químicas con actividad biológica conocida. Entre los métodos de estudio del ligando se encuentran los SAR (*relaciones estructura-actividad*) y dilucidación del farmacóforo (Escalona-Arranz, Carrasco-Velar, & Padrón-García, 2008).

1.5.2.1 SAR

Los métodos SAR (Structure-Activity Relationships) consideran las propiedades de las moléculas en tres dimensiones y son importantes en ellos aspectos como el análisis conformacional, la mecánica-cuántica, los campos de fuerzas y los gráficos moleculares interactivos. Estos últimos permiten la representación y la manipulación de la molécula en tres dimensiones, lo que proporciona una información espacial que es esencial para comparar moléculas y para estudiar la interacción entre ligandos y receptores macromoleculares. Estos estudios SAR son utilizados no sólo en el diseño de nuevos fármacos, sino que también aplicables al estudio de mecanismos de acción de los fármacos y a otras ramas de la ciencia como la ingeniería de proteínas y la química de polímeros.

1.5.2.2 Farmacóforo

Un farmacóforo es el conjunto de grupos químicos, unidos o no entre sí, que todas las moléculas activas sobre un mismo receptor tienen en común, y que son esenciales para asegurar interacciones óptimas con un blanco farmacológico específico, lo cual desencadenará o bloqueará una respuesta biológica. Un modelo de farmacóforo es un concepto abstracto que indica la capacidad de interacción molecular común de un grupo de compuestos dirigidos a un blanco farmacológico específico. En otras palabras, el farmacóforo puede ser considerado como el común denominador de un conjunto de moléculas activas.

1.5.3 Diseño basado en la estructura del receptor.

Los métodos que corresponden a esta estrategia consideran la estructura tridimensional de la macromolécula o biomolécula con la que interactúa el ligando, desencadenando un posible efecto farmacológico. Nos referiremos a la macromolécula como receptor (Schneider, 2013). De esta manera, la elección del método computacional empleado depende, en primera instancia, de que se conozca la estructura del ligando y/o del receptor. Cuando se conocen ambas se puede hacer uso de las dos estrategias. Sin embargo, cuando no se conoce ninguna, hay que generar primero información experimental.

1.5.3.1 Anclaje molecular (*Docking*).

El término anclaje molecular (*docking*) es un término computacional que implica la el estudio de la unión entre dos moléculas, un receptor y un ligando . Esto se realiza con el fin de diseñar ligandos más específicos que encajen con mayor precisión en el sitio de unión de la diana terapéutica en estudio (Dastmalchi & Siavoush, 2016). Si se dispone de complejos cristalizados ligando-receptor, se puede estudiar el sitio de unión de nuevas moléculas.

Mediante el uso programas de anclaje molecular, existen métodos automáticos para explorar las posibles uniones entre ligando y receptor, se puede realizar una exploración de todas las posibles posiciones relativas ligando-receptor, evaluando la interacción intermolecular entre ambos. Cada una de estas soluciones se evalúa mediante una función de puntaje (*scoring*).

1.5.4 Combinación de métodos

Recientemente, existe una tendencia hacia la integración de métodos basados tanto en estructura como en ligando, que usan información sobre la estructura de la proteína o las propiedades biológicas y fisicoquímicas de los ligandos unidos, respectivamente. Estos enfoques integrados se dividen en dos clases: métodos basados en la interacción o aquellos basados en la similitud de acoplamiento (López Vallejo, Vallejo, Franco, & Castillo, 2018).
Los *métodos basados en la interacción* se centran en identificar las interacciones clave entre la proteína y el ligando utilizando datos físico químicos disponibles. Estas interacciones se usan

luego para explorar bibliotecas de moléculas pequeñas para compuestos capaces de producir dicho perfil de interacción.

Los *métodos basados en similitud de acoplamiento* fusionan los métodos de acoplamiento basados en estructura con los métodos de similitud de ligandos. Con estas combinaciones, el cribado virtual se vuelve muy eficiente y permite explorar bibliotecas de hasta 10¨6 moléculas pequeñas. Si, además de conocer la estructura del receptor, se cuenta con información experimental sobre relaciones estructura-actividad para un grupo de moléculas que se unen al mismo receptor, se pueden combinar técnicas de diseño basado en el receptor y diseño basado en el ligando. Un ejemplo de esta combinación son los estudios de cribado virtual.

2.Hipótesis

A partir de una serie de naftoquinonas con actividad tripanocida se podría dilucidar una serie de moléculas con actividad similar y también encontrar nuevos posibles blancos para el desarrollo de antichagasicos.

3.Objetivos

- Evaluar el efecto de las naftoquinonas en TR / GR y comparar los datos experimentales e *in silico.*
- Visualizar por métodos computacionales, el modo de interacción de las naftoquinonas con blancos putativos de *T.cruzi* dilucidando patrones de contacto.
- Justificar las razones por las cuales se le confiere actividades tripanocidas a una serie de naftoquinonas usando herramientas bioinformáticas.
- Identificar blancos de acción putativos mediante tamizaje reverso.

4. Resultados

Capítulo 1

Tripanotión reductasa: un target para el desarrollo de drogas anti-*Trypanosoma cruzi*

Trypanothione Reductase: A Target for the Development of Anti-*Trypanosoma cruzi* Drugs
Vázquez, Karina; Paulino, Margot; Salas, Cristian O; Zarate-Ramos, Juan J; **Vera, Brenda**; Rivera, Gildardo
Mini Rev. Med. Chem.2017 Vol. 17 Num.0 Pag. 1-7
DOI: 10.2174/1389557517666170315145410

Resumen

Meta: Conocer la importancia de la tripanotión reductasa y los inhibidores desarrollados para este blanco parasitario.

Como se mencionó en la introducción de esta tesis, el tratamiento existente para el mal del Chagas es poco efectivo en la fase crónica de la enfermedad, motivo por el cual es necesario desarrollar nuevos medicamentos que sean eficientes y seguros para el tratamiento de esta patología.

Uno de los blancos parasitarios estudiados para el desarrollo de fármacos antichagasicos es la tripanotión reductasa (TR), una enzima clave en el metabolismo de *Trypanosoma cruzi*. En esta revisión, describimos la importancia de TR como blanco farmacológico, así como de los inhibidores conocidos y los publicados en la última década como posibles agentes terapéuticos para la enfermedad de Chagas.

En este trabajo se describen los diferentes compuestos que han sido estudiados como inhibidores de la TR. En algunos casos de estudio no se ha encontrado relación entre la inhibición de la actividad enzimática y la actividad tripanocida. Esto sugiere que puede haber otros mecanismos involucrados en la actividad tripanocida de estos inhibidores.
En el marco de mi tesis, era necesario conocer el estado del arte de moléculas con actividad anti-*T.cruzi* para poder proponer posibles inhibidores de TR o de otros blancos parasitarios.

Mi aporte en este trabajo fue la búsqueda, revisión y resumen de la bibliografía actualizada y disponible.

Send Orders for Reprints to reprints@benthamscience.ae

Mini-Reviews in Medicinal Chemistry, 2017, *17*, 000-000

REVIEW ARTICLE

Trypanothione Reductase: A Target for the Development of Anti-*Trypanosoma cruzi* Drugs

Karina Vázquez[1], Margot Paulino[2], Cristian O. Salas[3], Juan J. Zarate-Ramos[1], Brenda Vera[2] and Gildardo Rivera[4,*]

[1]*Facultad de Medicina Veterinaria y Zootecnia, Universidad Autónoma de Nuevo León, Escobedo, 66050, México;* [2]*Centro de Bioinformática Estructural DETEMA, Facultad de Química, Universidad de la Republica, P. O. 1157, Montevideo, Uruguay;* [3]*Departamento de Química Orgánica, Facultad de Química, Pontificia Universidad Católica de Chile, Santiago, 6094411, Chile;* [4]*Centro de Biotecnología Genómica, Instituto Politécnico Nacional, Reynosa, 88710, México*

ARTICLE HISTORY

Received: January 30, 2016
Revised: November 24, 2016
Accepted: February 17, 2017

DOI: 10.2174/1389557517666170315145410

Abstract: Chagas disease or American trypanosomiasis is a major parasitic disease in Latin America with restricted available treatment: nifurtimox and benznidazole. These two drugs are ineffective in the chronic phase of the disease; therefore, there is a need for the development of new, efficient and safe drugs for the treatment of this pathology. With this goal, one of the promising targets is trypanothione reductase (TR), a key enzyme in the metabolism of *Trypanosoma cruzi*. In this review, we analyse the importance of TR as a drug target, as well as the well-known and new inhibitors reported in the last decade as potential therapeutic agents for Chagas disease.

Keywords: Chagas disease, trypanothione reductase, *Trypanosoma cruzi*, target, drugs, inhibitors.

1. INTRODUCTION

Chagas disease or American trypanosomiasis was first discovered by Carlos Chagas in 1909. This fact is regarded as a landmark in the history of medicine, with the unprecedented identification of the causative agent, its vector and the impact of the disease on human beings [1, 2].

The causative agent is the parasite *Trypanosoma cruzi*, which has infected millions of people around the world [3]. While most cases are registered in endemic areas of Latin America, the migration of millions of people to Europe, North America, Japan and Australia over the past two decades has led to the development of cases in these regions [4-6]. Blood transfusion from infected individuals is the main mode of transmission, especially in countries that have no screening processes that identify the presence of the parasite in blood. Other modes include congenital and oral transmission with the latter due to the ingestion of food contaminated with feces carrying the parasite [7]. Based on this evidence, Chagas disease has become a worldwide health issue [6].

T. cruzi has a complex life cycle with three stages. During the first stage, the trypomastigote is found in the intestine and feces of several vectors, which include *Triatoma infestans,* a strictly hematophagous insect. Afterwards, trypomastigotes enter the host through the mucosa or the bloodstream through a bug bite, reaching the cells and becoming amastigotes, (mainly in the heart, esophagus and intestine); afterwards, amastigotes replicate and convert back to trypomastigotes, which are released into the bloodstream to infect new tissues. *Triatoma infestans* is infected by feeding on the blood of a human being or any other mammal carrying the parasite. When trypomastigotes are in the vector's intestine, they turn into epimastigotes, the third phase. They differentiate further into trypomastigotes, completing the parasite's life cycle [8, 9].

Triatoma infestans can be found in an area that stretches from the southern United States all the way to Argentina and Chile, where it has several common names, such as: kissing bug (Mexico), cone-nose bug (Guatemala, Honduras and El Salvador) and assassin bug (Argentina, Chile, Uruguay and Bolivia) [10, 11].

Chagas disease in human beings has an acute phase and a chronic phase, with a series of clinical symptoms associated with the evolution of the disease. The acute phase starts with transmission of the infection and lasts approximately 30 to 90 days. At this stage, blood testing will show high levels of parasitemia, generally asymptomatic. During the chronic phase, about 30% of the patients suffer from noticeable inju-

*Address correspondence to this author at the Centro de Biotecnología Genómica, Instituto Politécnico Nacional, Boulevard del Maestro, s/n, Esquina Elías Piña, Reynosa, 88710, México; Tel: +52 899 9243627; Fax: +52 899 9243628; E-mail: gildardors@hotmail.com

1389-5575/17 $58.00+.00

ries in the heart as well as in the digestive and nervous systems. Since the immune system of the host keeps reproduction of the parasite under control, blood testing shows low levels of parasitemia [12].

2. CHEMOTHERAPY OF CHAGAS DISEASE

The drugs that have been used as chemotherapy of Chagas disease for over 30 years are (*RS*)-3-methyl-*N*-[(1*E*)-(5-nitro-2-furyl)methylene]thiomorpholin-4-amine 1,1-dioxide (Nifurtimox, Lampit®, Bayer) and *N*-benzyl-2-(2-nitro-1*H*-imidazol-1-yl) acetamide (Benznidazole, Rochagan®, Roche) (Fig. **1**) [13]. Moreover, many other molecular scaffolds and putative pharmacological targets have been studied and this has generated important knowledge and alternative research lines [14-17]. In addition, nifurtimox and benznidazole were the starting point of research to have a deeper understanding of how these and other structures could function in the complex *T. cruzi* metabolism.

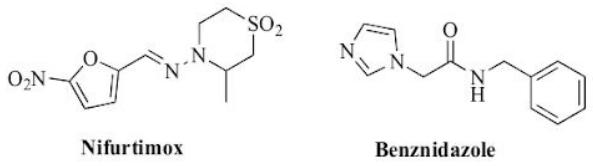

Fig. (1). Structure of drugs used in Chagas disease chemotherapy.

The mechanism of action of both nifurtimox and benznidazole is that they are the substrates of type I and II nitroreductase enzymes due to their chemical structures which include a nitro group linked to an aromatic ring. By the action of these nitroreductases, the nitro group reduces to an amino group with the formation of several free radicals and electrophilic metabolites, which in turn bind to macromolecules such as lipids, proteins and DNA, damaging the parasite. Hall *et al.* have proposed a mechanism through which type I nitroreductases act upon the nifurtimox molecule, producing a series of nitrile metabolites, which have been tested and proven cytotoxic. The production of these metabolites is shown in Fig. (**2**) [18, 19].

Nifurtimox and benznidazole show significant trypanocidal action during the acute phase of the disease, but this activity decreases considerably during the chronic phase. These two drugs also have serious adverse effects. Nifurtimox can produce anorexia, nausea and vomiting, leading to severe weight loss, sleeplessness and irritability, while the adverse effects of benznidazole include allergies, gastrointestinal syndromes and, less frequently, depression [20].

Due to the low effectiveness in the chronic phase and the severe adverse effects of nifurtimox and benznidazole, new options have been researched for Chagas disease; for example, ergosterol-synthesis inhibiting compounds. These inhibitors have shown trypanocidal activity both *in vitro* and *in vivo*, with an outstanding performance of posaconazole (POS; SCH 56592; Noxafil®, Fig. **3**), from the Schering-Plough Research Institute, which proved effective in antiparasitic treatment during the chronic phase of a female patient with positive trypanosomiasis parasitemia [21], and ravuconazole (ER-30346,Eisai Co.; BMS 207,147, Fig. **3**), from Bristol-Myers Squibb, a powerful parasitemia suppressant

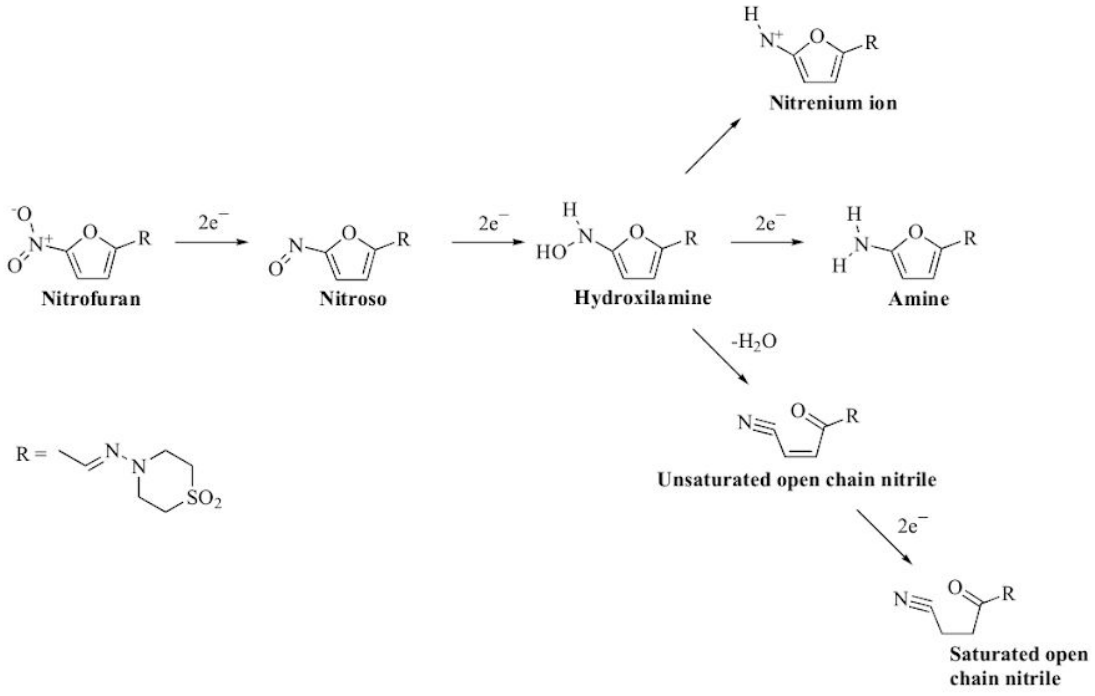

Fig. (2). Type I nitroreductases reduce the nitro group to generate hydroxylamine intermediaries. Hydroxylamine can be metabolized from: a) nitrenium ion, b) amine, c) saturated and unsaturated chains of nitrile [18].

in a study conducted on dogs infected with *T. cruzi* without side effects [22].

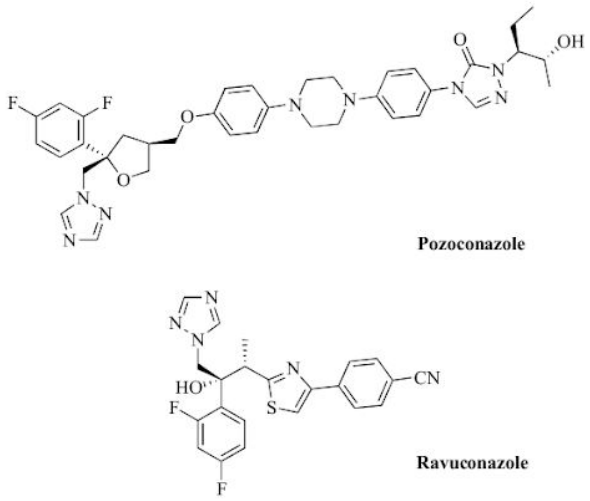

Fig. (3). Chemical structure of triazole derivatives as ergosterol synthesis inhibitors with trypanocidal activity.

Advances in the study of *T. cruzi* metabolism have led to the identification of diverse drug targets, each with its own advantages and drawbacks [23]. In this review, we analyze trypanothione reductase as a viable target for the development of new anti-*Trypanosoma cruzi* agents.

3. TRYPANOTHIONE BIOSYNTHESIS

Trypanothione (N^1,N^8-bis(glutathionyl)spermidine, $T(SH)_2$) is a low-molecular-weight thiol found in protozoa such as *T. cruzi*. This compound plays an important role in redox homeostasis that includes the reduction of several proteins involved in redox metabolism. In addition, $T(SH)_2$ addresses the decomposition of oxidants, such as H_2O_2, peroxynitrite and a range of short-chain fatty acid and phospholipid hydroperoxides [24, 25]. Also, $T(SH)_2$ reacts with a variety of electrophiles, such as those generated from the metabolism of nifurtimox and benznidazole [26, 27]. Therefore, $T(SH)_2$ is an important component of the mechanism involved in the detoxification and protection of *T. cruzi*.

The pivotal step in the biosynthesis of trypanothione (Fig. **4**) is carried out when two equivalents of the dithiol glutathione (GSH) binds to the polyamine spermidine with the catalytic action of the enzyme trypanothione synthetase (TryS). Previously, glutathione (GSH) synthesis starts with the formation of a γ-glutamylcysteine intermediate from L-glutamate and L-cysteine. This reaction is an ATP-dependent process and is catalysed by the enzyme γ-glutamylcysteine synthetase (GCS). On the other hand, spermidine is obtained from a polyamine, putrescine. Finally, once $T(SH)_2$ has been synthesized, this thiol could participate in several redox processes, which involve some oxidoreductases. Some of these have been identified: trypanothione reductase (TR), tryparedoxin (TXN) and tryparedoxin peroxidase (TXNPx). These enzymes are distributed in the cytosol (TXN and TXNPx), mitochondrion (TR, TXN, TXNPx), and the glycosome (TR) of *T. cruzi* [28-36].

Because of this, enzymes related to trypanothione biosynthesis have been considered drug targets for Chagas disease, since they are present only in trypanosomatids, which could offer selectivity towards the parasite [28].

4. TRYPANOTHIONE REDUCTASE

One of the most promising strategies to develop potent and specific antiparasitic drugs is based on metabolic differences

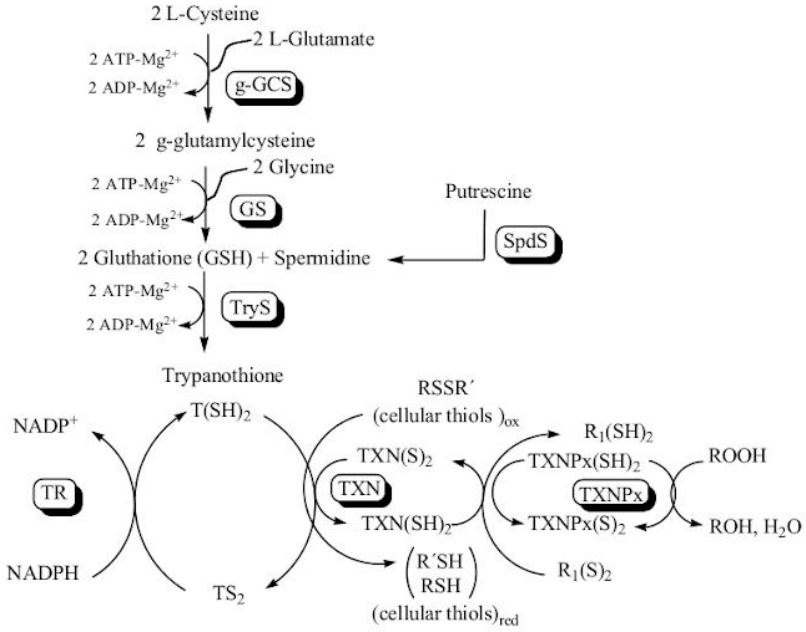

Fig. (4). Metabolism of trypanothione in trypanosomatids.

between the pathogen and the host. One example is related to how they avoid damage mediated by ROS, which is considerably dissimilar [37, 38]. Therefore, according to the role of $T(SH)_2$ in *T. cruzi*, mentioned in the biosynthesis of this thiol, these enzyme systems are attractive targets for drug design. Specifically, TR is essential in all trypanosomatids and it has been reported that parasites with lowered TR activity display an increased sensitivity towards ROS [39, 40]. In fact, an analysis used to reduce phenotypic TR expression resulted in decreased levels of trypanothione which was associated with an increased sensitivity against compounds derived from arsenic, antimony, and nitration [35, 36].

Comparative studies have been conducted between TR and glutathione reductase (GR), the counterpart in humans, finding that their three-dimensional structures are similar. Each enzyme has specific substrates, which would confer selectivity in the inhibition process. Thus, in principle, it should be possible to selectively inhibit the parasite enzyme without affecting the mammalian one, therefore highlighting the idea that TR is a good target for the development of new trypanocidal drugs [29].

5. TRYPANOTHIONE REDUCTASE INHIBITORS

TR has a large active site, which makes it challenging to identify drugs that bind to the pocket. There have been various forms of the inhibitor-binding site and a tendency to bind multiple ligands at the same time. However, knowing that both TR and GR have unique substrate specificity, several molecules have been explored as trypanothione reductase inhibitors (TRI), such as quinazoline, benzimidazole, and nitrobenzene derivatives, and polyamine and peptides analogues [41-48].

An example of a potent irreversible TRI is the compound thioridazine (Fig. **5**), a phenothiazine derivative, which showed 100% inhibition at 10 μM, causing a disruption of mitochondrial and kinetoplasts in trypomastigotes and condensation of these organelles in the plasmatic membrane of epimastigotes. Authors state that the quantitative effects of phenothiazines are mediated by the substituents on the ring, particularly at 2-position.

Thioridazine, used for acute infection at a dose of 80 mg/kg/day for 3 days one hour after infection, decreased parasitemia levels in mice infected with the Tulahuén strain of *T. cruzi* and eliminated parasitemia in 15 days (with no presence of parasites on microscopic examination) with a survival of 80% after one year of infection. The same dose for 12 days starting 180 days post infection produced a survival of 88% at 350 days. Additionally, the authors observed a decrease in cardiac histological and electrocardiographic abnormalities [49].

Clomipramine is one of the most potent TRI against *T. cruzi* with a Ki of 6.5 μM. Additionally *in vivo* activity against trypanosomes has been demonstrated, and in particular, it has been proven to cure mice in the acute and chronic phase of infection with *T. cruzi* when administered intraperitoneally at 5 mg/kg/day. Based on this potent inhibitor, various analogues were designed replacing the tricyclic ring with a dibenzosuberil group and evaluated as a TRI (Fig. **6**). The results allowed obtaining three compounds with Ki values of 7.6, 4.0 and 0.26 μM, as competitive inhibitors of the enzyme, obtaining a greater specificity for inhibiting TR than GR.

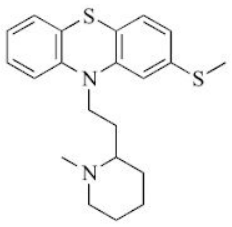

Fig. (5). Thioridazine, an irreversible TRI.

Subsequently, through studies of molecular docking, the authors indicated that the chlorine atom is involved in binding interactions with the active site residues in TR, indicating that halogenated aryl compounds are better TRI than similar non-halogenated compounds. Finally, the activity of these compounds was evaluated *in vitro* against *Trypanosoma brucei brucei* and *Trypanosome rhodesiense*, showing a trypanocidal effect with IC_{50} values of < 4.5 μM. However, they found no correlation between biological activity and TR inhibition, suggesting that the effects on the transport of these compounds through the cell membrane of the trypanosome are important for their trypanocidal effect. Despite these *in vitro* results, compound **7** showed the best inhibition of TR achieving a slight increase in animal life infected with *T. brucei* at a dose of 50 mg/kg/day; however, they also showed toxicity towards infected animals, leading researchers to not consider these types of compounds as potential anti-trypanosome drugs [50].

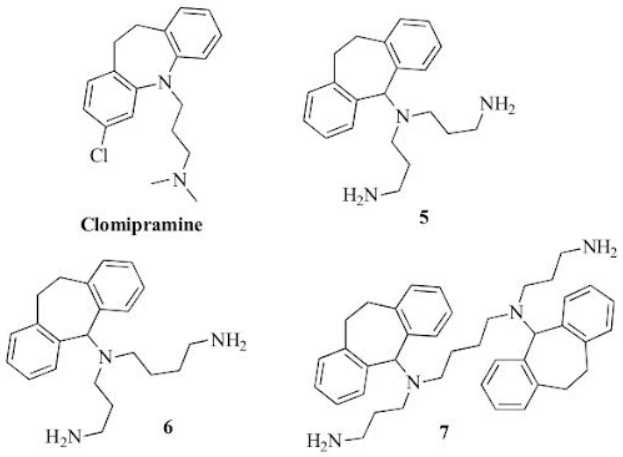

Fig. (6). Clomipramine, a TRI and analogue compounds.

In the generation of new and efficient anti-trypanosome drugs, Richardson *et al.*, conducted a screening of 1266 pharmacologically active compounds from the Sigma-Aldrich Library LOPAC1280. These compounds were evaluated as TRI and the 22 best compounds were evaluated in GR and *T. brucei* to determine their IC_{50}. In this study,

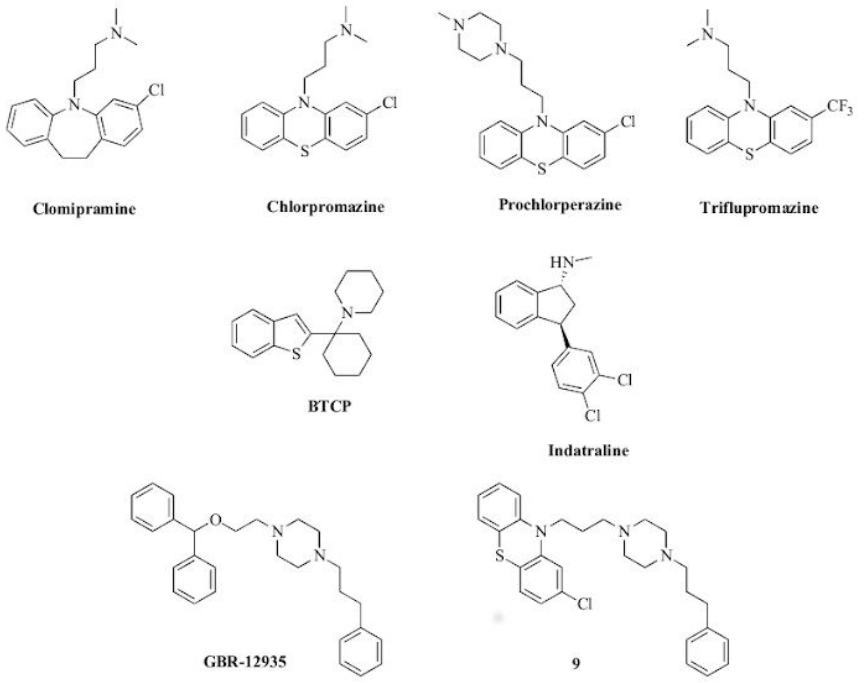

Fig. (7). Structure of TRI compounds obtained by screening and chemical synthesis.

several tricyclic compound derivatives were identified as potent inhibitors, such as clomipramine (IC_{50}= 3.8 μM on TR and $IC_{50} \geq 100$ μM), chlorpromazine (IC_{50}= 6.3 μM on TR and $IC_{50} \geq 100$ μM), prochlorperazine (IC_{50}= 7.4 μM on TR and $CI_{50} \geq 100$ μM), and triflupromizine (IC_{50} = 7.5 μM on TR and $CI_{50} \geq 100$ μM).

Interestingly, of the 13 best compounds from screening, researchers were able to determine three new classes of structures of potential TRI (Fig. **7**), which resemble known drugs. Following with the development of analogues to the compound GBR-12935, the authors proposed a change to the corresponding diphenylmethane moiety to the dibenzosuberol and phenothiazine tricyclic ring, moieties based on clomipramine and chlorpromazine, respectively. This enabled a 15-fold increase of the inhibitory activity of compound **9** to compound GBR-12935. Additionally, it was determined that the moiety phenylpropyl significantly increased activity against the enzyme, suggesting an interaction at the binding site [51].

At the beginning of the last decade, lunarine (Fig. **8**), a macrocyclic alkaloid, was identified as a TRI showing a kinetic of time-dependent inhibition from covalent modification of TR by Michael addition of a cysteine on the active site of C-10 or C-25 of lunarine [52]. Subsequently, Hamilton *et al*., proposed that this TR time-dependent inhibition involves the conjugate addition of Cys53 or Cys58 to one of the moieties of an α-β unsaturated amide of lunarine.

The authors made changes to the structure of lunarine and obtained a new series of compounds found to be competitive inhibitors; *cis*-3-oxo-8,9b-bis-(*trans*-N^4-(acrylamidospermidyl))-1,2,3,4,4a,9b-hexahydrodibenzofuran (Fig. **8**) showed the best trypanocidal activity with an IC_{50} value of 29 μM [53].

At the beginning of this decade, Walton *et al*. developed a series of compounds derived from indatraline (Fig. **7**) as TRI and evaluated them against *T. brucei*. Results showed that the *cis* derivative compounds had a lower TR inhibitory activity than indrataline, therefore following only with the development of *trans* analogues. A structural change was to increase the size and lipophilicity of the amino substituent; however, this did not improve its activity, suggesting that this group contributes little to the biological activity of the compounds. Additionally, when the methyl group was changed to a benzyl group, the biological activity increased, allowing the development of more indatraline analogues with a benzyl group, which by incorporating electron-donating substituents led to increased activity, while activity decreased with electron-withdrawing groups. A second modification was incorporated, a methoxy group at 6-position of the benzene ring, which increased the biological activity, suggesting that the presence of electron-donating groups are favourable in this position. Based on the above modifications proposed on the benzene ring, the researchers determined a preference for electron-donating groups for the synthesis of more analogues. Predominantly, these compounds showed lower inhibition activity on TR than indrataline and a lower EC_{50} on *T. brucei*; however, two indrataline analogues with a acetyl and tosyl substituent (EC_{50}= 3.64 μM, IC_{50}> 200 μM; EC_{50}= 4.33 μM, IC_{50}> 200 μM), respectively, showed an enzyme inactivity, with good activity against *T. brucei*, suggesting that these compounds may have another drug target. In addition, all compounds were evaluated as inhibitors of human GR with an inhibition <12% [54].

From 1,3,4-tiadiazolium-2-aminide derivatives that showed a growth inhibitory against four protozoa including *T. cruzi*, Rodrigues *et al*., developed a new series of four derivatives

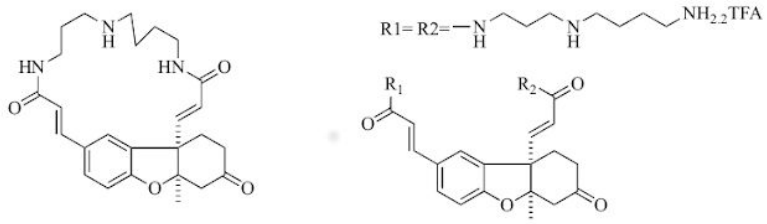

Lunarine **Lunarine analogue**

Fig. (8). Structure of lunarine and its analogue as TRI.

denominated, MI-HH, MI-3-OCH_3, OH-4-OCH_3 and MI-4-NO_2 (Fig. **9**) as potential TRI. The studies on enzymatic activity of TR demonstrated that the addition of these compounds did not modify NADPH consumption, with the exception of compound MI-4-NO_2, with 76% inhibition on extracts of *L. amazonensis*. The same behaviour was found with compound MI-4-NO_2 against *L. infantum*, *L. braziliensis* and *T. cruzi* with values of 70, 69.5 and 83%, respectively, suggesting TR as a pharmacological target. Subsequently, the compound MI-4-NO_2 was used as a trypanothione reductase inhibitor of *L. infantum* in enzyme kinetics, effectively reducing its activity. This effect on the enzyme was demonstrated by low maximum velocity (V_{max}) values and little or no effect on the apparent Michaelis constant (Km) that is a characteristic effect of non-competitive inhibition. The IC_{50} for TR was estimated at 1.63 ± 0.06 µM. Additionally, *in silico* (molecular docking) studies shows that the nitro group of MI-4-NO_2 forms an H-bond with the side chain Lys60 (O···N space of 3.47 Å); planarity of the nitro group apparently helps the *p*-nitro-phenyl group generate π-π interactions with the isoalloxazine ring from FAD cofactor, which is responsible for its redox behaviour; therefore it is expected that these interactions could interfere with enzyme activity. The authors suggest that these observations explain the best score of the compound MI-4-NO_2 and could be related to its experimental inhibitory activity [55].

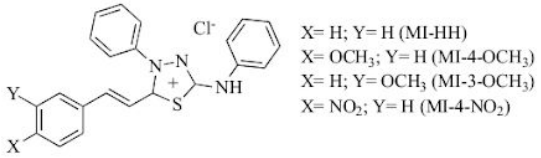

Fig. (9). Chemical structure of mesoionics 1,3,4-tiadiazolium-2-aminide derivatives.

Lu *et al.,* developed a potent trypanosomicidal agent, an anti-inflammatory, anti-oxidant and competitive inhibitor of thioredoxin reductase called ebsulfur (EbS, Fig. **10**), a sulphur analogue of ebselen (EbSe). EbS showed a potent growth inhibition of *T. brucei* (IC_{50}= 92 nM after 72 h incubation) 50 times more toxic than EbSe with a favourable selectivity index in mammalian cells. However, EbS was less toxic to other trypanosomatids such as epimastigotes of *T. cruzi* or promastigotes of *Leishmania tropica*. In addition, EbS irreversibly inhibited the activity of trypanothione reductase (K_{inact}= 0.38 min-1 and Ki= 10.4 µM) and was NADPH-dependent, forming a complex with trypanothione reductase and causing oxidation and inactivation of the enzyme. The result of biological activity indicates that EbS is more toxic for *T. brucei* to *T. cruzi*, causing a time-dependent trypanocidal effect. Furthermore, EbS demonstrated the activation of a cell death program of *T. brucei* through a translocation of phosphatidylserine and high production levels of intracellular reactive oxygen species killing the parasite [56].

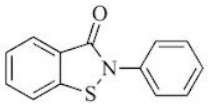

Fig. (10). Chemical structure of ebsulfur.

In the search for new TRI, Spinks *et al.* conducted a screening of 62 000 compounds, finding two new series of inhibitor compounds: quinoline and pyrimidinopyrazine derivatives (Fig. **11**). Analyzing the structure-activity relationship of quinoline derivatives results showed that a variation of 5-methyl furan decreases activity; the amide group with a basic substituent showed higher power than with alkyl or aryl amide substituents. On the other hand, a bromine atom on the aromatic ring of the quinolone can be removed to another position without affecting activity, although the change of the bromine atom by hydrogen or fluorine atom leads to a loss of activity. SAR from pyrimidinopyrazine derivatives shows that the methyl substituents on R_1 are well tolerated; however, deletion leads to loss of activity in position R_2. To maintain activity the methyl group can be replaced only by small alkyl groups, and in R_3, a large number of aromatic substituents were well tolerated.

To confirm the mechanism of action and selectivity of these compounds, enzyme assays with TR and GR were done with substrate concentrations at equal Km allowing direct comparison to the IC_{50} values. The results obtained for all compounds showed a significant selectivity for TR compared to GR, suggesting that the binding site of GR is smaller, less hydrophobic, and less negatively charged than TR. Additionally, these results show that the TR inhibition kinetic of these compounds is competitive, particularly, the quinolone series. This fact could indicate that they bind to the free enzyme or enzyme-substrate complex. In pyrimidi-

nopyrazine derivatives, the biological activity is linear and non-competitive; the compounds only bind to the enzyme-substrate complex. Additionally, the authors indicate that such compounds bind to a site distinct from the two substrate binding sites, since these compounds have certain structural similarities to the FAD co-factor. The authors suggest that disruption of orientation or displacement of FAD could explain the pattern of non-competitive inhibition [57].

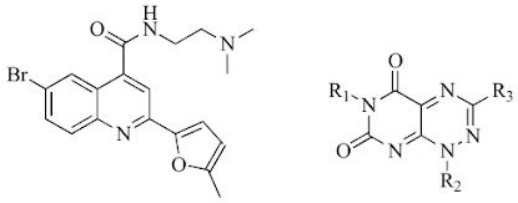

Fig. (11). Structures of quinoline and pyrimidinopyrazine derivatives as TRI.

CONCLUSION

In the development of new agents for the treatment of Chagas disease, TR has been considered a valid drug target. This allows the development of compounds with different structures that compete as irreversible inhibitors with trypanocidal activity. However, in some compounds there is no correlation between enzyme activity and trypanocidal activity. This suggests that there may be other mechanisms involved in the activity or pharmacokinetic factors interfering with the *in vivo* effect.

Undoubtedly, irreversible inhibitors are required to achieve death of the parasite; therefore the development of more TRI agents is needed. This must be based on advances in structure-activity relationships in order to find a new treatment option for Chagas disease.

CONFLICT OF INTEREST

The author(s) confirm that this article content has no conflict of interest.

ACKNOWLEDGEMENTS

Gildardo Rivera Sánchez wishes to thank the Comisión de Operación y Fomento de Actividades Académicas (COFAA- Instituto Politécnico Nacional), and the Programa de Estímulos al Desempeño de los Investigadores (EDI- Instituto Politécnico Nacional) for their financial support. KV is grateful for the financial support received from PRODEP 2016 and the School of Veterinary Medicine and Zootechnology of the Universidad Autónoma de Nuevo León.

REFERENCES

[1] Coura, J. R.; Borges-Pereira, J. Chagas disease: 100 years after its discovery. A systemic review. *Acta Trop* **2010**, *115*(1-2), 5-13

[2] Carabarin-Lima, A.; González-Vázquez, M.C.; Rodríguez-Morales, O.; Baylón-Pacheco, L.; Rosales-Encina, J.L.; Reyes-López, P.A.; Arce-Fonseca, M. Chagas disease (American trypanosomiasis) in Mexico: an update. *Acta Trópica* **2013**, *127*(2), 126–135.

[3] Stanaway, J.D.; Roth, G. The Burden of Chagas Disease: Estimates and Challenges. *Glob Heart.* **2015**, *10*(3), 139-44.

[4] Bonney, K.M. Chagas disease in the 21st century: a public health success or an emerging threat? *Parasite.* **2014**, *21*, 11.

[5] Strasen, J.; Williams, T.; Ertl, G.; Zollerm T.; Stich, A.; Ritterm O. Epidemiology of Chagas disease in Europe: many calculations, little knowledge. *Clin Res Cardiol.* **2014**, *103*(1), 1-10.

[6] Schmunis, G. A.; Yadon, Z. E. Chagas disease: a Latin American health problem becoming a world health problem. *Acta Trop* **2010**, *115(1-2)*, 14-21.

[7] Rueda, K.; Trujillo, J.E.; Carranza, J.C.; Vallejo, G.A. Oral transmission of *Trypanosoma cruzi* : a new epidemiological scenario for Chagas' disease in Colombia and other South American countries. *Biomedica.* **2014**, *34*(4), 631-41.

[8] Bern, C. Chagas' Disease. *N Engl J Med.* **2015**, *373*(5), 456-66.

[9] Goldenberg, S.; Avila, A.R. Aspects of *Trypanosoma cruzi* stage differentiation. *Adv Parasitol.* **2011**, *75*, 285-305.

[10] Sturm, N. R.; Campbell, D. A. Alternative lifestyles: the population structure of *Trypanosoma cruzi*. *Acta Trop* **2010**, *115(1-2)*, 3543.

[11] Torres-Pérez, F.; Acuna-Retamar, M.; Cook, J.A.; Bacigalupo, A.; García, A.; Cattan, P.E.; Statistical phylogeography of Chagas disease vector Triatoma infestans: testing biogeographic hypotheses of dispersal. *Infect Genet Evol.* **2011**, *11*(1), 167-74.

[12] Abad-Franch, F.; Santos, W.S.; Schofield, C.J Research needs for Chagas disease prevention. *Acta Trop,* **2010**, *115*(1-2), 44-54.

[13] Urbina, J.A. Specific chemotherapy of Chagas disease: relevance, current limitations and new approaches. *Acta Trop,* **2010**, *115*(1-2), 55-68.

[14] Calderón-Arancibia, J.; Espinosa-Bustos, C.; Cañete-Molina, Á.; Tapia, R. A.; Faúndez, M.; Torres, M. J.; Aguirre, A.; Paulino, M.; Salas, C.O. Synthesis and pharmacophore modelling of 2,6,9-trisubstituted purine derivatives and their potential role as apoptosis-inducing agents in cancer cell lines. *Molecules.* **2015**, *20*(4), 6808-6826.

[15] Carraro, R.; Iribarne, F.; Paulino, M. Analysis of cyclosporin A and a set of analogs as inhibitors of a T. cruzi cyclophilin by docking and molecular dynamics. *J Biomol Struct Dyn*. **2015**, 1-15.

[16] Vázquez, K.; Espinosa-Bustos, C.; Soto-Delgado, J.; Tapia, RA.; Varela, J.; Birriel, E.; Segura, R.; Pizarro, J.; Cerecetto, H.; González, M.; Paulino, M.; Salas, CO. New aryloxy-quinone derivatives as potential anti-Chagasic agents: synthesis, trypanosomicidal activity, electrochemical properties, pharmacophore elucidation and 3D-QSAR analysis. *RSC Adv*. **2015**, *5*, 65153-65166.

[17] Tapia, R.A.; Salas, C.O.; Vázquez, K.; Espinosa-Bustos, C.; Soto-Delgado, J.; Varela, J.; Birriel, E.; Cerecetto, H.; González, M.; Paulino, M. Synthesis and biological characterization of new aryloxyindole-4,9-diones as potent trypanosomicidal agents. *Bioorg Med Chem Lett*. **2014**, *24*(16), 3919-3922.

[18] Hall, B.S.; Bot, C.; Wilkinson, S.R. Nifurtimox activation by trypanosomal type I nitroreductases generates cytotoxic nitrile metabolites. *J Biol Chem,* **2011**, *286*(15), 13088-13095.

[19] Hall, B. S.; Wilkinson, S.R. Activation of benznidazole by trypanosomal type I nitroreductases results in glyoxal formation. *Antimicrob Agents Chemoter,* **2011**, *56*(1), 115-123.

[20] Maya, J.D.: Cassels, B.K; Iturriaga-Vásquez, P.; Ferreira, J.; Faúndez, M.; Galanti, N.; Ferreira, A.; Morrello, A. Mode of action of natural and synthetic drugs against *Trypanosoma cruzi* and their interaction with the mammalian host. *Comp Biochem Physiol A Mol Integr Physiol.* **2007**, *146*(4), 601-620.

[21] Pinazo, M.J.; Espinoza, G.; Gállego, M.; López-Chejade, P.L.; Urbina, J.A.; Gascón, J. Successful treatment with posaconazole of a patient with chronic Chagas disease and systemic lupus erythematosus. *Am. J. Trop. Med. Hyg*., **2010**, *82*(4), 583-587.

[22] Diniz Lde, F.; Caldas, I.S.; Guedes, P.M.; Crepalde, G.; de Lana, M.; Carneiro, C.M.; Talvani, A.; Urbina, J.A.; Bahia, M.T. Effects of Ravuconazole Treatment on Parasite Load and Immune Response in Dogs Experimentally Infected with *Trypanosoma cruzi*. *Antimicrob Agentes Chemothera*, **2010**, *54*(7), 2979-2986.

[23] Rivera, G.; Bocanegra-García, V.; Ordaz-Pichardo, C.; Nogueda-Torres, B:; Monge, A. New therapeutic targets for drug design against Trypanosoma cruzi, advances and perspectives. *Curr Med Chem*. **2009**, *16*(25), 3286-93.

[24] Flohe, L.; Hecht, H.J.; Steinert, P. Glutathione and trypanothione in parasitic hydroperoxide metabolism. *Free Radic. Biol. Med.,* **1999**, *27*(9-10), 966-984.

Capítulo 2

Análisis estructural y anclaje molecular de quinonas tripanocidas en tripanotión y glutatión reductasa : una comparación con datos bioquímicos

Structural analysis and molecular docking of trypanocidal aryloxy-quinones in trypanothione and glutathione reductases: a comparison with biochemical data.
Vera, Brenda; Vázquez, Karina; Mascayano, Carolina; Tapia, Ricardo A; Espinosa, Victoria; Soto-Delgado, Jorge; Salas, Cristian O; Paulino, Margot
J. Biomol. Struct. Dyn.2017 Vol.35, Num.18, Pag. 1785-1803
DOI: 10.1080/07391102.2016.1195283

Resumen

Meta: Dado un conjunto de ariloxi-quinonas sintetizadas y con actividades tripanocidas conocidas, describir este grupo de moléculas y proponer el modo de anclaje en tripanotión y glutatión reductasa. Relacionar los resultados in silico con datos bioquímicos y cinéticos.

Un conjunto de 28 ariloxi quinonas previamente sintetizadas y evaluadas en cultivos de epimastigotes de *Trypanosoma cruzi* resultaron ser más potentes y selectivas que Nifurtimox ®. La hipótesis de la que partimos para realizar el desarrollo de la siguiente investigación es que uno de los posibles mecanismos de la actividad tripanocida de estas quinonas podría ser la inhibición de la enzima tripanotión reductasa (TR).

En este trabajo se realizaron estudios bioquímicos, cinéticos y de acoplamiento molecular en TR y en su contraparte en humanos, la glutatión reductasa (GR).

Los ensayos bioquímicos indicaron que las naftoquinonas Nq-h, Nq-g y Nq-d inhiben TR y GR con cierta selectividad. Los estudios cinéticos demuestran que Nq-h inhibe por un mecanismo no competitivo a la TR.

El acoplamiento molecular se realizó en tres sitios: (1) el sitio catalítico, (2) la interfase de los dímero y (3) en los sitios de unión del NADPH de los receptores TR y GR. Las ariloxi quinonas mostraron una alta afinidad de unión en un sitio cercano al sitio de unión por lo que la cinética no competitiva podría estar justificada.

Los tres compuestos (Nq-h, Nq-g y Nq-d) presentan una cierta especificidad sobre TR, esta puede ser resultado de la presencia de una red de contactos con el anillo quinonico y por los residuos Lys62, Met400', Ser464' en TR, y un número menor de contactos en los respectivos

aminoácidos en GR.

El sustituyente nitrofenoxi del compuesto Nq-b contribuye en el mejor scaffold para el diseño de compuestos tripanocidas con baja toxicidad. Sin embargo, este compuesto presenta un efecto menos selectivo hacia TR que en el caso de Nqh, que tiene un sustituyente alfa-naftoxi , lo que indica que este blanco no es el mayor efector de la actividad antiparasitaria de las ariloxi quinonas.

Mis contribuciones en este trabajo: desarrollo de la metodología *in silico* y en análisis de resultados bioquímicos y computacionales.

Journal of Biomolecular Structure and Dynamics, 2017
Vol. 35, No. 8, 1785–1803, https://doi.org/10.1080/07391102.2016.1195283

Structural analysis and molecular docking of trypanocidal aryloxy-quinones in trypanothione and glutathione reductases: a comparison with biochemical data

Brenda Vera[a], Karina Vázquez[b,c], Carolina Mascayano[d], Ricardo A. Tapia[b], Victoria Espinosa[e], Jorge Soto-Delgado[f], Cristian O. Salas[b]* and Margot Paulino[a]*

[a]*Centro de Bioinformática estructural, DETEMA, Facultad de Química, UdelaR, Montevideo, Uruguay;* [b]*Facultad de Química, Pontificia Universidad Católica de Chile, Santiago, Chile;* [c]*Campus de Ciencias Agropecuarias, Facultad de Medicina Veterinaria y Zootecnia, Universidad Autónoma de Nuevo León, Nuevo León, Mexico;* [d]*Departamento de Ciencias del Ambiente, Facultad de Química y Biología, Universidad de Santiago, Chile, Santiago, Chile;* [e]*Centro de investigaciones biomédicas y aplicadas, Escuela de Medicina, Facultad de Ciencias Médicas, Universidad de Santiago, Chile, Santiago, Chile;* [f]*Departamento de Ciencias Químicas, Facultad de Ciencias Exactas, Universidad Andrés Bello, Quillota 980, Viña del Mar, Chile*

Communicated by Ramaswamy H. Sarma

(*Received 22 March 2016; accepted 25 May 2016*)

A set of aryloxy-quinones, previously synthesized and evaluated against *Trypanosoma cruzi* epimastigotes cultures, were found more potent and selective than nifurtimox. One of the possible mechanisms of the trypanocidal activity of these quinones could be inhibition of trypanothione reductase (TR). Considering that glutathione reductase (GR) is the equivalent of TR in humans, biochemical, kinetic, and molecular docking studies in TR and GR were envisaged and compared with the trypanocidal and cytotoxic data of a set of aryloxy-quinones. Biochemical assays indicated that three naphthoquinones (**Nq-h**, **Nq-g**, and **Nq-d**) selectively inhibit TR and the TR kinetic analyses indicated that **Nq-h** inhibit TR in a noncompetitive mechanism. Molecular dockings were performed in TR and GR in the following three putative binding sites: the catalytic site, the dimer interface, and the nicotinamide adenine dinucleotide phosphate-binding site. In TR and GR, the aryloxy-quinones were found to exhibit high affinity for a site near it cognate-binding site in a place in which the noncompetitive kinetics could be justified. Taking as examples the three compounds with TR specificity (TRS) (**Nq-h**, **Nq-g**, and **Nq-d**), the presence of a network of contacts with the quinonic ring sustained by the triad of Lys62, Met400′, Ser464′ residues, seems to contribute hardly to the TRS. Compound **Nq-b**, a naphthoquinone with nitrophenoxy substituent, proved to be the best scaffold for the design of trypanocidal compounds with low toxicity. However, the compound displayed only a poor and non-selective effect toward TR indicating that TR inhibition is not the main reason for the antiparasitic activity of the aryloxy-quinones.

Keywords: molecular docking; aryloxy-quinones; trypanothione reductase; glutathione reductase; Chagas disease

1. Introduction

Parasitic diseases are a major obstacle to human health and economic development in many parts of the world and cause high rates of mortality and morbidity (WHO, 2011). Current therapies against these diseases are unsatisfactory, with treatment failure being common due to widespread resistance and severe side effects (Bern, 2011; Bern et al., 2007; Rassi, Rassi, & Marin-Neto, 2010; Viotti et al., 2006; Yun et al., 2009). Thus, there is a need for the development of new, efficient, and safe drug (Carraro, Iribarne, & Paulino, 2016; Hoelz et al., 2015; Manoel-Caetano Fda & Silva, 2007; Molina et al., 2014; Woodcock & Woosley, 2008). In recent years, naphthoquinones and heterocyclic derivatives are considered privileged structures in the development of novel drugs against parasitic diseases such as trypanosomiasis (Prati et al., 2015; Salas, Faundez, Morello, Maya, & Tapia, 2011).

There are several proposed mechanisms of action f the trypanocidal activity of quinone derivatives. One them is the well-known ability of quinones for genera ing reactive oxygen species (ROS) through redox cyclin with molecular oxygen and consequently oxidative stre and cell death (Benites et al., 2010; Henry & Wallac 1996; Kovacic, 2007; O'Brien, 1991; Paulino et a 2008).

The metabolic differences between the parasite a host cells to avoid the damage mediated by ROS are co siderable (Gutteridge & Halliwell, 2000; Salas et a 2011). Trypanothione reductase (TR) constitutes a maj component of the general oxidative-stress defence *Trypanosoma cruzi* (Turrens, 2004) and is absent in mar mals. The main function of TR is to maintain a reducin intracellular environment by keeping trypanothione in t dithiol state (Gonzalez-Chavez, Olin-Sandoval, Rod guez-Zavala, Moreno-Sanchez, & Saavedra, 2015). TR

essential in all trypanosomatids. Parasites with lowered TR activity display an increased sensitivity toward hydrogen peroxide (Fairlamb, Blackburn, Ulrich, Chait, & Cerami, 1985; Gonzalez-Chavez et al., 2015). The counterpart of the parasite TR in the mammalian host is glutathione reductase (GR). A comparison with the available crystal structures of GR (Berkholz, Faber, Savvides, & Karplus, 2008; Karplus & Schulz, 1987, 1989; Pai, Karplus, & Schulz, 1988; Pai & Schulz, 1983) reveals that the overall structure of the two enzymes is highly conserved. There is an overall 40% sequence identify and both enzymes are homodimers. TR may also replace thioredoxin reductase, although trypanosomatids do possess a conventional thioredoxin.

The key feature of TR and GR is the mutually exclusive specificity for their cognate disulfide substrate. Thus, in principle, it should be possible to inhibit selectively the parasite enzyme without affecting the mammalian one. A detailed analysis of the enzymes (Iribarne, Paulino, Aguilera, Murphy & Tapia 2002) indicates that in both TR and GR, several alternative sites exist in addition to the binding sites for the disulfide substrate and nicotinamide adenine dinucleotide phosphate (NADPH) and the dimer interface.

For a set of aryloxy-quinones previously synthetized and tested for their trypanocidal and cytotoxic activities (Vazquez et al., 2015), it was proposed that their selective antiparasitic activities may correlate with the inhibition of TR. To prove this hypothesis, here, we report on the biochemical and kinetic analysis of recombinant *T. cruzi* TR and human GR inhibition. In parallel, *in silico* molecular docking studies of TR/GR complexes with aryloxy-quinones in all putative binding sites aimed at a deeper understanding of the atomic interactions between these compounds and TR and GR, respectively. As a result, quinone derivatives with good and selective TR inhibitor capacity and with low GR affinity can be proposed as candidates to develop more effective drugs against Chagas and other diseases caused by trypanosomatids.

2. Methodology

A set of 28 aryloxy-quinones (Figure 1) were previously synthetized and tested (Vazquez et al., 2015). The set of quinones was divided in three subsets based on three main scaffolds as naphthoquinones, quinolinequinones, and furanoquinones. Moreover, each main scaffold has different aryloxy substituents. To understand the manner in which these molecules function in the parasite, as well as in the couple TR/GR trypanosomatids and mammalian enzymes, in a first step of this work twenty of these molecules were selected to make TR/GR inhibition and kinetics studies. In a second step an *in silico,* strategy was applied to the entire set of quinones.

2.1. *Biochemical studies*

TcTR was prepared following a published procedure (Walsh, Bradley, & Nadeau, 1991). Trypanothione disulfide (TS_2) was generated enzymatically as described previously (Comini, Dirdjaja, Kaschel, & Krauth-Siegel, 2009).

2.1.1. *TR assays*

The activity of TR was measured in 40 mM Hepes, 1 mM EDTA, pH 7.5 at 25 °C. The assay mixture contained, in a total volume of 1 mL, 100 µM NADPH, 5–10 mU of TcTR, and 50 µL DMSO as control or the same volume with the tested compound dissolved at a final concentration of 100 µM when the quinone inhibition was tested. The reaction was started by the addition of 100 µM of TS_2 and NADPH consumption was measured by following the absorbance decrease at 340 nm at 25 °C ($\varepsilon = 6.22\ mM^{-1}\ cm^{-1}$) (Persch et al., 2014). From these data, the percentage of inhibition was calculated. Many compounds proved to be insoluble under the assay conditions and thus could only be measured at rather low concentrations. One representative compound of each subset of compounds (**Nq-h**, **Fq-c**, and **Qq-b**) was subjected to a detailed kinetic analysis.

2.1.2. *GR assays*

GR was purified from human erythrocytes by the method previously reported (Worthington & Rosemeyer, 1974). The enzyme was stored at a concentration of 5 mg/mL in potassium phosphate buffer, pH 7.0, I .1 M, containing .2 M KCl, 1 mM EDTA, and .1% (v/v) 2-mercaptoethanol.

The activity of human GR was measured in 200 mM KCl, 60 mM K_2HPO_4, and 1 mM EDTA, pH 6.9 at 25 °C. The assay mixture contained in a total volume of 1 mL, 100 µM NADPH, and 5–20 mU of hGR and 5 mM of inhibitor on DMSO.

After checking for nonspecific NADPH oxidation for two minutes, 1.1 mM of GSSG was added to start the enzymatic reaction. The decrease in NADPH concentration was monitored spectrophotometrically. Residual enzyme activity in the presence of inhibitor was determined relative to controls containing DMSO according to Nordhoff et al. (Fernandez-Blanco, Font, & Ruiz, 2016; Maran, Fernandez, Barbieri, Font, & Ruiz, 2009; Nordhoff, Bucheler, Werner, & Schirmer, 1993).

2.2. In silico *assays*

All calculations were done running the Molecular Operating Environment (MOE 2015.10, Chemical Computing Group Inc., http://www.chemcomp.com) suite on Linux, on a workstation with a quad-core processor hyperthread equipped.

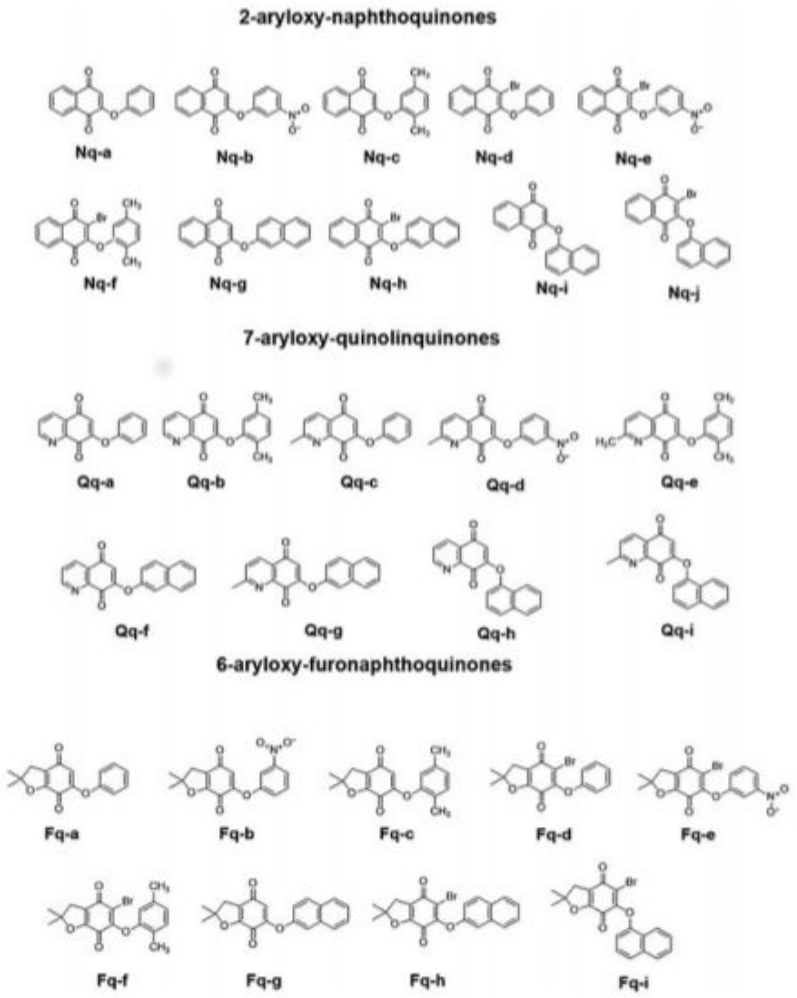

Figure 1. Chemical structures of aryloxy-quinones with trypanocidal interesting activities.

A molecular docking of 28 carbo and heterocyclic derivatives of aryloxy-quinones was done to study the interactions with the putative enzymatic receptors TR and GR. This procedure implies a ligand and a receptor preparation, the development of a validated docking procedure and the molecular docking itself.

2.2.1. *Ligand preparation: modeling and conformational analysis*

The three-dimensional (3D) structures of the 28 molecules under study (Vazquez et al., 2015) (Figure 1) were submitted to energy minimization by means of MMFF94x force field (Halgren, 1996a, 1996b) and the program suite MOE. To use all flexibility capacity of the program, a conformational analysis was performed for all naphthoquinones, quinolinequinones, and furanoquinones using the low-mode molecular dynamics (LowModeMD) approach (Labute, 2010) to search minimum energy conformers. The resulting conformations are saved to the output database provided they meet the energetic and geometric criteria.

An energy minimization was done and terminated when the root mean square (RMS) gradient test fall below .005 kcal/mol. The maximum number of energy minimization iterations was selected as 500. Two conformations are judged equal if the optimal heavy atom RMS superposition distance is less than the specified tolerance of .25 Å. All conformations with an energy greater than the sum of the global minimum energy plus a cutoff of 7 kcal/mol were discarded.

2.2.2. *Crystal structure of the putative targets*

2.2.2.1. Trypanothione reductase. The catalytic function of TR is the reduction of its cognate substrate TS_2 to the

dithiol form $T(SH)_2$. TR is active as a homodimer with a subunit mass of about 52 kD. The two identical catalytic sites are composed of residues of both subunits and comprise at least two regions, namely the NADPH site and the disulfide substrate site, which are separated by the flavin ring (Paulino et al., 2005).

The crystal structure of *T. cruzi* TR complexed with its physiological substrate TS_2 was obtained from the Protein Data Base (PDB 1BZL), 2.4 Å resolution (Bond et al., 1999). The homodimeric protein is composed of two peptide chains each containing 486 amino acids, two molecules of the cofactor flavin adenine dinucleotide (FAD) and two molecules of ligand, the *bis*(gamma-glutamyl–cysteinyl–glycinyl)spermidine (TS_2). Both TR cocrystallized ligands are posed each one in both catalytic sites.

2.2.2.2. Glutathione reductase. The crystal structure of human GR was obtained from the PDB base (4GR1) with 2.4 Å resolution (Janes & Schulz, 1990). GR is a homodimer with two chains of 478 amino acids and a molecule of the cofactor FAD each. It is cocrystallized with a molecule of 4-N-malonyl cysteinyl-2,4-diaminobutyrate disulfide (RGS).

2.2.3. Quinones putative binding sites

To identify possible quinones-binding site in the crystal structures of GR and TR, the Site Finder module of the MOE 2015.10 was used. Forty-four putative sites in TR and fifty-five55 in GR were detected. The site finder shows the findings as red (polar) or grey (apolar) spheres and a number that is the total count of spheres represents the size of a site. The sites have been analyzed in their size as well their structure and amino acid composition. The greater detected sites in both enzymes were the catalytic sites described earlier in the crystallographic structures. The Site Finder detected too the NADPH-binding site in both enzymes. Finally, for both enzymes, a site localized in the interface surface between both monomers conforming the dimer was identified (Figure 2). Several crystal structures of GR–inhibitor complexes have shown binding of the ligands at this cavity (e.g. Bilzer et al., 1984; Savvides & Karplus, 1996).

2.2.3.1. Catalytic-binding site and neighborhoods. Cys53 and Cys58 form the catalytic redox-active site dithiol/disulfide of TR and are located at the bottom of the cleft near the isoalloxazine ring of FAD (Bond et al., 1999). In GR, the respective residues are Cys58 and Cys63 (Janes & Schulz, 1990; Karplus, Pai, & Schulz, 1989; Pai & Schulz, 1983; Pai et al., 1988).

When the TS_2-binding site in TR is described based on a list of contacting amino acids at a 4.5 Å distance of TS_2, it could observed that amino acids from both A and B chains participate in the binding (Bond et al., 1999).

Research from our groups gave detailed information about these structural characteristics (Hikichi, Paulino, Hansz, & Tapia, 1995; Iribarne, Paulino, Aguilera, & Tapia, 2009; Iribarne et al. 2002; Paulino et al., 2005).

The overall structure of the active site of GR is similar to that of TR. However, in contrast to the negatively charged TS_2 binding site in TR, the GSSG-binding site in GR displays an overall positive charge.

A hydrophobic region named "Z-site" was defined in 1991 by el-Waer, Douglas, Smith, and Fairlamb (1991). They suggested the Z-site as a relevant binding pocket for TR inhibitors although Glu466 and Glu467, the residues mainly responsible for the electrostatic interactions with the inhibitors, are conserved in GR and TR (de Paula da Silva, Bernardes, da Silva, Zani, & Carvalho, 2012). Thus, it is difficult to assume a specific binding of TR inhibitors at this site. Indeed, although docking simulations yielded the Z-site as favored binding site, the crystal structure revealed the inhibitor at the hydrophobic wall lining the TS_2-binding site (Persch et al., 2014). Here we will demonstrate that for aryloxyquinones, a mixture of both catalytic and Z-site residues, in its neighborhood, could confer selectivity.

2.2.3.2. Alternative putative binding sites. In each active site of the homodimer, the cofactor FAD is found, together with the dithiol/disulfide bridge, essential for catalysis. During catalysis, reducing equivalents flow from NADPH to the disulfide substrate (e.g. trypanothione) with FAD and the disulfide bridge as intermediates. Two proton relays, one at each site, modulate the transfer. This complexity justifies the proposal of the NADPH site as a putative-binding site, in the same way by which the endogenous substrate binding site was proposed before.

At the subunit interface, both enzymes have a cavity that was marked in the Site Finder strategy, as a likely binding site. This is in accordance with previous crystal structures of GR inhibitor complexes showing ligand binding at this site (e.g. Bilzer et al., 1984; Savvides & Karplus, 1996). In comparison to GR, the cavity of TR is more extended and narrow, contacting both catalytic sites in neighborhood of the above-described Z-site (Figure 2). This topology like a bridge between both catalytic sites caused us to think that this site may bind molecules. For this reason, in the docking approaches, we compared this region with other sites.

2.2.4. Molecular docking

Separate configurational databases in which each one of naphthoquinones, quinolinequinones, and furanoquinones

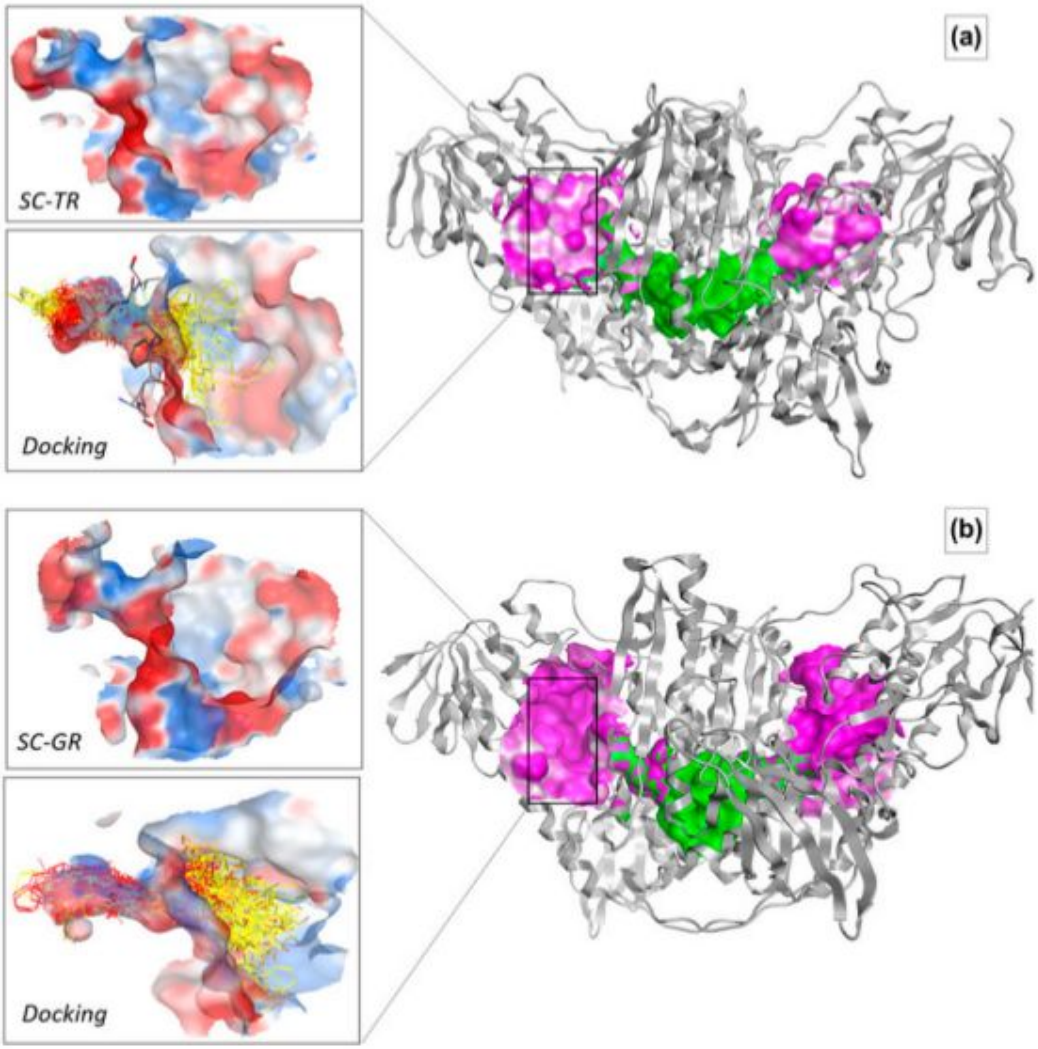

Figure 2. Catalytic site (purple) and interface site (green) of (A) trypanothione reductase and (B) glutathione reductase. In the top left corner of each figure, the electrostatic surfaces of the TR (SC-TR) and GR (SC-GR) catalytic sites are shown. Electrostatic positive and negative surfaces were colored in red and blue, respectively.
Notes: In the bottom left corner of Figures 2(A) and (B), the docked naphthoquinones in the catalytic site of trypanothione reductase and glutathione reductase were shown. In red: molecule conformers with high scores ranging from −13.4 to −10.1 kcal/mol. In yellow, molecule conformers with low scores ranging lower scored from −10.1 to −5.3 kcal/mol.

configurations were used. As ligand, it was used a configurational database of molecules.

Four sites are assayed separately. The catalytic binding sites were defined from a 4.5 Å sphere around the cocrystallized ligand of TR and GR, respectively. The interface site definition was made through the Site Finder procedure above described. In the case of NADPH, a 4.5 Å sphere around the FAD adenine moiety defined the site.

Docking validation tests were performed with three set of conformational databases for naphthoquinones, quinolinequinones, and furanoquinones and the Catalytic Site 1. Two placement methods: Triangle Matcher and Alpha PMI (Udatha, Sugaya, Olsson, & Panagiotou, 2012) were assayed. Affinity dG (AdG) (Halgren, 1996a, 1996b) and London dG were assayed for scoring and re-scoring. Finally, MMFF94x force field was used to energy minimize the resulting structures.

2.2.5 *Protein–ligand interaction fingerprints (PLIF)*

The PLIF descriptors implemented in the MOE were used as a benchmark with respect to interaction fingerprints. Interactions are classified as hydrogen bonds,

ionic interactions, and surface contacts according to the residues. The PLIF descriptors for all protein-bound ligands were generated with the default parameter set in MOE and presented in Population Display and the Barcode display.

The Population Display is a histogram showing the number of ligands (*Y*-axis) with which each residue (plotted in the *X*-axis) interacts. In the Barcode representation of binding interactions, they are horizontal lines (rows) that correspond to each of the studied compounds.

Additionally, two other analysis of PLIF results were performed and PLIF-ContactMap and PLIF-HeatMap were generated.

2.2.6. *H-Bond–ligand interactions*

The ligand interactions application provides a tool to visualize an active site of a complex in diagrammatic form. A selection of interacting entities, which includes hydrogen-bonded residues, close but nonbonded residues, solvent molecules and ions are drawn about the ligand, their positions in 2D being chosen to be representative of the observed 3D distances, as well as taking into account aesthetic considerations.

3. Results and discussion

3.1. *Enzymatic inhibition and kinetics*

3.1.1. *TR and GR inhibition screening*

Table 1 summarizes the experimental data obtained for all aryloxy-quinones investigated in this study. The trypanocidal activity toward *T. cruzi*, cytotoxicity vs. J-774 cells (Vazquez et al., 2015), as well as the *in vitro* TR/GR inhibitor activities are given.

Considering the three subsets of aryloxy-quinones studied, a naphthoquinone (**Nq-h**) proved to be the most active inhibitor of TR. However, no correlation between TR inhibition and the antiparasitic activity efficiency was observed. Whereas compound **Nq-b** showed the highest trypanocidal activity, it was a comparably weak inhibitor of TR and was even more active against GR. Thus, the compound is a good example that other mechanisms are responsible for the cellular mode of action of the quinones.

Nq-b is a naphthoquinone with a nitro substituent in its aryloxy moiety which may be the reason for its excellent trypanocidal activity (IC_{50} *T. cruzi* epimastigote = .02 μM). It is even more potent than nifurtimox (IC_{50} *T. cruzi* epimastigote = 7 μM) and possibly acts by a similar mechanism.

Nq-h was the most effective and selective inhibitor of TR. Its trypanocidal activity was good; although ten fold lower than that of **Nq-b**. The halogen (Br) on the naphthoquinone and the O-naphthyl substituent suggest that the electronegativity as well as the planar aromaticity may confer selectivity for TR vs. GR inhibition.

3.1.2. *TR kinetic assays*

Nq-h, **Qq-b**, and **Fq-c** were selected as representatives for the naphthoquinone, quinolinquinone, and furanquinone subsets and subjected to a detailed kinetic analysis. The type of inhibition was derived from Lineweaver–Burk plots (Supplementary Material Figure I). The inhibitor constants K_i were calculated from direct plots. The data obtained are shown in Table 2. All three compounds inhibited TR with a noncompetitive type of inhibition indicating that their binding site does not coincide with that for TS_2. With a K_i–value of 1.1 μM, **Nq-h** was clearly the best TR inhibitor.

3.2. *The 3D structure of the assayed quinones database and it Structure–Activity Relationships (SAR)*

Table 3 summarizes the main structural characteristics and results to allow a SAR analysis of the trypanocidal and TR inhibitory activities.

3.2.1. *SAR with respect to the trypanocidal activity*

Being that the aim of this search for a trypanocidal nontoxic drug is to improve the design of nifurtimox (better growth inhibition together with a lesser toxicity), it was been considered that a quinone with a good trypanocidal activity must inhibit *T. cruzi* growth in a concentration under .17 μM, a medium activity will correspond to concentrations between .17 and 7 μM, and quinones with inhibitory concentrations over 7 μM (that of nifurtimox) will be considered with low activity.

As we concluded in a previous paper (Vazquez et al., 2015), when comparing the naphthoquinones, furanoquinones, and quinolinequinones, the naphthoquinone moiety proved to be the best substructure for trypanocidal activity and lower toxicity. This is because the naphthoquinones were specially analyzed here. Inside the naphthoquinone sample, we could observe many variants including the addition of nitro, bromine, phenyl, or naphthyl moieties.

The presence of two putative redox active moieties: the quinonic ring and the nitrophenyloxy group (**Nq-b**) is an example of a very good improvement giving to the molecule very good (the best) activity in *T. cruzi*. With respect to the toxicity (J-774 cells), a comparison with nifurtimox seems put in evidence that the presence of the quinonic planar structure together with a phenoxy group, gave to the molecule selectivity in favor to the

Table 1. First column, coded name of quinones. Second and third columns: IC_{50} for the *T. cruzi* growth inhibition and cytotoxicity in J-774 IC_{50} in μM. Fourth and Fifth columns: percentages of trypanothione and glutathione reductase inhibition and in parentheses are annotated the related concentrations in μM.

Molecule	IC_{50} *T cruzi* Epimastigote*	J-774 IC_{50}*	% TR inhibition	% GR inhibition
Naphthoquinones				
Nq-a	.05 ± .04	<12.5	62% (5)	50 (7.32)
Nq-b	.02 ± .01	12.5	57% (100)	50 (1.4)
Nq-c	.17 ± .05	<12.5	46% (2.5)	50 (3.9)
Nq-d	.11 ± .04	18	53% (5)	50 (>100)
Nq-e	.11 ± .04	46	41% (10)	50 (>100)
Nq-f	Insoluble	Insoluble	Insoluble	50 (>100)
Nq-g	.15 ± .04	<12.5	43% (2.5)	50 (>100)
Nq-h	.14 ± .05	<12.5	64% (5)	50 (>100)
Nq-i	.17 ± .04	<12.5	Precipitated	50 (>100)
Nq-j	.17 ± .06	19	Precipitated	50 (>100)
Furanquinones				
Fq-a	1.00 ± .02	21	24% (12.5)	50 (>100)
Fq-b	2.30 ± .03	61	4% (1.5)	50 (>100)
Fq-c	.54 ± .13	44	25% (10)	50 (>100)
Quinolinquinones				
Qq-b	2.30 ± .03	18	52% (50)	50 (>100)
Qq-c	.14 ± .05	12.5	65% (10)	50 (>100)
Qq-d	.44 ± .09	12.5	46% (10)	50 (1.69)
Qq-e	.23 ± .07	<12.5	31% (3.1)	50 (3.33)
Qq-g	.98 ± .17	16	35% (12.5)	50 (6.32)
Qq-i	.17 ± .05	<12.5	36% (10)	50 (3.09)
Nifurtimox	7.00 ± .3	316 ± .5	–	–

*Data are from Vazquez et al. (2015).

Table 2. Aryloxy-naphthoquinone derivatives kinetics of TR inhibition.

Molecule	K_i (μM)	Inhibition kinetics
Nq-h	1,1	Noncompetitive
Qq-b	6,0	Noncompetitive
Fq-c	18,5	Noncompetitive

parasite inhibition (low toxicity than nifurtimox). Finally, the addition of a halogen when a nitro moiety is present (like in **Nq-e**) seems to lower the *T. cruzi* selective growth inhibition.

The presence of a halogen or a dimethyl-phenyloxy (comparing **Nq-a** with **Nq-d** or **Nq-a** with **Nq-c**) did not helped to improve the *T. cruzi* growth inhibition either to lower the toxicity.

The results of molecules with an alpha or beta naphtyloxy moieties, with or without a bromine atom in the structure, seems indicate that in which refers the *T. cruzi* growth inhibition these moieties have quite similar impact. In some cases (comparing **Nq-i** with **Nq-j**), the bromination contributes to lower the toxicity when a beta naphthyloxy is present in the structure. The halogenation of an alpha naphtyloxy moiety as in the case of the **Nq-h** seems not to give to the molecule a special either selective activity (compared with **Nq-g**).

3.2.2. *SAR with respect to the TR/GR inhibitory activity*

The nitro moiety, so good in the design of a trypanocidal molecule, is not related with a good and selective TR inhibition. This is the case of **Nq-b** and **Nq-e**, which are not selective TR inhibitors even if they are nontoxic and trypanocidal molecules.

A naphthoquinone scaffold accompanied by a phenyl nitro compound like that of **Nq-b** is depicted as the ideal scaffold to reach higher *T. cruzi* inhibition together with very low toxicity, even if the action mechanism will not be the selective inhibition of TR.

The phenoxy group is good when it has a bromination in the naphthyl moiety (**Nq-d**).

The alpha naphthyloxy group as in **Nq-h** and **Nq-g**, seems to be related to a selective TR inhibition. When the alpha naphthyloxy group has an halogen (**Nq-h**), the selectivity is as good than when it is absent (**Nq-g**).

They are no TR inhibition data to analyze the influence of a beta naphthyl (as it is the case of **Nq-j** of **Nq-i**) even if both have low activity in GR.

In the last columns of the Table 3, main questions referring these observations were YES/NO answered. In consequence, those molecules with both YES answers (*T. cruzi* and TR-selective inhibition): **Nq-h**, **Nq-d**, and **Nq-g**, were selected to further discussion.

Nq-h, **Nq-d**, and **Nq-g** are good and selective *T. cruzi* inhibitors and at the same time of TR. For these

Table 3. Summary of the structural characteristics for the assayed sets of naphtoquinones (Columns 2 to 6). Columns 7 and 8: color-coded *T. cruzi* inhibition growth and J-774 measurements (Vazquez et al., 2015): *T. cruzi* growth inhibition was considered TRYPANOCIDAL (GREEN) for compound concentrations below .17 μM; MEDIUM for concentrations between .17 and 7 μM and LOW (RED) those equal or higher than 7 μM (that of Nfx). Columns 9 and 10: color coded TR and GR inhibition results. TR inhibition was considered good (GREEN) when inhibitions of more than 43% were detected with concentrations below 5 μM. All other cases were considered low (RED); GR inhibition was considered low (RED) when a 50% inhibition was obtained for concentrations above 100 μM; all other cases were considered a low inhibition (GREEN). Column 11: Index of selectivity (IS) evaluated from data of Table 1 for the *T. cruzi* inhibition as the ratio between the J-774 by the *T. cruzi* growth inhibition concentrations. Values over 90 were considered as SELECTIVES (GREEN), between 45 and 90 MEDIUM SELECTIVITY (YELLOW) and BAD SELECTIVITY (RED) (<45). Column 12: The Index of Selectivity for the inhibition of TR (TRS) was calculated as the ratio between the values in the fourth by the fifth columns of the Table 1 and were classified as SELECTIVE TR INIHIBITION (GREEN) when a value over 20 was obtained. Column 13: the ratio of free energies in TR by GR (data from Supplementary Material Table A). Selectivity is assigned to rates over 1.11 (GREEN). Last two columns: main questions are YES/NO answered.

Molecule	Nitro	Br	Naphtyloxy	Phenyloxy	Methylphenyloxy	*T. cruzi* activity	Putative human	TR inhibition	GR inhibition	*T. cruzi* selectivity (IS)	TR selectivity (TRS)	*In silico* free energies TR/GR ratio	Inhibt *T. cruzi* with low toxicity?	Inhibit selectively TR?
Iq-a				x		Highly tripapnocidal	Nontoxic	Inhibition	Inhibition	250	1.5	1	YES	NO
Iq-b	x			x		Higher tripanocidal activity	Nontoxic	Low inhibition	Inhibition	1250	01	1.05	YES	NO
Iq-c					x	Tripanocidal	Medium toxicity	Inhibition	Inhibition	74	1.4	1.01	YES	NO
Iq-d		x		x		Tripanocidal	Nontoxic	Inhibition	Low inhibition	164	20	.93	YES	YES
Iq-e	x	x		x		Tripanocidal	Nontoxic	Low inhibition	Low inhibition	418	10	.99	YES	NO
Iq-f		x			x	ins	ins	ins	Low inhibition	–	–	1.01		
Iq-g			x α			Tripanocidal	Medium toxicity	Inhibition	Low inhibition	83	40	1.11	YES	YES
Iq-h		x	x α			Tripanocidal	Medium toxicity	Inhibition	Low inhibition	89	20	1.2	YES	YES
Iq-i			x β			Tripanocidal	Medium toxicity	ins	Low inhibition	74	–	1.03	YES	NO
Iq-j		x	x β			Tripanocidal	Non-toxic	ins	Low inhibition	112	–	89	YES	NO

three cases, the hypothesis of a selective inhibition of TR associated with a good and selective inhibition of *T. cruzi* growth is true. Considering that the **Nq-h** was the best, we could say that for the set of studied aryloxy-quinones, a naphthoquinone moiety, accompanied with an alpha naphthyloxy substituent is the scaffold to lead the design of a trypanocidal, nontoxic and TR-selective inhibitor drug.

3.3. *Molecular docking*

The previous observations were limited by the lacking of all necessary experimental results. This is because in this work we had the proposal of doing all *in silico* evaluation of the complete set of the quinones under study. The *in silico* will be in this case, complementary to all the discussion envisaged in the Section 3.2.

3.3.1. *Docking validation*

The validation step aimed into obtaining the broader range of energies to assure a good conformation sampling. The full set of 10 naphthoquinones, nine quinolinequinones, and nine furanquinones was used to generate three conformational databases of 63, 59, and 64 conformers, respectively, and they were docked in the Catalytic Site 1 of the TR (1BZL).

The results are presented in the Table 4. The best results were obtained for the Alpha PMI and the London ⊗G methods.

As the second criterion of validation, we look for a maximum overlap between the cocrystallyzed and docked TS_2. The Alpha PMI and the London ⊗G methods were used to dock the TS_2 in the catalytic Site 1. The overlapping between the cocrystallyzed and docked TS_2 was measured and resulted an root mean square deviation (RMSD) of 2.02 Å.

In consequence, the procedure was declared validated.

3.3.2. *Docking in the catalytic sites of TR and GR*

The three conformational databases were used as "ligand" in the docking.

As "Receptor," they were settled all atoms of TR or GR. As "Site," it was defined a sphere of 4.5 Å around the crystallographic ligand TS_2 or RGS, respectively. After selection, TS_2 (or RGS) molecules were deleted and FAD atoms remained as unselected atoms.

With the aim of comparing within the experimental results shown in the Table 1, in the Supplementary Material Table A, were detailed the ΔG of the best docked conformation for each set of aryloxy-quinones. All poses were classified in two ranges of high and low energies. All high energetic poses were red-colored ant the other in yellow. The results are shown in the Figure 2 and in Supplementary Material Figures II and III.

As it could be observed inside the left bottom frame of the Figure 2(A), two populations of naphthoquinones are detected in TR. The red colored poses, that is, the more energetic bindings, are in a site in the borderline between the Z site and the catalytic site.

When the furane and quinoline quinones were docked against the catalytic site 1 of TR, similar results were obtained being the more energetic bindings near to the catalytic site in the borderline with the Z site (Supplementary Material Figures II(a) and III(a)).

To describe graphically, this new aryloxy-quinones site, an electrostatic map was obtained for TR and GR (Figure 2(A) and (B) left top frames). The Electrostatic Feature Map in MOE is an application of the Poisson–Boltzmann Equation to the prediction of electrostatically preferred locations of hydrophobic, H-bond acceptor and H-bond donor locations.

The best energies in the docking against GR were observed in a subsite of the catalytic site 1 similar to that detected for TR (left bottom frame in Figure 2(B) and Supplementary Material Figures II(b) and III(b)).

3.3.3. *Docking in the alternative sites of TR and GR*

The docking for the three conformational databases in the interface site of TR (1BZL) and y GR (4GR1) shown that all best scored poses were placed in the middle of the interface but with lesser free energies than in the other assayed sites (data not shown). As an example, in the Supplementary Material, Figure IV shows the naphthoquinones docked in the interface site of TR and GR.

The results of the docking in the NADPH sites in TR and GR are shown in the Supplementary Material Table A and Figure V for the case of naphthoquinones.

3.4. *Analysis of docked complexes in TR and GR*

3.4.1. *Analysis of docking in the catalytic site by PLIF*

A massive analysis of contacts between docked quinones in TR and GR was performed by means of PLIF. For data visualization, the Barcode and Population Display and PLIF-ContactMap and PLIF-HeatMap tools were used.

All Side chain H-donor or acceptor (ChDon/ChAcc), Backbone H-donor or acceptor (BkDon/BkAcc), Solvent H-donor and acceptor (O), Ionic attraction (I), and Surface contact (Surf) were analyzed.

3.4.1.1. Barcode and Population Display. The Figure 3(a) and (b) show the Barcode Display and Figure 4(a) and (b) show the Population Display

Table 4. All combinations of docking conditions assayed to docking validation. Binding energy values are in kcal/mol.

Placement	Alfa PMI		TM	
Score function	Affinity dG	London dG	Affinity dG	London dG
Naphthoquinones	−6.72 to −5.6	−13.6 to −.69	−6.96 to −1.74	−7 to −1.65
Furanequinones	−7.11 to −5.5	−13.7 to −2.99	−7 to −1.65	−10.83 to −6
Quinolinequinones	−6.88 to −5.69	−13.7 to −2.29	−6.65 to −1.7	−10 to −5.85

(or histogram) made for all 28 docked quinones in GR and TR, respectively.

Two list of contacts emerges and they are, in the case of TR is: Lys62, Thr66, Leu399′, Met400′, His401′, Lys402′, Asp432′, Asn433, His461′, Thr463′, and Ser464′.

In the case or GR, the list of contacts is: Lys67, Asn71, Tyr106, Ile113, Tyr114, Ile343, Arg347, Thr404′, Met406′, Leu438′, His467′, Thr469′, Ser470′, Glu473′, and Thr476′.

Those contacts that have counterpart in TR/GR are highlighted in bold: Lys62 in TR is Lys67 in GR; Thr66 in TR is Asn71 in GR; Leu399′ in TR is Met406′ in GR (a nonconservative change); His461′ in TR is the His467′ in GR; Thr463′ in TR is Thr469′ in GR and Ser464′ in TR is Ser470′ in GR.

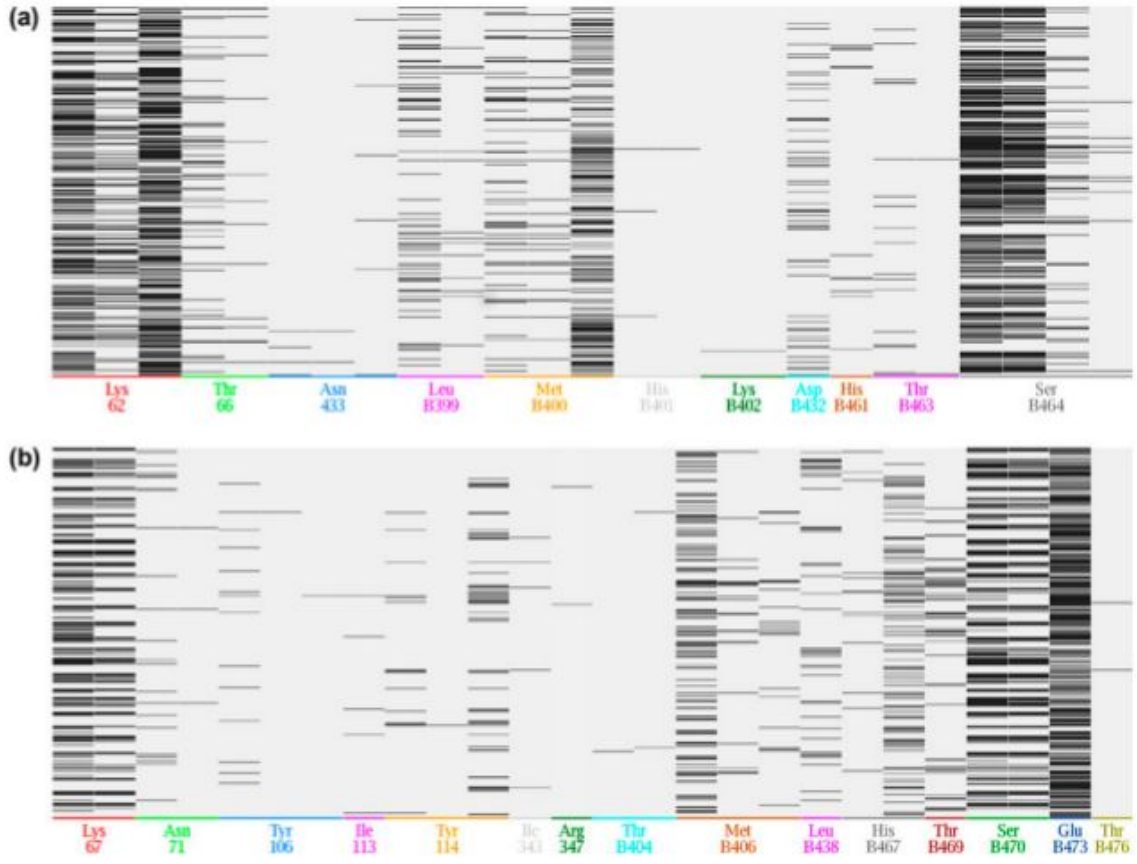

Figure 3. Barcode display analysis of PLIF results.
Notes: The horizontal rods correspond to each of the studied compounds. A black rod indicates the presence of an interaction with residues shown in the *X*-axis at the bottom of each graph. 3(a) Barcode display in TR. 3(b) Barcode display in GR.

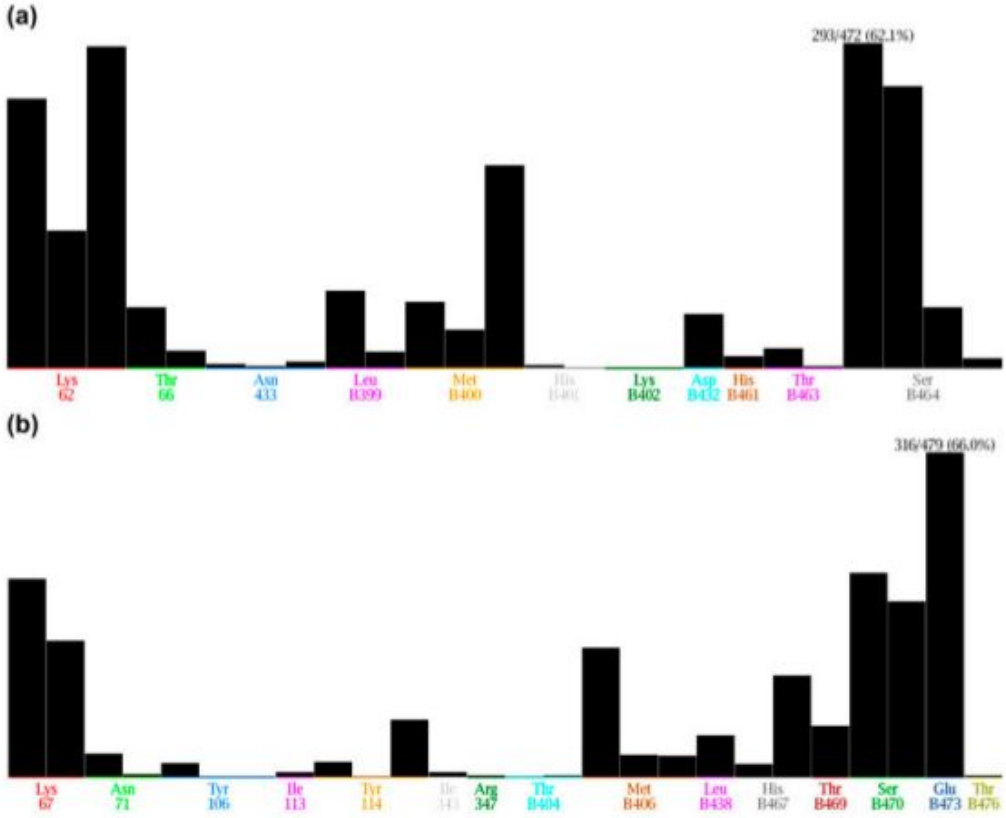

Figure 4. Histogram (Population Display) of PLIF results showing the number of ligands (*Y*-axis) with which each residue (plotted in the *X*-axis) interacts. 4(a) Population display in TR. 4(b) Population display in GR.

All other contacts of docked quinones in TR does not have a counterpart in GR and vice versa.

In the Figure 4(a) and (b), the *Y*-axis shows the relative counts for the bits, directly related with the number of contacts. For example, the **Lys62** has the three higher bars and that means that this amino acid makes three kinds of contacts with the most of quinones. On the contrary, Asn433 has three bars with very low *Y*-value meaning that it forms three different and nonfrequent contacts.

Lys62 is of most importance for the TR binding and is evidenced by the three columns in the Figure 3(a). In the case of GR, Lys67 forms hydrogen bonds with all the analyzed quinones evidenced by the two columns if the Figure 3(b). Even if the mammalian enzyme offers a more electrostatic region to binding and that the Lys62 is conserved in GR, some selectivity for TR could be evidenced by an increased number of contacts.

Leu399′ in TR is a contact detected for quinones that is a nonconserved residue in GR (Met406′). This contact seems to be important to the pose of quinones in the TR. However, Met406′ makes more contacts in GR than Leu399′ in TR, allowing to conclude that both residues are of similar important in the TR or GR binding.

The **Met400′** in TR appears, as a surface contact in the PLIF analysis for **Nq-h**, Qq-d, and Fq-b and it is absent as contact in GR. For this reason, we could propose this contact as important for the TR specificity (TRS). This residue deserved special consideration in the interaction analysis of quinones by de Molfetta, de Freitas, da Silva, and Montanari (2009).

Referring the contact with **Ser464′** in TR (Ser470′ in GR), it appears more frequently in TR than in GR as an important H-bonding interaction in the PLIF analysis.

In GR (Figure 4(b)), there is a differential contact found in the **Glu473′** (not present in TR) giving to this environment the electrostatic differential characteristic pointing to a selective binding in favor of TR.

3.4.1.2. PLIF-ContactMap and PLIF-HeatMap. The PLIF-ContactMap and the PLIF-HeatMap were created from the PLIF analysis as an ad hoc designed tool to observe all docked conformations by means of a colorful image of binding in TR and GR that confirmed and completed the previous observations. They are presented

in the Table 5 and in the Supplementary Material Table B.

In the case of PLIF-ContactMap, to each given contact, it was assigned a number representing the percentage of conformers of a quinone making a contact with a given amino acid in TR or GR. For data visualization, the numbers of contacts were highlighted by means of a color gradient from dark red (100%) to light blue (4%). The result is shown in the Table 5 (PLIF-ContactMap). Alternatively, the percentage of contacts was associated with the intensity of the color from dark to light red (PLIF-HeatMap).

Lys62 in TR makes two kinds of H-bond acceptor and surface contacts with high percentage of conformations making contacts (e.g. 64% for **Nq-h**). **Met400′** has unique and colorful annotations in TR representing the contacts made by a high percentage of quinones conformations (e.g. 55% for **Nq-h**). Finally, higher percentage of conformations make four kind of contacts (two H-bond side-chain acceptor and two backbone H-bond acceptor) with **Ser 464′** in TR (e.g. 69% for **Nq-d**). The PLIF-HeatMap (Supplementary Material Table B) presents a similar picture.

3.4.2. Analysis of docking in the alternatives binding sites

When the interface site was selected in the TR (Supplementary Material Table A), all quinones finally were posed near the catalytic site, indicating a tendency to bind in this subsite (Supplementary Material Figure IV). However, when the same strategy was used for GR, it is noticeable that all quinones were placed in the middle of the interface site (Supplementary Material Figure IV). Earlier studies in GR (Karplus & Schulz, 1989) shown that a putative site with allosteric properties placed in the dimer interface should be considered as a putative-binding site. Tridimensional and molecular dynamics analysis (Hikichi et al., 1995) show that the GR dimer interface is quit adequate to lodge planar molecules as they are too the aryloxy-quinones here studied. However, if we take into account the scoring obtained for all of assayed sites, the dimer interface seems not to be the best for binding.

When the NADPH was used to center a putative binding site (Supplementary Material Table A), in the case of TR the scores of all quinones ranked in lower values than in the aryloxy-quinones site near the catalytic one described in the 3.4.1 Section. In principle, then, the NADPH site could be not considered as a secondary one for binding and for inhibition, remaining as more relevant the binding near the catalytic site. On the contrary, in the GR enzyme, it seems to be a site with similar "appealing" for quinones than the active site, with similar scores for both sites. Any case, the NADPH site in GR seems to be a good alternative for binding. This result is in agreement with previous observations (Karplus et al., 1989). Then, for a molecule with a high binding energy either in the catalytic or the NADPH site in GR, it will be predictable a nonselective in TR inhibition.

3.4.3. 3D Graphical analysis and modeling

3.4.3.1. Putative modeling of selective TR inhibitors. Taking the observations related to the catalytic and the NADPH sites together, it could be suggested that if a quinone must be designed as a noncompetitive TR inhibitor, it must be bound near the catalytic site for TR but allowing the nonproducing posing of TS_2. In addition, this compound must have low binding energies in the catalytic either the NADPH GR sites.

In the Figure 5, an hypothetical complex of a TR with **Nq-h** posed near the catalytic site (as described in the 3.4.1 Section) with the cocrystallized TS_2 in the crystallographic pose is shown. The TR-TS_2-**Nq-h** energy minimized model was used as putative virtual complex to show that there is enough room inside the catalytic site to lodge the TS_2 and the inhibitors. Furthermore, this model could agree with a noncompetitive inhibition.

Based again in our results, to add selectivity against GR, it will be necessary that the quinone, even if it will be posed in the NADPH site or in the catalytic site, the bound will be so weak to no interfere with the GR activity. This is being sustained, for example in the case of **Nq-h**, by a low GR score, concomitantly with a very low GR inhibition capacity.

Moreover, if the aim of an anti-Chagasic drug should be to design optimal and selective TR inhibitors with maximal trypanocidal activity, structures like that of **Nq-h** could be used as leads to the improvement of the design.

3.4.3.2. Graphical analysis of best and selective TR inhibitors and comparison with the best trypanocidal assayed quinonic compounds. In the Table 3, we add three more columns containing the score in TR and GR, and finally, the ratio between both measurements (TR/GR) as a theoretical determination of the TRS.

If we take as good specificity a ratio over 1.1, the prediction of the TRS is that **Nq-h** and **Nq-g** are selective, and all other naphthoquinones are nonselective. We were successful into predict two of three TR selective inhibitors, and all (7) nonselective TR inhibitors. It was just only one failure into predict the **Nq-d** as nonselective (being selective). In view of this result, we could be confident that the *in silico* methods have a very good capacity to predict if a molecule will be a selective TR inhibitor and to give an atomic description of the interaction.

Table 5. PLIF-ContactMap: Contact percentage detected by PLIF between a given aminoacid and all conformers of each quinone in TR and GR. *X*-Axis: TR (grey) and GR (yellow) contact codes are detailed: Side chain H-acceptor (ChAcc), Backbone H-acceptor (BkAcc), and Surface contact (Surf). Blocks are colored by means of a color gradient from blue (low percentage of contact) to red (high percentage of contact). Red blocks indicate a highly frequent contacts. Black frames were used to groupe similar residues in TR/GR. *Y*-axis: aryloxy-quinones set.

TR	GR	Lys62			Lys67		Thr66		Asn71		Tyr106			Ile113	Tyr114			Ile343	Arg347	Asn433			Leu399'		Met406'			Met400'			His401'		Thr404'		Lys402'		Asp432'	Leu483'	His461'		His467'		Thr463'		Thr469'	Ser464'				Ser470'			Glu473'	Thr476'
Molecule		Ch Ac c1	Ch Acc 2	Surf	Ch Ac c1	Ch Acc 2	Ch Acc 1	Ch Acc 2	Ch Acc 1	Ch Acc 2	Ch Ac c1	Ch Ac c2	Surf		Ch Ac c1	Ch Ac c2	Surf			Ch Ac c1	Ch Ac c2	Surf	Bk Acc 1	Bk Ac c2	Bk Ac c1	Bk Ac c2	Surf	Bk Ac c1	Bk Ac c2	Surf	Ch ChA cc1	Ac c2	Bk Acc	Su rf	Ch Ac c1	Ch Ac c2	Surf	Surf	Ch Ac c1	Ch Ac c1	Ch Ac c2	Bk Acc 1	Bk Ac c2	Bk Ac c1	Ch ChA cc1	Ac c2	Bk Acc	Bk Acc	Ch Ac c1	Ch Acc 2	Surf		Ch Ac c1
Nq-a		50	28	44	27	27	22	22	13	0	0	0	0	0	0	0	0	0	0	0	0	6	17	0	33	7	0	17	6	28	0	0	0	0	0	0	0	7	0	7	0	0	0	0	61	61	11	0	40	33	60	0
Nq-b		48	22	52	36	21	9	4	14	0	0	0	0	0	0	0	0	0	0	0	0	0	17	9	21	0	0	13	9	22	0	0	0	0	0	0	9	7	9	0	14	0	0	0	65	61	13	0	36	36	57	0
Nq-c		52	26	83	38	33	4	0	0	0	5	5	0	0	5	0	10	0	0	0	0	4	13	4	19	0	10	9	4	39	0	0	0	5	0	0	13	0	0	0	19	13	0	5	65	52	9	0	43	38	57	0
Nq-d		54	15	46	44	19	15	8	25	0	6	0	0	0	0	0	0	0	0	0	0	0	8	0	25	0	0	8	8	46	8	0	0	0	0	0	15	25	0	0	0	0	0	13	69	62	8	0	44	38	63	0
Nq-e		64	14	64	40	33	21	7	7	0	0	0	0	0	0	0	0	0	0	7	7	0	7	0	27	0	0	7	7	43	0	0	0	0	0	0	14	13	0	0	13	0	0	20	71	71	21	0	47	40	67	0
Nq-f		50	6	88	33	28	6	0	0	0	0	0	0	6	6	6	11	0	0	6	0	6	6	0	28	0	6	13	0	56	0	0	0	0	0	0	19	0	0	0	17	13	6	17	75	69	13	6	33	33	61	0
Nq-g		44	28	39	32	21	11	6	16	0	5	0	0	0	0	0	26	0	5	0	0	0	33	6	11	0	0	17	11	39	0	0	0	0	0	0	6	11	17	5	37	6	0	0	33	28	6	0	42	42	63	0
Nq-h		36	27	64	18	18	9	9	0	0	6	0	0	0	0	0	29	6	0	5	0	0	18	5	12	0	0	9	5	55	0	0	0	0	5	5	18	0	5	0	29	9	0	0	27	18	9	0	29	29	82	0
Nq-i		50	15	75	53	41	0	0	6	0	0	0	0	0	0	0	0	0	0	0	0	0	10	0	35	0	0	5	5	45	0	0	0	0	0	0	10	47	0	6	6	5	0	0	65	50	15	0	65	53	65	0
Nq-j		38	25	81	33	22	13	6	0	0	6	0	0	0	0	0	11	0	0	6	6	0	0	0	33	17	0	0	0	81	0	0	0	0	0	0	13	6	0	6	17	6	0	22	69	50	19	0	28	28	67	0
Qq-a		54	23	38	43	29	23	8	7	0	0	0	0	0	0	0	0	0	0	0	0	0	8	0	43	14	0	15	8	23	0	0	0	0	0	0	8	0	0	7	7	8	0	7	85	77	8	0	50	36	57	0
Qq-b		56	33	56	50	45	11	0	0	0	5	0	0	0	5	0	5	0	0	0	0	0	28	11	10	0	5	22	17	17	22	0	0	0	0	0	0	5	0	0	20	0	6	10	0	61	50	6	55	45	50	0
Qq-c		60	60	40	45	27	10	0	9	0	0	0	0	0	0	0	0	0	0	0	0	0	20	10	18	9	9	10	10	10	0	0	0	0	0	0	0	0	10	9	27	0	0	0	70	70	0	0	36	36	45	0
Qq-d		50	38	63	38	15	0	0	8	0	0	0	0	8	0	0	8	0	0	0	0	0	19	13	31	0	8	13	6	13	0	0	0	0	0	0	0	8	13	0	38	6	0	0	56	50	13	0	23	23	46	0
Qq-e		55	30	55	38	29	10	0	0	0	0	0	0	0	0	0	14	0	0	0	0	0	15	0	19	5	14	10	10	20	0	0	5	5	0	0	0	5	0	0	33	0	0	0	50	45	5	0	38	38	62	0
Qq-f		35	24	65	39	22	24	6	11	0	6	0	0	0	17	0	17	6	0	0	0	0	18	6	17	0	0	29	12	59	0	0	0	0	0	0	24	11	0	0	22	6	0	0	35	24	18	6	44	39	50	6
Qq-g		33	28	44	28	22	6	0	6	0	6	0	0	0	17	6	22	0	0	0	0	0	28	6	22	0	0	6	6	44	0	0	0	0	0	0	6	6	11	0	22	11	0	0	33	33	0	0	33	28	72	0
Qq-h		41	18	71	53	47	0	0	0	0	0	0	0	0	0	0	0	0	0	0	0	6	12	0	33	0	0	6	6	41	6	0	0	0	0	0	24	33	0	0	13	0	0	7	53	47	6	0	67	47	53	0
Qq-i		72	44	67	47	42	6	6	5	5	0	0	0	5	5	0	16	0	0	0	0	6	17	0	21	0	0	17	17	44	0	0	0	0	0	0	17	11	0	5	21	0	0	5	50	39	11	0	68	63	63	0
Fq-a		69	31	46	43	21	0	0	0	0	0	0	0	0	0	0	0	0	0	0	0	0	23	0	50	7	7	23	15	8	0	0	0	0	0	0	8	0	0	0	7	0	0	14	77	62	8	0	43	29	71	0
Fq-b		76	18	59	43	43	0	0	0	0	7	0	0	0	0	0	0	0	0	0	0	0	12	0	21	0	0	18	12	18	0	0	0	0	0	0	18	0	0	0	14	0	0	0	71	59	6	0	50	43	71	0
Fq-c		76	35	82	50	44	18	0	0	0	0	0	0	0	6	0	6	6	0	0	0	0	18	0	31	6	0	6	6	29	0	0	0	0	0	0	6	0	0	0	38	0	0	13	71	65	12	0	50	50	69	0
Fq-d		50	33	58	50	36	33	8	0	0	7	0	0	0	0	0	7	0	0	0	0	0	0	0	29	7	0	8	0	50	0	0	0	0	0	0	8	14	0	7	14	0	0	29	100	83	17	8	50	36	86	0
Fq-e		53	29	71	38	19	18	6	5	5	5	0	0	0	0	0	19	0	0	0	0	0	0	0	33	10	5	12	0	53	0	0	0	0	0	0	12	5	0	10	24	0	0	24	88	82	24	12	33	29	76	0
Fq-f		50	8	67	65	25	17	0	0	0	0	0	0	5	0	0	0	0	0	0	0	0	0	0	35	10	30	8	0	50	0	0	0	0	0	0	8	0	0	0	15	8	0	30	83	83	25	8	35	25	70	0
Fq-g		53	29	65	37	16	18	6	5	5	5	0	0	0	5	0	32	5	0	0	0	0	41	0	26	0	0	29	18	29	0	0	0	0	0	0	6	21	0	0	16	0	0	11	71	53	6	6	32	26	89	0
Fq-h		50	39	39	30	17	22	0	0	0	9	0	4	4	13	0	43	0	4	0	0	0	11	6	22	9	4	11	6	44	0	0	0	0	0	0	17	4	0	9	39	0	0	17	56	44	6	0	30	17	83	4
Fq-i		37	16	95	47	21	16	0	5	0	0	0	0	0	0	0	16	5	0	0	0	5	5	5	42	26	16	11	5	63	5	5	0	0	0	0	11	5	0	5	37	5	5	37	79	79	37	11	37	37	74	0

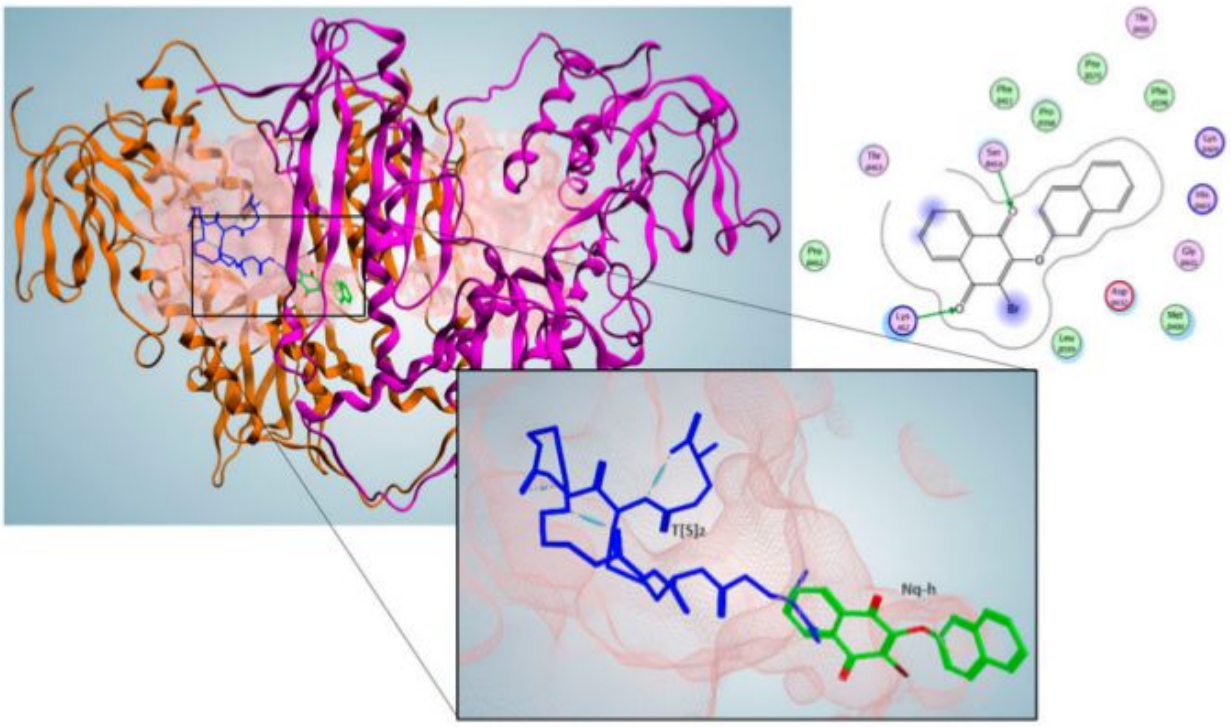

Figure 5. Putative complex TR-TS_2-**Nq-h**.
Notes: Top: Trypanothione reductase draw of backbone in orange and magenta ribbons. A dotted light pink surface is showing the catalytic site and interface sourroundings. A black rectangle is amplified in the middle: the TS_2 is shown in blue rods. The **Nq-h** quinone is shown in green rods. Right: 2D picture of the ligand interactions analysis showing the contacts made by **Nq-h** in TR. Green arrows indicate H-bond side-chain interactions. Blue light shadows are places where there is ligand exposition.

Nq-g, **Nq-d**, and **Nq-h** were further analyzed and shown in the Figures 6 and 7 (TR and GR, respectively). To do that, further energy minimization was done for the six complexes of those molecules docked in the TR and GR. The fact that – as it is clear in the Figure 6 – the place occupied by quinones in the docking is in the binding site of one of the carboxylate moieties of trypanothione, could have the meaning that the anchorage of the TS_2 in the presence of the quinones is prevented, generating a bad and nonproductive linkage.

The Figure 6(d) shows clearly that the Lys62, Met400′, and Ser464′ are the most frequent and intense contacts for a TR-specific binding. This conclusion reinforce the massive observations (PLIF analysis) made in the Section 3.4.1.

To compare with another interesting molecule with low score free energy to TR, we analyzed the **Nq-b**, the best trypanocidal molecule with low toxicity in the J-774 cells. In it best pose in TR, the nitro phenyl group is placed in the same region that the quinone ring in the **Nq-h** being the **Nq-b** quinone ring redirected toward the interface. The low score obtained for this **Nq-b** pose indicated that the nitro group, with its charge localized in the nitrogen and oxygen atoms, is not adequate to bound this region in which the Lys62 and the Ser464′ are sustaining the quinone rings of three best and specific TR ligand quinones above-mentioned (**Nq-h**, **Nq-g**, and **Nq-d**). The difference in the charge distribution (very concentrate in the nitro group and polarized in the oxygens of quinone rings) must be the key to understand the difference in their TR activity. Then, the same key moiety, which gave best trypanocidal activity to the quinones (a naphthoquinone with a nitrophenyl group), seems to be the responsible for a weak union to TR, making this design not corresponding to a selective TR inhibitor. In summary, we are showing that the action mechanism of naphthoquinones with a nitro group in it structure, making these molecules the best design for a nontoxic and trypanocidal compounds is not associated with the TR-selective inhibition. Moreover, the lack of TRS could be explained too taking into account the global electrostatic charge of both TR and GR catalytic sites. The GR-catalytic site has a global negative charge, and it will be very appealing to a negative-charged nitro compound. However, the very good specific trypanocidal properties of the **Nq-b** compound is related to it good reactivity in the ROS mechanisms and some capacity to lower the toxicity with respect to nifurtimox.

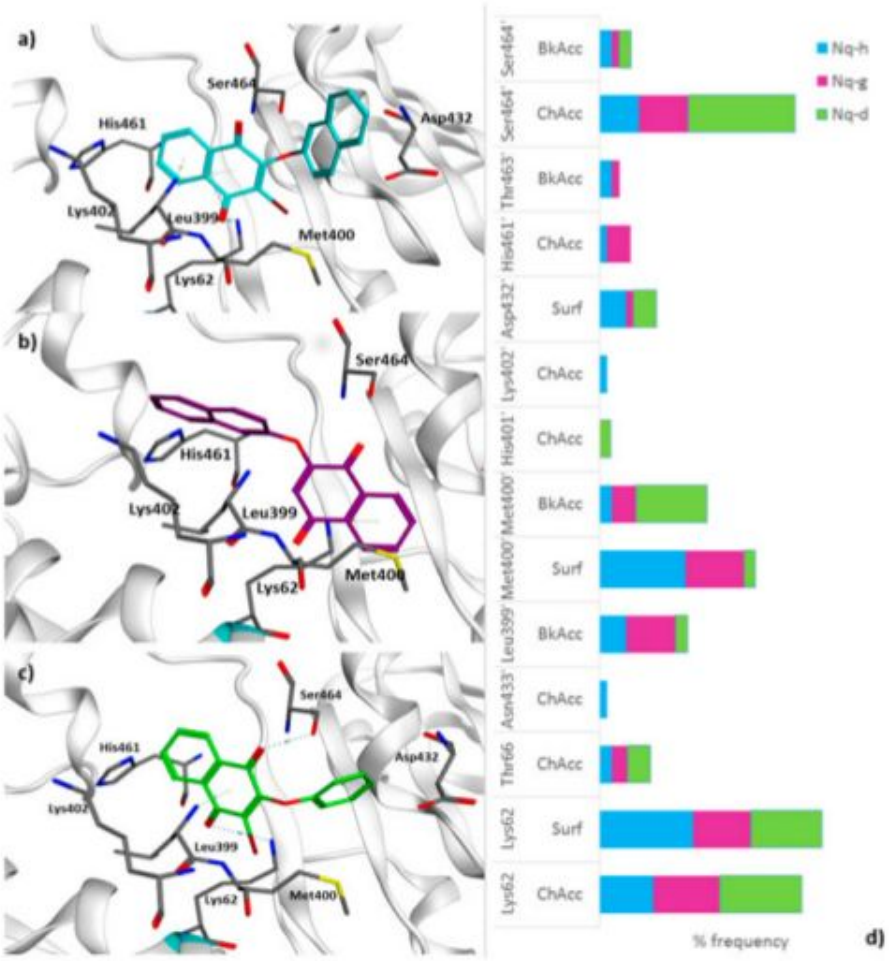

Figure 6. The best scored poses in trypanothione reductase of (a) **Nq-h** (cyan rods), (b) **Nq-g** (magenta rods) and (c) **Nq-d** (green rods) (d) Ligand interaction fingerprint report: Lys62: ChDon and Surf; Thr66: ChDon; Asn433′: ChDon and Surf; Leu399′: BkDon; Met400′: BkDon and Surf; His401′: ChDon; Lys402′: ChDon; Asp432′: Surf; His461′: ChDon; Thr463′: BkDon; Ser464′: BkDon and ChDon.
Notes: ChDon = sidechain atoms act as H-bond acceptors or donors. BkDon = backbone atoms act as H-bond acceptors or donors. Surf = surface contact interactions.

To associate the previous consideration with the role of different residues in the TR-selective inhibition, for the case of **Nq-h**, **Nq-g**, and **Nq-d**, we could consider for one hand (Figure 6), the presence of a network of contacts with the quinonic ring sustained by the **Lys62**, **Ser464′**, and **Leu399′** residues. The alpha naphthyl moieties (**Nq-h** and **Nq-g**) contribute to the posing and are oriented to the interface (**Nq-h**) or to the catalytic site (**Nq-g**). In the case of **Nq-d**, its phenyl moiety accomplishes with the same role posing the quinonic ring near to the Lys62, Ser464′, and Leu399′. On the other hand, the **Met400**, in the neighborhood of the bromine atoms (**Nq-h** and **Nq-g**) makes important surface contacts (Figure 6) giving better proper specificity to the TR anchorage. In the case of the nonbrominated **Nq-d**, with its quinonic ring pointing to the polar region of Met400, a backbone donor H-bonding is giving the differential contact needed to confer TRS.

Once again, it was demonstrated for one hand that a molecule containing a naphthoquinone ring together to a brominated alfa naphthoxy or phenyloxy moiety seems to be a very good model to lead the design of a trypanocidal and nontoxic antitrypanosomatid (e.g. anti-Chagas) drug. On the other hand, this pharmacological property was associated with a selective TR inhibition capacity mediated by a great number of contacts with the triad **Lys62**, **Ser464′**, and **Met400**, with the **Leu399′** accomplishing an important and subtle role in the spatial orientation inside the site.

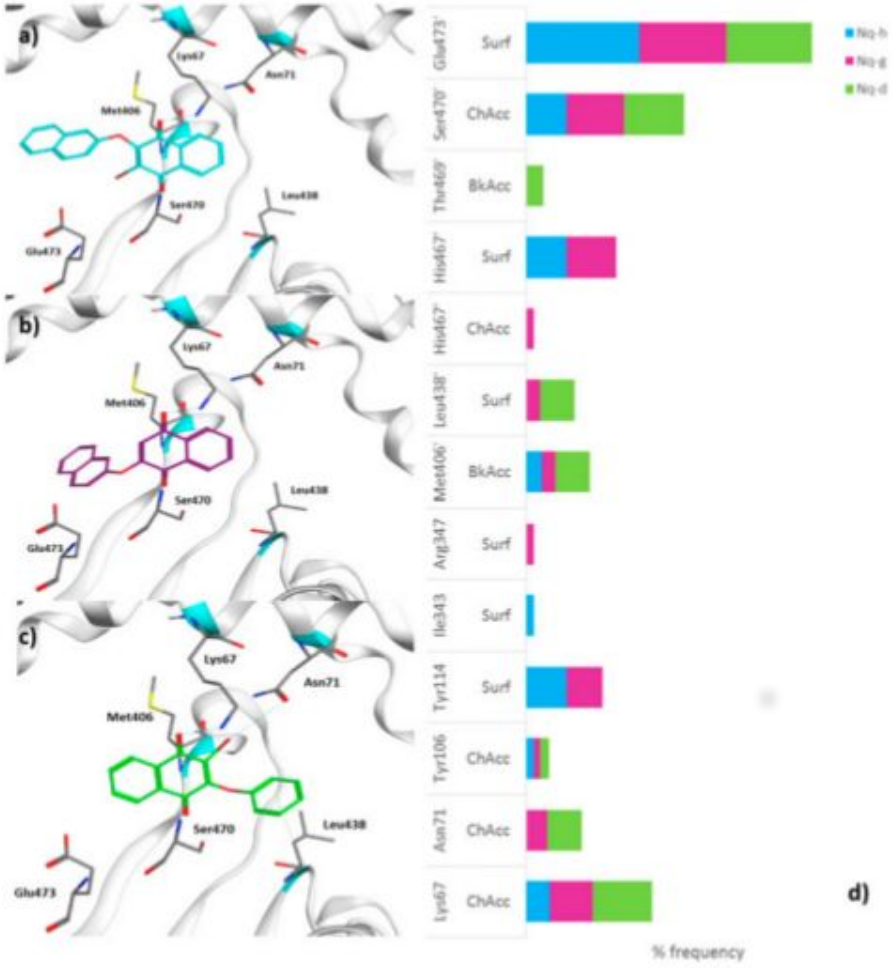

Figure 7. The best scored poses in glutathione reductase of (a) **Nq-h** (cyan rods), (b) **Nq-g** (magenta rods) and (c) **Nq-d** (green rods).
Notes: Ligand interaction fingerprint report: Lys67(Lys62 in TR): ChDon; Asn71(Thr66 in TR): ChDon, Tyr106: ChDon; Tyr114: Surf; Ile343: Surf; Arg347: Surf; Met406′ (Leu399′ in TR): BkDon; Leu438′ (Asp432′ in TR): Surf; His467′ (His461′ in TR): ChDon and Surf; Thr469′ (Thr463′ in TR): BkDon; Ser470′ (Ser464′ in TR): BkDon; Glu473′: Surf. Note that these quinones have no interaction with Ile113, Thr404′, Thr476′. ChDon = side-chain atoms act as H-bond acceptor or donors. BkDon = backbone atoms act as H-bond acceptors or donors. Surf = surface contact interactions.

4. Conclusions

The aryloxy-quinones presented a tendency to have good docking scores in a new subsite inside the catalytic one, configuring a good model for the noncompetitive type of inhibition obtained experimentally. In this putative binding of quinones, there is enough room for the substrate trypanothione that would be anchored but in a way that would interfere with the overall catalysis.

In the TR aryloxy-quinones-binding site, the main contacts were detected with Lys62, Met400′, and Ser464′. In GR, a similar sub site was occupied by quinones, but there is a differential contact found in the Glu473′ giving to this environment the electrostatic differential characteristic pointing to a selective binding in favor of TR.

For most of the compounds studied, a relationship between trypanocidal activity and TR inhibition could not be observed. However, three of the naphthoquinones, namely **Nq-h**, **Nq-g**, and **Nq-d**, proved the hypothesis of a relationship between a good and nontoxic activity in *T. cruzi,* accompanied with low toxicity in mammalian cells associated with a specific TR inhibition.

Overall, our studies provided a more thorough understanding of the experimental trypanocidal results and revealed for selected compounds TR/GR as key enzymes in the action mechanisms of some aryloxy-quinones.

Interaction with other cellular targets cannot be discarded. Evidence for this is the very good and non-toxic activity of **Nq-b**, a nitro compound. A promising

approach to optimize these compounds are *in silico* techniques such as for example the reverse docking that allows to find other targets that could contribute to the aryloxy-quinones trypanocidal action. A strategy involving the cycles of biochemical, parasitological and *in silico* assays, appears to be the best strategy for compound optimization and required to reach the final goal of a new anti-Chagas nontoxic drugs.

Abbreviations

TS_2	bis(gamma-glutamyl-cysteinyl-glycinyl) spermidine
RGS	4-*N*-malonyl cysteinyl-2,4-diaminobutyrate disulfide
DMSO	Dimethyl sulfoxide
ROS	Reactive oxygen species
TR	Trypanothione reductase
GR	Glutathione reductase
MMFF94x	Merck Molecular Force Field
PLIF	Protein–ligand interaction fingerprints
PDB	Protein data bank
MOE	Molecular-operating environment
ps	Picosecond
FAD	Flavin adenine dinucleotide
NADPH	Nicotinamide adenine dinucleotide phosphate
RMS	Root mean square

Supplementary material

The supplementary material for this paper is available online at http://dx.doi.org/10.1080/07391102.2016.1195283.

Acknowledgements

We are grateful to PEDECIBA-UDELAR Master in Bioinformatics ANII-Uruguay. KV thanks to PROMEP-México. CS thanks to financial support from FONDECYT. Authors are very grateful to Professor Dr R. Luise Krauth-Siegel (Biochemie-Zentrum der Universität Heidelberg (BZH)) for her valuable comments and technical and academic support in the TR assays.

Disclosure statement

No potential conflict of interest was reported by the authors.

Funding

This work was supported by the PROMEP-México [grant number 103.5-10-5345]; FONDECYT [Research grant number 1120128].

References

Benites, J., Valderrama, J. A., Bettega, K., Pedrosa, R. C., Calderon, P. B., & Verrax, J. (2010). Biological evaluation of donor-acceptor aminonaphthoquinones as antitumor agents. *European Journal of Medicinal Chemistry, 45*, 6052–6057. doi:10.1016/j.ejmech.2010.10.006

Berkholz, D. S., Faber, H. R., Savvides, S. N., & Karplus, P. A. (2008). Catalytic cycle of human glutathione reductase near 1 Å resolution. *Journal of Molecular Biology, 382*, 371–384. doi:10.1016/j.jmb.2008.06.083

Bern, C. (2011). Antitrypanosomal therapy for chronic Chagas' disease. *New England Journal of Medicine, 364*, 2527–2534. doi:10.1056/NEJMct1014204

Bern, C., Montgomery, S. P., Herwaldt, B. L., Rassi, A., Jr, Marin-Neto, J. A., Dantas, R. O., … Moore, A. C. (2007). Evaluation and treatment of Chagas disease in the United States. *JAMA, 298*, 2171–2181. doi:10.1001/jama.298.18.2171

Bilzer, M., Krauth-Siegel, R. L., Schirmer, R. H., Akerboom, T. P. M., Sies, H., & Schulz, G. E. (1984). Interaction of a glutathione S-conjugate with glutathione reductase kinetic and X-ray crystallographic studies. *European Journal of Biochemistry, 138*, 373–378. doi:10.1111/j.1432-1033.1984.tb07925.x

Bond, C. S., Zhang, Y., Berriman, M., Cunningham, M. L., Fairlamb, A. H., & Hunter, W. N. (1999). Crystal structure of *Trypanosoma cruzi* trypanothione reductase in complex with trypanothione, and the structure-based discovery of new natural product inhibitors. *Structure, 7*, 81–89. http://dx.doi.org/10.1016/S0969-2126(99)80011-2

Carraro, R., Iribarne, F., & Paulino, M. (2016). Analysis of cyclosporin A and a set of analogs as inhibitors of a *T. cruzi* cyclophilin by docking and molecular dynamics. *Journal of Biomolecular Structure & Dynamics, 34*, 399–413.http://doi.org/10.1080/07391102.2015.1038584

Comini, M. A., Dirdjaja, N., Kaschel, M., & Krauth-Siegel, R. L. (2009). Preparative enzymatic synthesis of trypanothione and trypanothione analogues. *International Journal for Parasitology, 39*, 1059–1062. doi:10.1016/j.ijpara.2009.05.002

de Molfetta, F. A., de Freitas, R. F., da Silva, A. B., & Montanari, C. A. (2009). Docking and molecular dynamics simulation of quinone compounds with trypanocidal activity. *Journal of Molecular Modeling, 15*, 1175–1184. doi:10.1007/s00894-009-0468-3

de Paula da Silva, C. H. T., Bernardes, L. S. C., da Silva, V. B., Zani, C. L., & Carvalho, I. (2012). Novel aryl β-aminocarbonyl derivatives as inhibitors of *Trypanosoma cruzi* trypanothione reductase: Binding mode revised by docking and GRIND2-based 3D-QSAR procedures. *Journal of Biomolecular Structure & Dynamics, 29*, 702–716. http://doi.org/10.1080/07391102.2011.672633

el-Waer, A., Douglas, K. T., Smith, K., & Fairlamb, A. H. (1991). Synthesis of N-benzyloxycarbonyl-l-cysteinyl-glycine 3-dimethylaminopropylamide disulfide: A cheap and convenient new assay for trypanothione reductase. *Analytical Biochemistry, 198*, 212–216. doi:10.1016/0003-2697(91)90531-W

Fairlamb, A. H., Blackburn, P., Ulrich, P., Chait, B. T., & Cerami, A. (1985). Trypanothione: A novel bis(glutathionyl)spermidine cofactor for glutathione reductase in trypanosomatids. *Science, 227*, 1485–1487. doi:10.1126/science.3883489

Fernandez-Blanco, C., Font, G., & Ruiz, M. J. (2016). Interaction effects of enniatin B, deoxinivalenol and alternariol in Caco-2 cells. *Toxicology Letters, 241*, 38–48. doi:10.1016/j.toxlet.2015.11.005

Gonzalez-Chavez, Z., Olin-Sandoval, V., Rodriguez-Zavala, J. S., Moreno-Sanchez, R., & Saavedra, E. (2015). Metabolic control analysis of the *Trypanosoma cruzi* peroxide detoxification pathway identifies tryparedoxin as a suitable drug target. *Biochimica et Biophysica Acta (BBA) – General Subjects, 1850*, 263–273. doi:10.1016/j.bbagen.2014.10.029

Gutteridge, J. M., & Halliwell, B. (2000). Free radicals and antioxidants in the year 2000. A historical look to the future. *Annals of the New York Academy Science, 899*, 136–147. doi:10.1111/j.1749-6632.2000.tb06182.x

Halgren, T. A. (1996a). Merck molecular force field. I. Basis, form, scope, parameterization, and performance of MMFF94. *Journal of Computational Chemistry, 17*, 490–519. doi:10.1002/(SICI)1096-987X(199604)17:5/6<490:AID-JCC1>3.0.CO;2-P

Halgren, T. A. (1996b). Merck molecular force field. V. Extension of MMFF94 using experimental data, additional computational data, and empirical rules. *Journal of Computational Chemistry, 17*, 616–641. doi:10.1002/(SICI)1096-987X(199604)17:5/6<616:AID-JCC5>3.0.CO;2-X

Henry, T. R., & Wallace, K. B. (1996). Differential mechanisms of cell killing by redox cycling and arylating quinones. *Archives of Toxicology, 70*, 482–489. doi:10.1007/s002040050302

Hikichi, N., Paulino, M., Hansz, M., & Tapia, O. (1995). A molecular dynamics study of glutathione reductase. *Journal of Molecular Structure: THEOCHEM, 335*, 243–254. doi:10.1016/0166-1280(94)04005-D

Hoelz, L. V. B., Leal, V. F., Rodrigues, C. R., Pascutti, P. G., Albuquerque, M. G., Muri, E. M. F., & Dias, L. R. S. (2015). Molecular dynamics simulations of the free and inhibitor-bound cruzain systems in aqueous solvent: Insights on the inhibition mechanism in acidic pH. *Journal of Biomolecular Structure & Dynamics*, 1–10. http://doi.org/10.1080/07391102.2015.1100139

Iribarne, F., Paulino, M., Aguilera, S., & Tapia, O. (2009). Assaying phenothiazine derivatives as trypanothione reductase and glutathione reductase inhibitors by theoretical docking and molecular dynamics studies. *Journal of Molecular Graphics and Modelling, 28*, 371–381. doi:10.1016/j.jmgm.2009.09.003

Iribarne, F., Paulino, M., Aguilera, S., Murphy, M., & Tapia, O. (2002). Docking and molecular dynamics studies at trypanothione reductase and glutathione reductase active sites. *Journal of Molecular Modeling, 8*, 173–183. doi:10.1007/s00894-002-0082-0

Janes, W., & Schulz, G. E. (1990). The binding of the retro-analogue of glutathione disulfide to glutathione reductase. *Journal of Biological Chemistry, 265*, 10443–10445. doi:10.2210/pdb4gr1/pdb

Karplus, P. A., & Schulz, G. E. (1987). Refined structure of glutathione reductase at 1.54 Å resolution. *Journal of Molecular Biology, 195*, 701–729. doi:10.2210/pdb3grs/pdb

Karplus, P. A., & Schulz, G. E. (1989). Substrate binding and catalysis by glutathione reductase as derived from refined enzyme: Substrate crystal structures at 2 Å resolution. *Journal of Molecular Biology, 210*, 163–180. doi:10.1016/0022-2836(89)90298-2

Karplus, P. A., Pai, E. F., & Schulz, G. E. (1989). A crystallographic study of the glutathione binding site of glutathione reductase at 0.3-nm resolution. *European Journal of Biochemistry, 178*, 693–703. doi:10.1111/j.1432-1033.1989.tb14500.x

Kovacic, P. (2007). Unifying mechanism for anticancer agents involving electron transfer and oxidative stress: Clinical implications. *Medical Hypotheses, 69*, 510–516. doi:10.1016/j.mehy.2006.08.046

Labute, P. (2010). LowModeMD—implicit low-mode velocity filtering applied to conformational search of macrocycles and protein loops. *Journal of Chemical Information and Modeling, 50*, 792–800. doi:10.1021/ci900508k

Manoel-Caetano Fda, S., & Silva, A. E. (2007). Implications of genetic variability of *Trypanosoma cruzi* for the pathogenesis of Chagas disease. *Cadernos de Saúde Pública, 23*, 2263–2274. doi:10.1590/S0102-311X2007001000002

Maran, E., Fernandez, M., Barbieri, P., Font, G., & Ruiz, M. J. (2009). Effects of four carbamate compounds on antioxidant parameters. *Ecotoxicology and Environmental Safety, 72*, 922–930. doi:10.1016/j.ecoenv.2008.01.018

Molina, I., Gomez i Prat, J., Salvador, F., Trevino, B., Sulleiro, E., Serre, N., … Pahissa, A. (2014). Randomized trial of posaconazole and benznidazole for chronic Chagas' disease. *New England Journal of Medicine, 370*, 1899–1908. doi:10.1056/NEJMoa1313122

Nordhoff, A., Bucheler, U. S., Werner, D., & Schirmer, R. H. (1993). Folding of the four domains and dimerization are impaired by the Gly446–>Glu exchange in human glutathione reductase. Implications for the design of antiparasitic drugs. *Biochemistry, 32*, 4060–4066. doi:10.1021/bi00066a029

O'Brien, P. J. (1991). Molecular mechanisms of quinone cytotoxicity. *Chemico-Biological Interactions, 80*, 1–41. doi:10.1016/0009-2797(91)90029-7

Pai, E. F., & Schulz, G. E. (1983). The catalytic mechanism of glutathione reductase as derived from x-ray diffraction analyses of reaction intermediates. *Journal of Biological Chemistry, 258*, 1752–1757. Retrieved from http://www.jbc.org/content/258/3/1752.abstract#cited-by

Pai, E. F., Karplus, P. A., & Schulz, G. E. (1988). Crystallographic analysis of the binding of NADPH, NADPH fragments, and NADPH analogues to glutathione reductase. *Biochemistry, 27*, 4465–4474. doi:10.1021/bi00412a038

Paulino, M., Iribarne, F., Dubin, M., Aguilera-Morales, S., Tapia, O., & Stoppani, A. O. (2005). The chemotherapy of Chagas disease: An overview. *Mini-Reviews in Medicinal Chemistry, 5*, 499–519. doi:10.2174/1389557053765565

Paulino, M., Alvareda, E. M., Denis, P. A., Barreiro, E. J., Sperandio da Silva, G. M., Dubin, M., … Tapia, O. (2008). Studies of trypanocidal (inhibitory) power of naphthoquinones: Evaluation of quantum chemical molecular descriptors for structure–activity relationships. *European Journal of Medicinal Chemistry, 43*, 2238–2246. doi:10.1016/j.ejmech.2007.12.023

Persch, E., Bryson, S., Todoroff, N. K., Eberle, C., Thelemann, J., Dirdjaja, N., … Diederich, F. (2014). Binding to large enzyme pockets: Small-molecule inhibitors of trypanothione reductase. *ChemMedChem, 9*, 1880–1891. doi:10.1002/cmdc.201402032

Prati, F., Bergamini, C., Molina, M. T., Falchi, F., Cavalli, A., Kaiser, M., … Bolognesi, M. L. (2015). 2-Phenoxy-1,4-naphthoquinones: From a Multitarget Antitrypanosomal to a Potential Antitumor Profile. *Journal of Medicinal Chemistry, 58*, 6422–6434. doi:10.1021/acs.jmedchem.5b00748

Rassi, A., Jr, Rassi, A., & Marin-Neto, J. A. (2010). Chagas disease. *The Lancet, 375*, 1388–1402. doi:10.1016/S0140-6736(10)60061-X

Salas, C. O., Faundez, M., Morello, A., Maya, J. D., & Tapia, R. A. (2011). Natural and synthetic naphthoquinones active against *Trypanosoma Cruzi*: An initial step towards new drugs for Chagas disease. *Current Medicinal Chemistry, 18*, 144–161. doi:10.2174/092986711793979779

Savvides, S. N., & Karplus, P. A. (1996). Kinetics and crystallographic analysis of human glutathione reductase in complex with a xanthene inhibitor. *Journal Biological Chemistry, 271*, 8101–8107. doi:10.1074/jbc.271.14.8101

Turrens, J. F. (2004). Oxidative stress and antioxidant defenses: A target for the treatment of diseases caused by parasitic protozoa. *Molecular Aspects of Medicine, 25*, 211–220. doi:10.1016/j.mam.2004.02.021

Udatha, D. B., Sugaya, N., Olsson, L., & Panagiotou, G. (2012). How well do the substrates KISS the enzyme? Molecular docking program selection for feruloyl esterases. *Scientific Reports, 2*, 323. doi:10.1038/srep00323

Vazquez, K., Espinosa-Bustos, C., Soto-Delgado, J., Tapia, R. A., Varela, J., Birriel, E., … Salas, C. O. (2015). New aryloxy-quinone derivatives as potential anti-Chagasic agents: Synthesis, trypanosomicidal activity, electrochemical properties, pharmacophore elucidation and 3D-QSAR analysis. *RSC Advances, 5*, 65153–65166. doi:10.1039/C5RA10122K

Viotti, R., Vigliano, C., Lococo, B., Bertocchi, G., Petti, M., Alvarez, M. G., … Armenti, A. (2006). Long-term cardiac outcomes of treating chronic Chagas disease with benznidazole versus no treatment. *Annals of Internal Medicine, 144*, 724–734. doi:10.7326/0003-4819-144-10-200605160-00006

Walsh, C., Bradley, M., & Nadeau, K. (1991). Molecular studies on trypanothione reductase, a target for antiparasitic drugs. *Trends in Biochemical Sciences, 16*, 305–309. doi:10.1016/0968-0004(91)90124-E

WHO (2011). Working to overcome the global impact of neglected tropical diseases – Summary. *Releve epidemiologique hebdomadaire/Section d'hygiene du Secretariat de la Societe des Nations = Weekly epidemiological record/Health Section of the Secretariat of the League of Nations, 86*, 113–120. doi:10.1016/S0140-6736(09)61877

Woodcock, J., & Woosley, R. (2008). The FDA critical path initiative and its influence on new drug development. *Annual Review of Medicine, 59*, 1–12. doi:10.1146/annurev.med.59.090506.155819

Worthington, D. J., & Rosemeyer, M. A. (1974). Human glutathione reductase: Purification of the crystalline enzyme from erythorocytes. *European Journal of Biochemistry, 48*, 167–177. doi:10.1111/j.1432-1033.1974.tb03754.x

Yun, O., Lima, M. A., Ellman, T., Chambi, W., Castillo, S., Flevaud, L., … Palma, P. P. (2009). Feasibility, drug safety, and effectiveness of etiological treatment programs for Chagas disease in Honduras, Guatemala, and Bolivia: 10-year experience of Medicines Sans Frontiers. *PLoS Neglected Tropical Diseases, 3*, e488. doi:10.1371/journal.pntd.0000488

Capítulo 3

Identificación de blancos putativos mediante *target fishing* de naftoquinonas tripanocidas

Resumen

Meta: Proponer nuevos blancos putativos de naftoquinonas tripanocidas .

En este capítulo, se describe el uso de dos métodos de cribado virtual usados para recuperar los posibles blancos de una molécula dada (*query o "anzuelo"*). Estos métodos se fundamentan en la búsqueda de similitud estructural de la molécula dada y mapeo de farmacóforo. Para este caso, usamos como anzuelos las quinonas Nq-b y Nq-h , que como se describió en el capítulo anterior, presentan las mejores actividades tripanocidas y selectivas. De tal forma, en este apartado se estudiaron una combinación de anzuelos y de métodos, planteando así las siguientes cuatro estrategias: 1) Nq-b_Pharmmapper, 2) Nq-b_SHAFT, 3) Nq-h_Pharmmapper y 4) Nq-h_SHAFT.

Los resultados de estas estrategias fueron analizadas usando el programa R studio para la manipulación y la visualización de la información. Además, para la trazabilidad y búsqueda de información de cada blanco reportado, se realizaron consultas en las bases de datos PDB, UniProt, KEGG, STRING y TryTripDB, entre otras.

Como resultado, se muestra una serie de proteínas dónde estas moléculas pudieran generar un efecto biológico. Para visualizar mejor el listado de cada estrategia, se realizaron agrupaciones de cada conjunto de salida, según su clasificación enzimática, su ubicación en el organismo y en la célula. Además, cada uno de estos blancos fueron ubicados en los mapas metabólicos y de enfermedades para conocer su relación con alguna vía metabólica o patología clínica.

Los posibles blancos para estas naftoquinonas además de estar presentes en el metabolismo del *T. cruzi*, están ampliamente relacionadas con vías metabólicas involucradas en el tratamiento de cáncer y de otras patologías.

3.1 Introducción

En contraste con el *virtual screening* , que se utiliza para buscar grandes bibliotecas de compuestos para moléculas que tienen más probabilidades de unirse a un blanco específico, el objetivo del *reverse virtual screening*, también conocido como *target fishing* es identificar proteínas que pueden anclar o interactuar con moléculas pequeñas bioactivas usando como "anzuelo" (*query*) una molécula de consulta (Koutsoukas et al., 2011; L. Wang & Xie, 2014).

Este método computacional permite, entre otras cosas, la predicción de la bioactividad de un compuesto, la identificación del modo de acción de medicamentos conocidos, el estudio de polifarmacología de drogas (Reddy & Zhang, 2013), el reposicionamiento de medicamentos (Achenbach, Tiikkainen, Franke, & Proschak, 2011; Ashburn & Thor, 2004; Pérez-Nueno, Karaboga, Souchet, & Ritchie, 2014) o la predicción de los efectos adversos de un compuesto(Bender et al., 2007; Lounkine et al., 2012). La gran cantidad de de información almacenada en las bases de datos, permite el desarrollo de este tipo de métodos (Cereto-Massagué et al., 2015).

La "pesca de blancos" o target fishing es uno de los pasos iniciales en el desarrollo racional de un fármaco. Este procedimiento nos permite traer (de bases de datos de proteínas blanco) proteínas que pueden anclar o interactuar con moléculas pequeñas bioactivas. Además, nos permite encontrar posibles blancos no relacionados con compuestos terapéuticos (L. Wang & Xie, 2014).

En el proceso de diseño racional de fármacos, los estudios de polifarmacología son de gran interés. Este término describe la capacidad de las pequeñas moléculas para interactuar con múltiples proteínas blanco. Con el objetivo de diseñar drogas más efectivas y menos tóxicas, los métodos de *target fishing* son una forma prometedora de explorar alternativas para los medicamentos ya existentes y proponer el reposicionamiento de un medicamentos y encontrar nuevos usos para los ya conocidos (Z. Liu et al., 2013) .

3.1.1 Métodos computacionales para realizar *target fishing*

Se han desarrollado varios métodos computacionales para predecir los blancos moleculares de un compuesto (Koutsoukas et al., 2011; Varnek & Tropsha, 2008).

En una reciente revisión de estas metodologías, se muestra la tendencia por año en el uso de estas aplicaciones y de algunos de los programas representativos Figura 4. Las herramientas más usadas en estos últimos años son las que incorporan información farmacofórica y de similitud estructural, seguidas por los métodos híbridos (Huang et al., 2018).

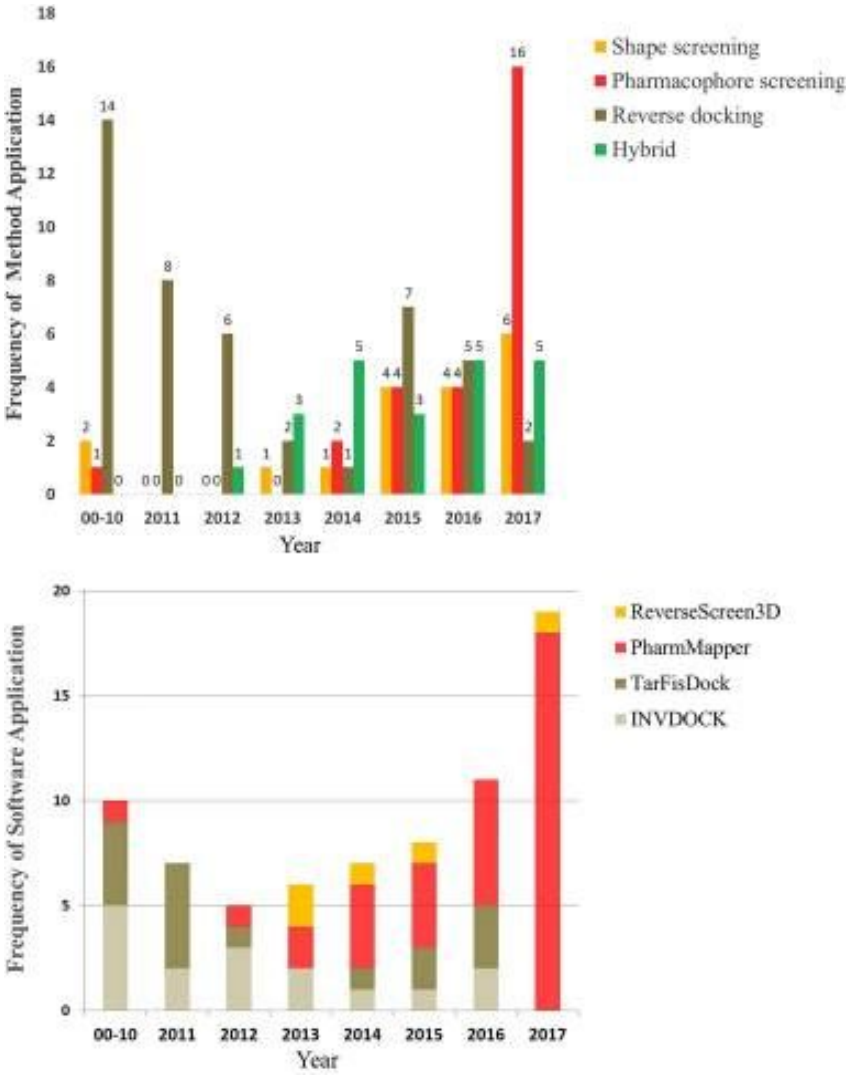

Figura 4. El número y la tendencia de las aplicaciones que utilizan los tres métodos de tamizaje reverso y el software representativo desde el año 2000.

Pharmmapper es un programa que representa a los métodos basados en farmacóforos y SHAFT es un método híbrido por que considera en su algoritmo la similitud estructural y datos farmacofóricos.

Una de las herramientas más conocidas es **PharmMapper**, un servidor de tamizaje reverso basado en el estudio de la similitud entre un ligando dado y un conjunto de modelos farmacóforicos obtenidos de las bases de datos TargetBank, BindingDB, DrugBank y PDTD (X. Wang et al., 2017).

Otro método utilizado para realizar tamizaje reverso es **SHAFTS (SHApe-FeaTure Similarity)** que tiene como objetivo encontrar blancos considerando la similitud estructural de la molécula *query* con los ligandos co-cristalizados del Protein Data Bank (X. Liu, Jiang, & Li, 2011).

SHAFTS es un método hibrido por que considera tanto la forma como las características farmacofóricas. Este algoritmo funciona enumerando todos los posibles tripletes de características de la molécula de consulta y de las conformaciones de ligandos co-cristalizados en la base de datos. Entregando como resultado, la proteína que tenga un ligando similar a la molécula dada.

3.2 Metodología

3.2.1 Selección de las moléculas *query* (anzuelos)

Las naftoquinonas Nq-b y Nq-h fueron utilizadas como molécula consulta Figura 5. Estas moléculas tienen actividades tripanocidas y de selectividad conocidas (Capítulo 2). Las estructuras fueron modeladas usando MOE 2014 y guardadas en formato mol2.

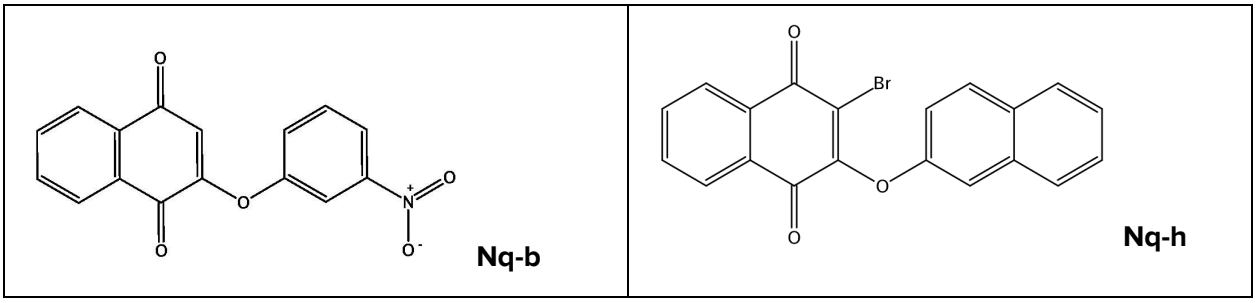

Figura 5. Estructura química de las naftoquinonas Nq-b y Nq-h

3.2.1 Predicción de blancos

El servidor PharmMapper y el algoritmo de SHAFT fueron utilizados para encontrar proteínas diana de las naftoquinonas Nq-b y Nq-h.

PharmMapper es un servidor web de acceso libre diseñado para identificar posibles blancos putativos para moléculas pequeñas dadas. (X. Wang et al., 2017) Este servidor utiliza el método de mapeo de farmacóforos altamente eficiente y robusto, y puede identificar los posibles candidatos de la base de datos en algunas horas.

PharmMapper cuenta con un amplio repertorio interno de base de datos de farmacóforos de proteínas blanco extraídos de TargetBank, DrugBank, BindingDB y PDTD.

Se utilizó la versión 2017. Esta versión aplica *Cavity1.1* para detectar los sitios de unión en la superficie de una estructura de proteína dada y los clasifica por *druggability score*. Adicional, Pharmmmapper usa un programa de modelado de farmacóforos basado en receptores llamado *Pocket 4.0* para extraer las características de los farmacóforos dentro de las cavidades de los receptores de las bases de datos. Toda esta información queda contenida en una gran base de datos llamada PharmTargetDB.

Con la versión de Pharmmapper 2017 se tiene acceso un total de 23236 proteínas que cubren 16159 modelos de farmacóforo que se pronostican como sitios de unión a fármacos y 52431 modelos de farmacóforo. En comparación con la última versión (v.2010), los modelos de farmacóforo objetivo incluidos en esta versión han aumentado más de seis veces, de 7302 a más de 53000.

Para usar el servidor PharmMapper se ingresó en formato Mol2 las naftoquinonas *query* para ser mapeadas contra todas las dianas en PharmTargetDB.

El algoritmo SHAFTS (SHApe-Feature Similarity) fue usado en su versión integrada en el servidor ChemMapper. Este algoritmo tiene como primer etapa enumerar todos los posibles tripletes de características de la molécula *query* y de las características de las moléculas asociadas a los posibles blancos. Esta información es guardada en una tabla de partición *hashing* donde la clave para la búsqueda es el tipo de vértice y la distancia entre los nodos de cada triplete. Los tripletes generados de la molécula de consulta son comparados con los guardados en la tabla de *hashing* y aquellos que tengan la misma clave son definidos como un posible alineamiento. SHAFT califica los alineamientos estructurales con base a la similitud geométrica y a la similitud farmacofórica.

Se ejecutó el algoritmo introduciendo en formato mol2 las naftoquinonas query y seleccionando como base de consulta al Protein Data Bank y usando como corte un score 1.5.

3.2.2 Clasificación de proteínas blanco

El resultado para cada método es un listado de proteínas blanco predichas para cada molécula dada. Este listado tiene como identificador el ID del PDB. Este ID puede ser convertido a un identificador UniProtKB usando el recurso *Retrieve/ID mapping* de UniProt. En esta sección se puede ingresar el listado de IDs PDB para ser buscados en la base de datos UniProt y obtener información sobre cada proteína dada.

UniProt permite darle trazabilidad a cada ID ingresado y recuperar información del subset de proteínas dadas, como ser su localización subcelular, función molecular y los procesos biológicos en los que participan estos posibles blancos.

Para lograr una manipulación y una macro visualización de ambas metodologías, se utilizó el programa *R studio* y se transformó la salida de la información en formato tablas a gráficos. Los gráficos de esta sección fueron creados usando el paquete *ggplot2* de R para mostrar el número y tipo de proteínas obtenidas para cada uno de los métodos y para cada una de las moléculas anzuelo.

Además, se usó la enciclopedia KEGG ("KEGG: Kyoto Encyclopedia of Genes and Genomes," n.d.) que reúne información sobre las vías de señalización, metabólicas y de enfermedades para ubicar y enriquecer la información sobre cada posible blanco encontrado. Finalmente, para el listado de blancos humanos encontrados se realizó un análisis de enriquecimiento funcional. Para esto se construyó una red de interacción proteína-proteína usando la base de datos STRING V10.5 Para ampliar el conocimiento de los blancos putativos se obtuvo información funcional tal como los procesos biológicos en los que participa usando *Gene Ontology*, las funciones moleculares y su ubicación en alguna ruta metabólica o de asociación con alguna enfermedad (*KEGG Pathways).*

3.2.3 Docking Molecular

Se realizó un anclaje molecular (*docking*) con el objetivo de evaluar las energías libres de unión entre los blancos parasitarios encontrados y las quinonas de estudio. El programa MOE (MOE,

2009) fue utilizado para la preparación de los receptores, ligandos, acoplamiento y análisis. Con el objetivo de ampliar las formas de unión del las naftoquinonas en los receptores se realizó un estudio conformacional usando LowModeMD, un método estocástico para la generación de conformaciones (Labute, 2010) . Para la preparación de los receptores se realizó una minimización de energía usando el campo de fuerza MMFF94x.

El protocolo de *docking* fue validado y usado anteriormente para anclar naftoquinonas (Capítulo 2). Este protocolo consistió en seleccionar como sitio de *docking* una esfera de 4.5 A cercana al ligando co cristalizado. El método de posicionamiento (*placement*) seleccionado fue alfa PMI y de puntaje (*scoring)* London dG.

3.3 Resultados y discusión

3.3.1 Predicción de blancos putativos

Usando el algoritmo SHAFT y como anzuelo a las molécula Nq-b y Nq-h, se obtuvieron 245 y 284 blancos putativos, respectivamente. Para el caso de Pharmmapper, 233 y 188 blancos fueron recuperados usando las moléculas Nq-b y Nq-h como anzuelos, respectivamente.

Para conocer si los resultados de ambas metodologías eran similares, se construyó un diagrama de Venn para identificar la intersección del conjunto de cada una de las salidas (Figura 6). Como resultados de este planteamiento, se observa que 36 proteínas fueron identificadas en ambos métodos usando como *query* a la naftoquinona Nq-b, y usando el algoritmo SHAFTS se muestra que 52 proteínas son similares en ambos conjuntos cuando el query es la naftoquinona Nq-h.

Considerando lo anterior, se recuperaron más blancos usando el algoritmo SHAFT y a la 3h como query (284 blancos) , pero no fue el mismo caso para esta molécula usando el método Pharmmapper, ya que se obtuvieron el menor número de blancos putativos para este caso (188 blancos).

Si bien, ambas metodologías tienen el objetivo de encontrar blancos a partir de una molécula dada, estas dos metodologías entregaron resultados diferentes porque ambos programas usan estrategias diferentes para encontrar un blanco. Como se mencionó el la sección de metodologías, con el algoritmo SHAFT se pueden encontrar blancos que tenga asociados a su

estructura cristalográfica un ligando similar a la molécula *query*, estos ligandos mayoritariamente se encuentran en las regiones catalíticas de las proteínas cristalizadas. En cambio, la estrategia que usa Pharmmapper está basada en el mapeo farmacóforico, es decir, usa el farmacóforo de la molécula *query* (*farmacóforo del ligando*) y la compara con la base de datos de los farmacóforos de sitio que existen en cada proteína cristalizada (*farmacóforo de receptor*).

El uso de cada metodología estará en función de lo que se quiera buscar. Para este caso , usamos las dos metodologías porque no queríamos limitarnos a encontrar blancos en los que solamente nuestros blancos pudieran tener algún efecto en las regiones catalíticas de estos, más bien, se amplió la búsqueda usando un mapeo farmacofórico para encontrar más blancos en los que nuestras moléculas pudieran generar algún efecto biológico en regiones fuera del sitio catalítico. Es decir, ampliando la posibilidad de anclaje en los bolsillos de todo el receptor y no solo en los bolsillos catalíticos de las proteínas.

Figura 6. Número de proteínas encontradas mediante los métodos de SHAFT y Pharmmapper usando como query las moléculas Nq-b y Nq-h

El cribado virtual de proteínas blanco demostró teóricamente, que las naftoquinonas Nq-b y Nq-h podrían interaccionar con diferentes enzimas tales como: hidrolasas, isomerasas, ligasas, liasas, oxidorreductasas y transferasas. Siendo para todos los casos, las transferasas, el grupo más grande de las proteínas encontradas seguido por las hidrolasas y oxidorreductasas (Figura 7).

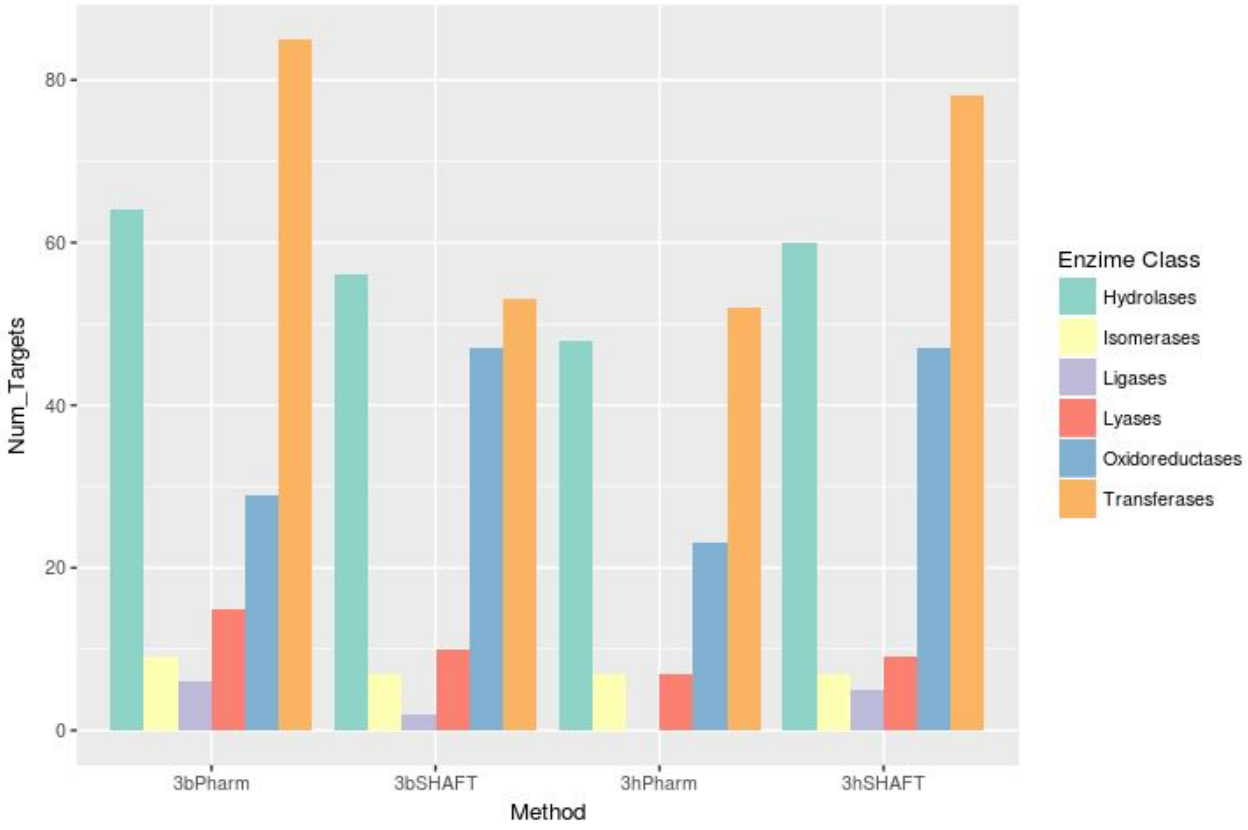

Figura 7. Clasificación enzimática de los blancos putativos obtenidos por de cribado virtual

Estas proteínas predichas como blancos se encuentran mayoritariamente en organismos eucariotes, seguido por bacterias y algunas presentes en arqueas Figura 8.

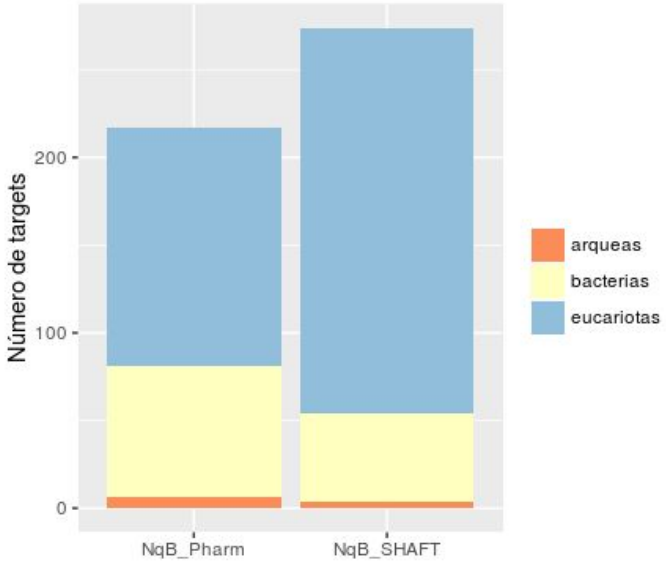

Figura 8. Número de blancos putativos encontrados en diferentes organismos

De las 233 proteínas obtenidas en Pharmmapper usando Nq-b como “anzuelo” : 51 son humanas y corresponden al 22 % de toda la salida

Este conjunto de proteínas humanas está integrado por 5 oxidorreductasas, 19 transferasas, 14 hidrolasas y 3 isomerasa. En este listado de resultados se encuentra la enzima glutatión reductasa.

Las proteínas predichas por ambos métodos constituyen mediadores bioquímicos de especial interés en funciones catalíticas y en varias vías de señalización molecular (Figura 9). Además, se pudo identificar los componente celulares en los que se encuentran este set de blancos (Figura 10). El 75% de las proteínas humanas encontradas tienen función catalítica y el 69% son citoplasmáticas.

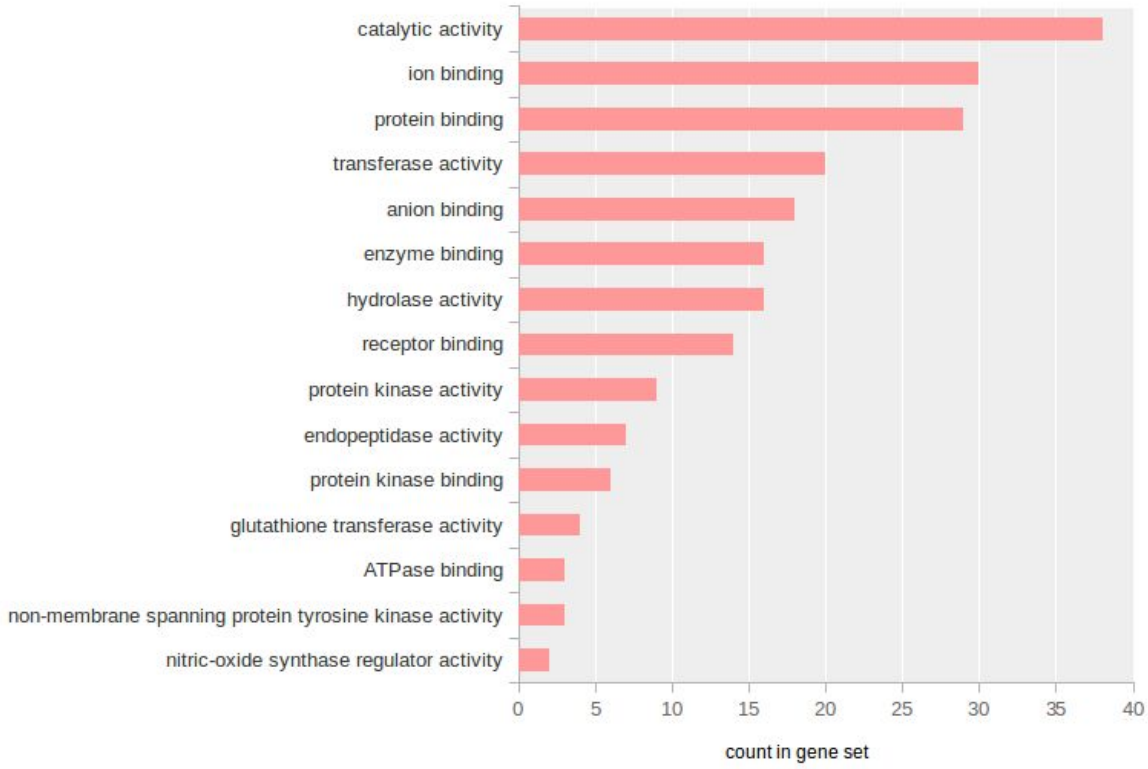

Figura 9. Clasificación en función de la función enzimática de los posibles blancos estudiado.

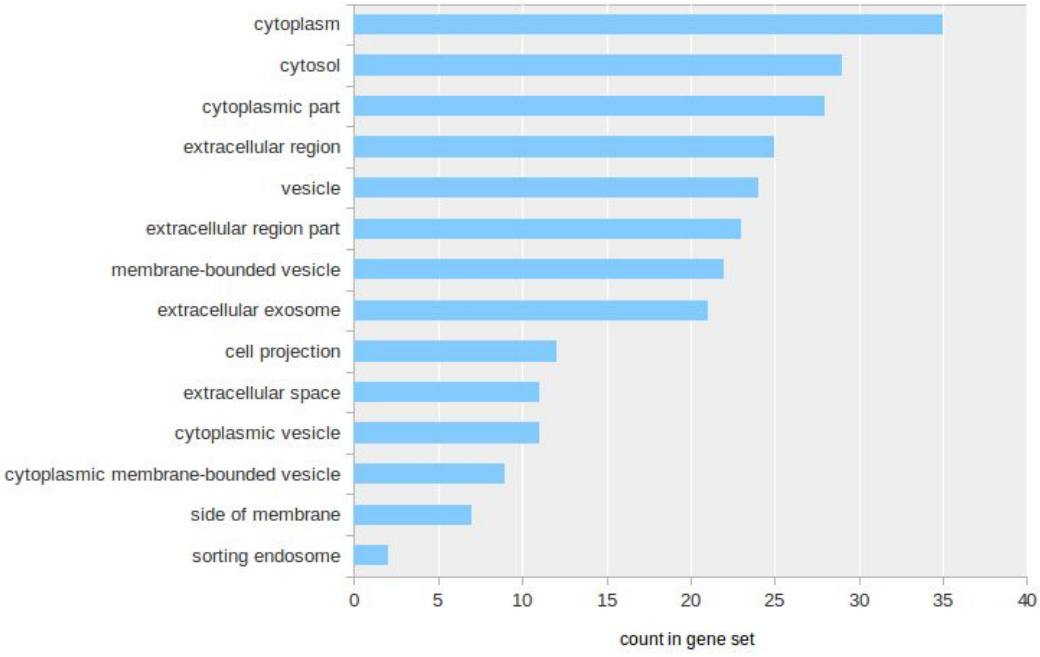

Figura 10. Ubicación de los posibles blancos estudiado en la célula.

3.3.2 Blancos putativos en *T. cruzi* obtenidos por *target fishing*

Se usó la base de datos BindingDB como recurso de comparación de los blancos obtenidos en el *target fishing*. En esta base de datos se encuentran anotados los blancos farmacológicos que se encuentran ampliamente estudiados para el desarrollo de fármacos. BindingDB cuenta con información categorizada por organismo, lo que permitió identificar que para el *T.cruzi* existen 10 blancos anotados (Tabla 1).

Con ambas estrategias (SHAFTS y Pharmmapper) y usando a la naftoquinona Nq-h como anzuelo, se recuperaron el 50% de los blancos reportados en el BindingDB. Por otro lado, usando la molécula Nq-b se obtienen mejores resultados en la pesca de proteínas del *T.cruzi*. Usando el método de SHAFTS se recuperaron sólo el 30 % y usando PharmMapper el 70% de las proteínas reportadas por Binding DB como blancos del *T.cruzi*. Es importante mencionar que con las cuatro estrategias de búsqueda, se identificó a la TR como blanco putativo para estas naftoquinonas.

De manera clara y para este caso, se puede ver que Pharmmapper reporta más blancos que SHAFTS, y usando a la molécula Nq-b de anzuelo se predicen -mejor- blancos para el *T. cruzi*

Una vez conociendo estos resultados, se realizaron estudios de anclaje molecular para conocer la afinidad de las naftoquinonas para cada uno de los blancos reportados por BindingDB y encontrados por cribado reverso.

Las energías de anclaje para estas moléculas en los receptores se encuentran resumidas en la Tabla 1. Se puede observar que el rango de energías está comprendido entre -14.81 a -7.27 kcal/mol, siendo el mejor anclaje la molécula Nq-b en el sitio catalítico de la triosafosfato isomerasa y con la energía de anclaje menor , se encuentra la interacción de las naftoquinonas en la enzima dihidroorotato deshidrogenasa.

Tabla 1. Identificación de blancos de *T.cruzi* usando cuatro estrategias de *target fishing*. Se muestran las energías de unión del anclaje molecular de naftoquinonas en los sitios catalíticos de cada blanco propuesto.

*T. cruz*i targets	Nq-h		Nq-b		Energía de unión Kcal/mol	
	SHAFTS	PharmMapper	SHAFTS	PharmMapper	Nq-b	Nq-h
6-phospho-1-fructokinase				x	-12,15	-13,23
Bifunctional dihydrofolate reductase-thymidylate synthase	x		x	x	-7,78	-7,27
Cruzipain				x	-11,08	-9,4
Farnesyl diphosphate synthase	x	x			-11,83	-13,28
Glyceraldehyde-3-phosphat e dehydrogenase		x		x	-13,42	-11,62
Hexokinase	x				-8,39	-10,11
Phosphodiesterase		x	x	x	-10,52	-10,68
Trans-sialidase	_	_	_	_	-11,09	-12,4
Triosephosphate isomerase	x	x		x	-14,81	-14,49
Trypanothione reductase	x	x	x	x	-11,7	-13,4

3.3.3 Blancos putativos humanos obtenidos por *target fishing*

Como se mencionó anteriormente , el método Nqb_Pharmmapper fue el más informativo, por tal motivo fue el seleccionado para realizar el análisis de la salida de datos relacionado a los blancos humanos.

Usando Nqb como *query* y Pharmmaper como estrategia de búsqueda, se obtuvieron 233 proteínas. De este conjunto , 51 son humanas y corresponden al 22 % de toda la salida.

Realizando consultas a la base de datos de UniProt, se encontró que las proteínas humanas de este conjunto de entrada, están relacionadas mayoritariamente en procesos de cáncer. El 35 % de los blanco putativos de la naftoquinona Nq-b están relacionados con enfermedades causadas por mutaciones y un 12 % relacionadas a protooncogenes (Figura 11).

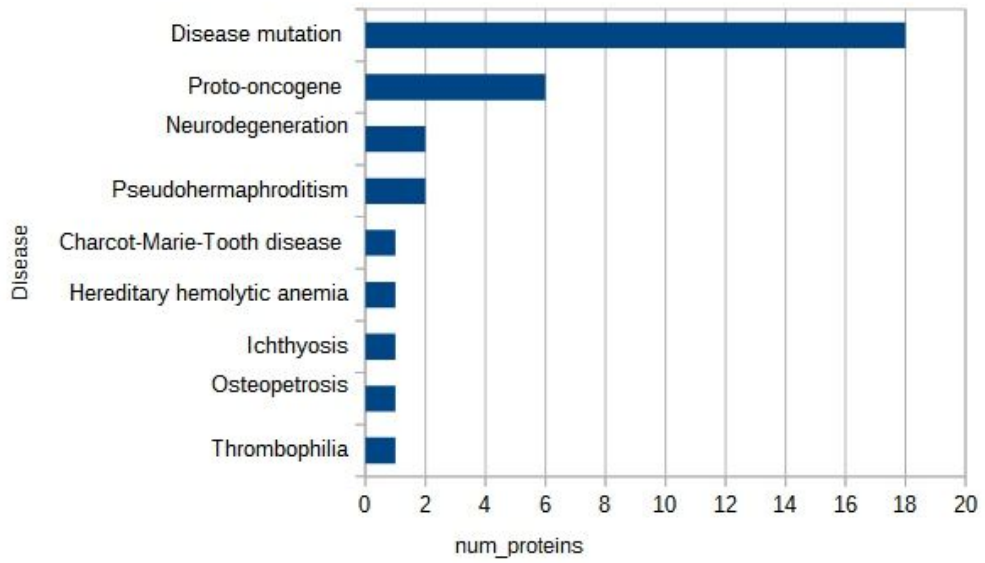

Figura11. Enfermedades en las que se encuentran relacionadas las proteínas humanas predichas por *target fishing*. Datos obtenidos de la base UniProt 2018

Para poder identificar el contenido del conjunto de Proteínas Humanas, se usó el programa STRING en su versión 10.5 (von Mering et al., 2005).

Se realizó una red de asociaciones predichas para el conjunto de 51 proteínas humanas Figura 12. Esta red presenta en nodos a cada proteína y las líneas de unión entre cada nodo representan el tipo de relaciones que hay entre ellas, ya sea una interacción reportada, predicha o relacionada con co expresión, *text mining* u homología. De tal forma, los nodos más conectados serán las proteínas que tienen más evidencias de relaciones funcionales entre ellas. En esta red proteína-proteína se puede encontrar altamente conectada a la enzima glutatión reductasa (GSR) que como se mencionó en el Capítulo 2, fue estudiada como contraparte de la enzima parasitaria TR. Esta red puede aportar gran información sobre la relación que existe entre las proteínas predichas.

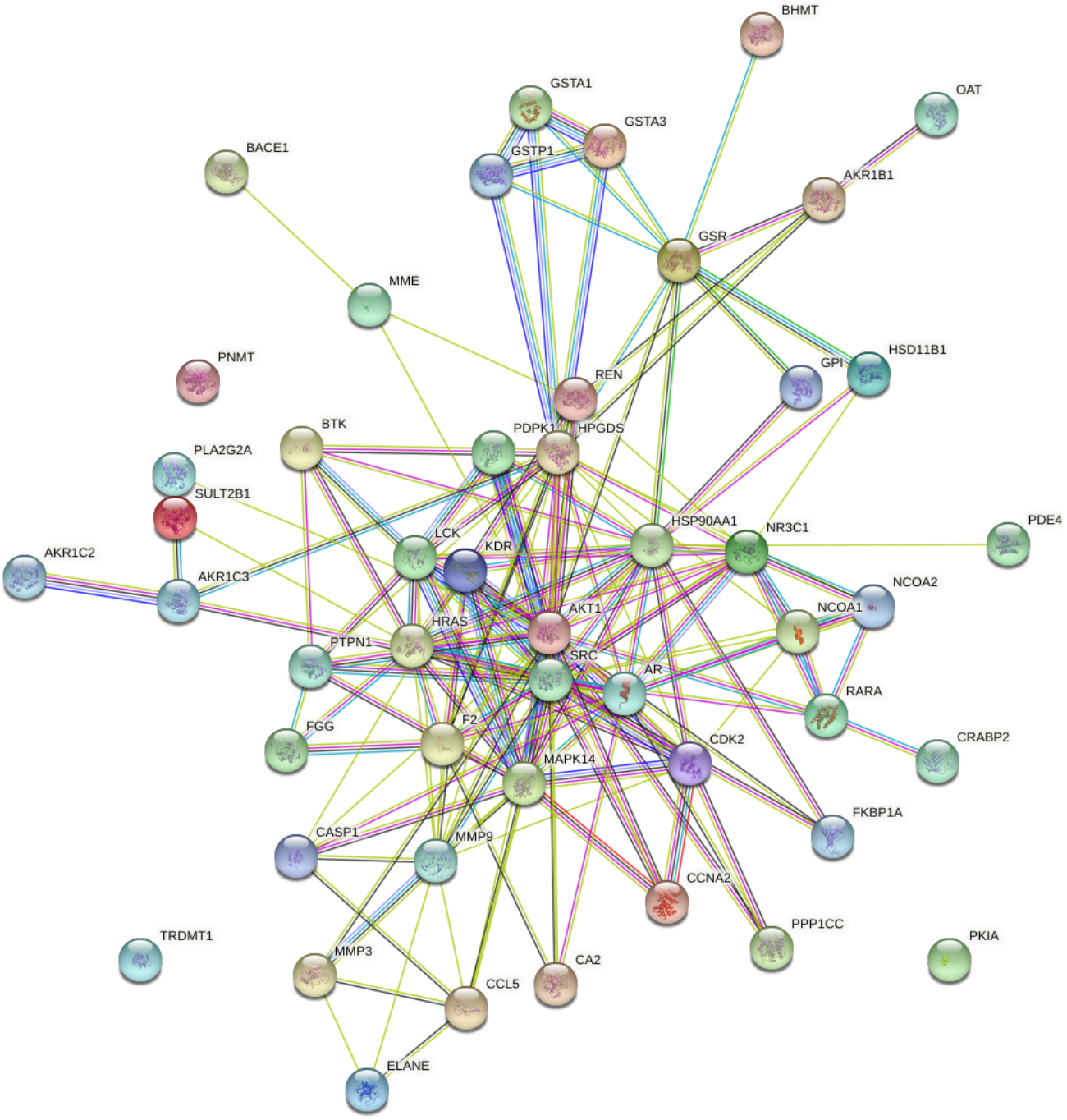

Figura 13. Grafo de las interacciones directas e indirectas para el set de salida de proteínas humanas según la base de datos String 10.5. Cada nodo es una proteína y las líneas que los unen corresponde a una evidencia de asociación. El código de colores de cada línea indica el tipo de asociación entre proteínas: Línea roja - indica *gene fusions*, Línea verde - genes continuos o *gene neighborhood*, Línea azul - evidencia

de concurrencia *gene co occurrence*, Línea morada - evidencia experimental, Línea amarilla - evidencia *text mining*, Línea azul clara - evidencia de base de datos, Línea negra - evidencia de co expresión.

Para enriquecer el estudio se utilizó la enciclopedia KEGG, esta es una colección de referencia que contiene información curada manualmente y representa el conocimiento actual sobre las interacciones, reacciones y relaciones de las proteínas de varios organismos ("KEGG PATHWAY Database," n.d.).

Usando como input el mismo set de proteínas humanas, se logró mapear la información. En resumen y coincidiendo con los datos de UniProt, el conjunto de proteínas está -mayoritariamente- relacionado con blancos relacionados en procesos biológicos relacionados al cáncer (Figura 14).

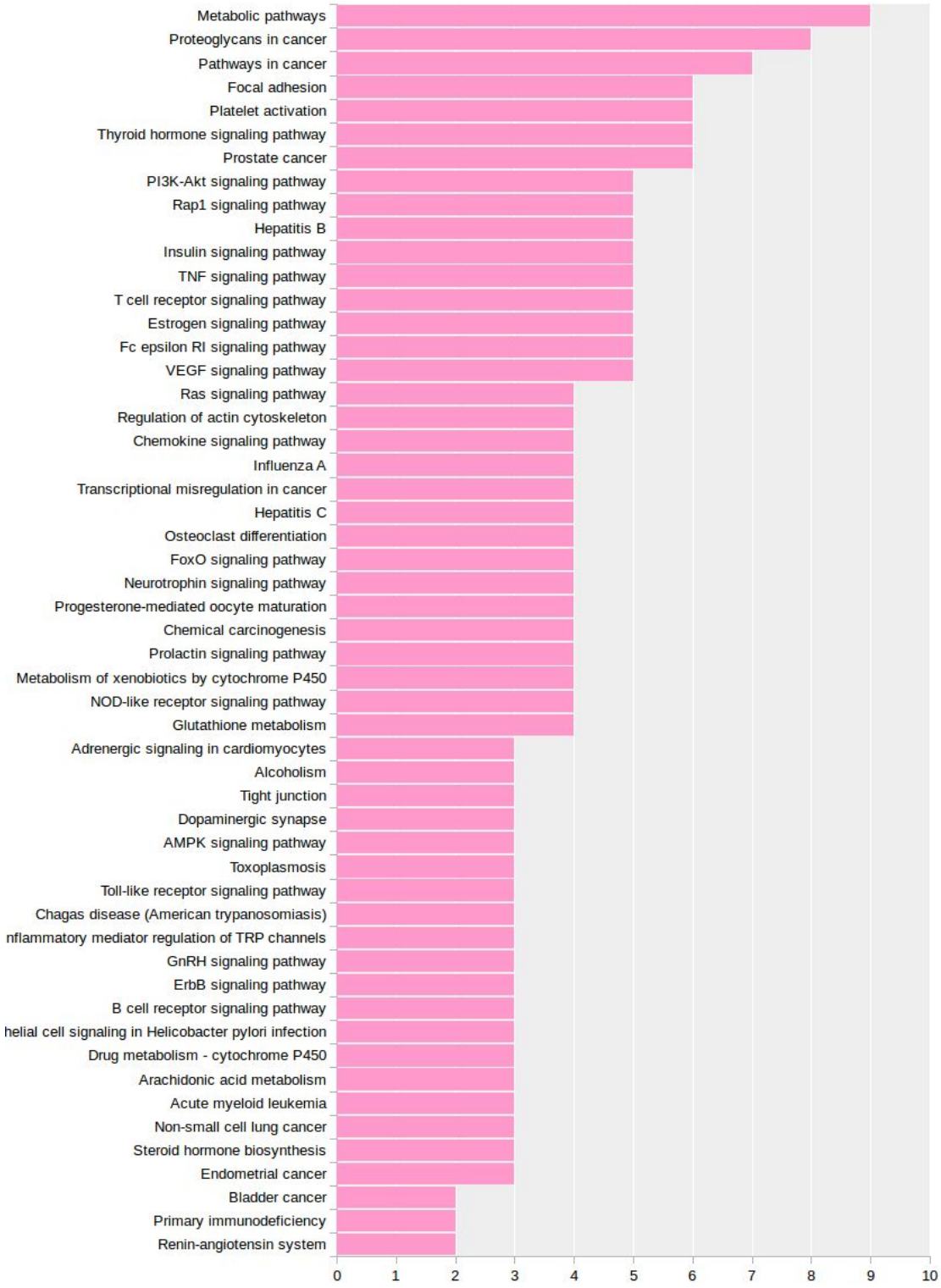

Figura 14. Número de proteínas y su relación con alguna patología o vía de señalización

5. Conclusiones Generales

Capítulo 1

- La tripanotión reductasa es un blanco farmacológico validado para el desarrollo de nuevos agentes para el tratamiento de la enfermedad de Chagas.
- No hay evidencia de correlación entre la actividad tripanocida y la inhibición de la actividad enzimática en varios de los compuestos presentados en esta revisión.
- Los inhibidores de TR propuestos son una opción para el tratamiento de la Enfermedad de Chagas.

Capítulo 2

- Se nombró como sitio Q a la región cercana al sitio catalítico de la TR donde el anclaje molecular presentó las mayores y mejores interacciones de las quinonas estudiadas.
- Las ariloxi quinonas presentaron los mejores puntajes de interacción en el sitio Q, lo que responde a un buen modelo para comprender la inhibición no competitiva demostrada experimentalmente.
- Los residuos Lys 62, Met 400' y Ser464' contribuyen principalmente en la unión de las ariloxi quinonas en TR.
- El Glu473' presenta en GR un contacto diferencial contra TR. Esta diferencia genera un cambio electrostático en el entorno y podría apuntar a la selectividad a favor de TR.
- No hay relación entre la actividad tripanocida en epimastigotes de *T. cruzi* y la inhibición de TR en la mayoría de quinonas estudiadas.
- Las quinonas Nq-h, Nq-g y Nq-d presentaron buena actividad tripanocida en epimastigotes de *T. cruzi*, además de baja toxicidad en células mamíferas.
- Las ariloxi quinonas podrían inhibir a otros blancos metabólicos del *T.cruzi*.

- Las quinonas Nq-h y Nq-b son buenos representantes de la serie estudiada en esta tesis, ya que son las moléculas más tripanocidas y selectivas, respectivamente.

Capítulo 3

- Se reportan un listado de proteínas para considerarlas en ensayos *in vivo* e i*n vitro* así como para el desarrollo de drogas antichagásicas.
- Se propone una serie de posibles blancos para naftoquinonas con el propósito de entender los posibles mecanismos de acción de estas moléculas y/o para proponer nuevos usos farmacológicos de éstas quinonas.
- Usando Pharmmapper y SHAFT se recuperaron 9 proteínas consideradas blancos validados del *T. cruzi.*
- Pharmmapper es la estrategia de "*target fishing*" recomendada para la busqueda de blancos a partir de naftoquinonas.
- Un gran número de blancos putativos para naftoquinonas estarían en condiciones de ser presentados para un estudio de reposicionamiento, por ejemplo, para el tratamiento de cáncer.

Referencias

Achenbach, J., Tiikkainen, P., Franke, L., & Proschak, E. (2011). Computational tools for polypharmacology and repurposing. *Future Medicinal Chemistry*, *3*(8), 961–968.

Ashburn, T. T., & Thor, K. B. (2004). Drug repositioning: identifying and developing new uses for existing drugs. *Nature Reviews. Drug Discovery*, *3*(8), 673–683.

Bartel, L. C., Montalto de Mecca, M., Fanelli, S. L., Rodriguez de Castro, C., Diaz, E. G., & Castro, J. A. (2007). Early nifurtimox-induced biochemical and ultrastructural alterations in rat heart. *Human & Experimental Toxicology*, *26*(10), 781–788.

Bender, A., Scheiber, J., Glick, M., Davies, J. W., Azzaoui, K., Hamon, J., … Jenkins, J. L. (2007). Cover Picture: Analysis of Pharmacology Data and the Prediction of Adverse Drug Reactions and Off-Target Effects from Chemical Structure (ChemMedChem 6/2007). *ChemMedChem*, *2*(6), 733–733.

Castro, J. A., de Mecca, M. M., & Bartel, L. C. (2006). Toxic side effects of drugs used to treat Chagas' disease (American trypanosomiasis). *Human & Experimental Toxicology*, *25*(8), 471–479.

CDC-Centers for Disease Control, & Prevention. (2009). CDC - Chagas Disease - Epidemiology & Risk Factors. Retrieved from https://www.cdc.gov/parasites/chagas/epi.html

Cerecetto, H., & Gonzalez, M. (2002). Chemotherapy of Chagas Disease: Status and New Developments. *Current Topics in Medicinal Chemistry*, *2*(11), 1187–1213.

Cereto-Massagué, A., Ojeda, M. J., Valls, C., Mulero, M., Pujadas, G., & Garcia-Vallve, S. (2015).

Tools for in silico target fishing. *Methods* , *71*, 98–103.

Cortés-Ruiz, E. M., Palomino-Hernández, O., Rodríguez-Hernández, K. D., Espinoza, B., & Medina-Franco, J. L. (2018). Computational Methods to Discover Compounds for the Treatment of Chagas Disease. *Advances in Protein Chemistry and Structural Biology*, *113*, 119–142.

Dastmalchi, & Siavoush. (2016). *Methods and Algorithms for Molecular Docking-Based Drug Design and Discovery*. IGI Global.

Escalona-Arranz, J. C., Carrasco-Velar, R., & Padrón-García, J. A. (2008). *Introducción al diseño racional de fármacos*.

Goodman, L. S., Hardman, J. G., Limbird, L. E., & Gilman, A. G. (2001). *Goodman and Gilman's the Pharmacological Basis of Therapeutics*. McGraw-Hill.

Hopfinger, A. J. (1985). Computer-assisted drug design. *Journal of Medicinal Chemistry*, *28*(9), 1133–1139.

Hotez, P. J., Dumonteil, E., Woc-Colburn, L., Serpa, J. A., Bezek, S., Edwards, M. S., … Bottazzi, M. E. (2012). Chagas Disease: "The New HIV/AIDS of the Americas." *PLoS Neglected Tropical Diseases*, *6*(5), e1498.

Huang, H., Zhang, G., Zhou, Y., Lin, C., Chen, S., Lin, Y., … Huang, Z. (2018). Reverse Screening Methods to Search for the Protein Targets of Chemopreventive Compounds. *Frontiers in Chemistry*, *6*. https://doi.org/10.3389/fchem.2018.00138

Imming, P., Sinning, C., & Meyer, A. (2006). Drugs, their targets and the nature and number of drug targets. *Nature Reviews. Drug Discovery*, *5*(10), 821–834.

Jannin, J., & Villa, L. (2007). An overview of Chagas disease treatment. *Memorias Do Instituto Oswaldo Cruz*, *102 Suppl 1*, 95–97.

KEGG: Kyoto Encyclopedia of Genes and Genomes. (n.d.). Retrieved October 22, 2018, from

https://www.genome.jp/kegg/

KEGG PATHWAY Database. (n.d.). Retrieved October 23, 2018, from https://www.genome.jp/kegg/pathway.html

Koutsoukas, A., Simms, B., Kirchmair, J., Bond, P. J., Whitmore, A. V., Zimmer, S., … Bender, A. (2011). From in silico target prediction to multi-target drug design: current databases, methods and applications. *Journal of Proteomics*, *74*(12), 2554–2574.

Labute, P. (2010). LowModeMD—Implicit Low-Mode Velocity Filtering Applied to Conformational Search of Macrocycles and Protein Loops. *Journal of Chemical Information and Modeling*, *50*(5), 792–800.

Liu, X., Jiang, H., & Li, H. (2011). SHAFTS: a hybrid approach for 3D molecular similarity calculation. 1. Method and assessment of virtual screening. *Journal of Chemical Information and Modeling*, *51*(9), 2372–2385.

Liu, Z., Fang, H., Reagan, K., Xu, X., Mendrick, D. L., Slikker, W., & Tong, W. (2013). In silico drug repositioning – what we need to know. *Drug Discovery Today*, *18*(3-4), 110–115.

López Vallejo, F., Vallejo, F. L., Franco, J. L. M., & Castillo, R. (2018). Diseño de fármacos asistido por computadora. *Educación Química*, *17*(4), 452.

Lounkine, E., Keiser, M. J., Whitebread, S., Mikhailov, D., Hamon, J., Jenkins, J. L., … Urban, L. (2012). Large-scale prediction and testing of drug activity on side-effect targets. *Nature*, *486*(7403), 361.

Marin-Neto, J. A., Rassi, A., Jr, Morillo, C. A., Avezum, A., Connolly, S. J., Sosa-Estani, S., … BENEFIT Investigators. (2008). Rationale and design of a randomized placebo-controlled trial assessing the effects of etiologic treatment in Chagas' cardiomyopathy: the BENznidazole Evaluation For Interrupting Trypanosomiasis (BENEFIT). *American Heart Journal*, *156*(1), 37–43.

Murta, S. M., Gazzinelli, R. T., Brener, Z., & Romanha, A. J. (1998). Molecular characterization of susceptible and naturally resistant strains of Trypanosoma cruzi to benznidazole and nifurtimox. *Molecular and Biochemical Parasitology*, *93*(2), 203–214.

Nagel, R. (1987). Genotoxicity studies with two antichagasic drugs. *Mutation Research*, *191*(1), 17–20.

Naveja, J. J., Oviedo-Osornio, C. I., & Medina-Franco, J. L. (2018). Computational Methods for Epigenetic Drug Discovery: A Focus on Activity Landscape Modeling. *Advances in Protein Chemistry and Structural Biology*, *113*, 65–83.

Pérez-Nueno, V. I., Karaboga, A. S., Souchet, M., & Ritchie, D. W. (2014). GES Polypharmacology Fingerprints: A Novel Approach for Drug Repositioning. *Journal of Chemical Information and Modeling*, *54*(3), 720–734.

Reddy, A. S., & Zhang, S. (2013). Polypharmacology: drug discovery for the future. *Expert Review of Clinical Pharmacology*, *6*(1), 41–47.

Salvatella, R., & Rosa, R. (2007). LA INTERRUPCION EN URUGUAY DE LA TRANSMISIÓN VECTORIAL DE Trypanosoma cruzi, AGENTE PE LA ENFERMEDAD DE CHAGAS, POR CONTROL DE Tríatoma infestam. *Revista de Patologia Tropical*, *29*(2). https://doi.org/10.5216/rpt.v29i2.17010

Salvatella, R., Rosa, R., Gonzalez, M., Basmadjián, Y., Combol, A., Benavidez, U., … Calegari, L. (1999). Seroprevalencia de la infección por Trypanosoma cruzi en escolares de seis y doce años de edad de tres departamentos endémicos de Uruguay. *Boletín Chileno de Parasitología*, *54*(3-4). https://doi.org/10.4067/s0365-94021999000300003

Schmunis, G. A., & Yadon, Z. E. (2010). Chagas disease: a Latin American health problem becoming a world health problem. *Acta Tropica*, *115*(1-2), 14–21.

Schneider, G. (2013). *De novo Molecular Design*. John Wiley & Sons.

Senior, K. (2007). Chagas disease: moving towards global elimination. *The Lancet Infectious Diseases*, *7*(9), 572.

Tropsha, A., & Zheng, W. (2001). Computer Aided Drug Design. In *Computational Biochemistry and Biophysics*.

Varnek, A., & Tropsha, A. (2008). *Chemoinformatics Approaches to Virtual Screening*. Royal Society of Chemistry.

von Mering, C., Jensen, L. J., Snel, B., Hooper, S. D., Krupp, M., Foglierini, M., … Bork, P. (2005). STRING: known and predicted protein–protein associations, integrated and transferred across organisms. *Nucleic Acids Research*, *33*(Database Issue), D433.

Wang, L., & Xie, X.-Q. (2014). Computational target fishing: what should chemogenomics researchers expect for the future of in silico drug design and discovery? *Future Medicinal Chemistry*, *6*(3), 247–249.

Wang, X., Shen, Y., Wang, S., Li, S., Zhang, W., Liu, X., … Li, H. (2017). PharmMapper 2017 update: a web server for potential drug target identification with a comprehensive target pharmacophore database. *Nucleic Acids Research*, *45*(W1), W356–W360.

Website. (n.d.). Retrieved October 22, 2018, from http://apps.who.int/iris/bitstream/10665/42443/1/WHO_TRS_905.pdf

Wermuth, C. G. (2003). *The Practice of Medicinal Chemistry*. Elsevier.

Anexo

I. INPUT DE STRING_ 51 PROTEÍNAS HUMANAS

SULT 2B1	*Sulfotransferase family, cytosolic, 2B, member 1; Sulfotransferase that utilizes 3'-phospho-5'-adenylyl sulfate (PAPS) as sulfonate donor to catalyze the sulfate conjugation of many hormones, neurotransmitters, drugs and xenobiotic compounds. Sulfonation increases the water solubility of most compounds, and therefore their renal excretion, but it can also result in bioactivation to form active metabolites. Sulfates hydroxysteroids like DHEA. Isoform 1 preferentially sulfonates cholesterol, and isoform 2 avidly sulfonates pregnenolone but not cholesterol (365 aa)*
GSTA3	*Glutathione S-transferase alpha 3; Conjugation of reduced glutathione to a wide number of exogenous and endogenous hydrophobic electrophiles. Catalyzes isomerization reactions that contribute to the biosynthesis of steroid hormones. Efficiently catalyze obligatory double-bond isomerizations of delta(5)-androstene-3,17-dione and delta(5)-pregnene-3,20-dione, precursors to testosterone and progesterone, respectively (222 aa)*
GSR	*Glutathione reductase; Maintains high levels of reduced glutathione in the cytosol (522 aa)*

MAPK14	*Mitogen-activated protein kinase 14; Serine/threonine kinase which acts as an essential component of the MAP kinase signal transduction pathway. MAPK14 is one of the four p38 MAPKs which play an important role in the cascades of cellular responses evoked by extracellular stimuli such as proinflammatory cytokines or physical stress leading to direct activation of transcription factors. Accordingly, p38 MAPKs phosphorylate a broad range of proteins and it has been estimated that they may have approximately 200 to 300 substrates each. Some of the targets are downstream kinases which are a [...] (360 aa)*
NR3C1	*Nuclear receptor subfamily 3, group C, member 1 (glucocorticoid receptor); Isoform Alpha-D3- Has lowest transcriptional activation activity of all isoforms created by alternative initiation (PubMed-15866175, PubMed-23820903). Has transcriptional repression activity (PubMed-23303127) (778 aa)*
RARA	*Retinoic acid receptor, alpha; Receptor for retinoic acid. Retinoic acid receptors bind as heterodimers to their target response elements in response to their ligands, all-trans or 9-cis retinoic acid, and regulate gene expression in various biological processes. The RXR/RAR heterodimers bind to the retinoic acid response elements (RARE) composed of tandem 5'-AGGTCA-3' sites known as DR1-DR5. In the absence of ligand, the RXR-RAR heterodimers associate with a multiprotein complex containing transcription corepressors that induce histone acetylation, chromatin condensation and transcrip [...] (462 aa)*
HSD11B1	*Hydroxysteroid (11-beta) dehydrogenase 1; Catalyzes reversibly the conversion of cortisol to the inactive metabolite cortisone. Catalyzes reversibly the conversion of 7-ketocholesterol to 7-beta-hydroxycholesterol. In intact cells, the reaction runs only in one direction, from 7-*

		ketocholesterol to 7-beta-hydroxycholesterol (By similarity) (292 aa)
	ELANE	*Elastase, neutrophil expressed; Modifies the functions of natural killer cells, monocytes and granulocytes. Inhibits C5a-dependent neutrophil enzyme release and chemotaxis (267 aa)*
	KDR	*Kinase insert domain receptor (a type III receptor tyrosine kinase); Tyrosine-protein kinase that acts as a cell-surface receptor for VEGFA, VEGFC and VEGFD. Plays an essential role in the regulation of angiogenesis, vascular development, vascular permeability, and embryonic hematopoiesis. Promotes proliferation, survival, migration and differentiation of endothelial cells. Promotes reorganization of the actin cytoskeleton. Isoforms lacking a transmembrane domain, such as isoform 2 and isoform 3, may function as decoy receptors for VEGFA, VEGFC and/or VEGFD. Isoform 2 plays an importan [...] (1356 aa)*
	CDK2	*Cyclin-dependent kinase 2; Serine/threonine-protein kinase involved in the control of the cell cycle; essential for meiosis, but dispensable for mitosis. Phosphorylates CTNNB1, USP37, p53/TP53, NPM1, CDK7, RB1, BRCA2, MYC, NPAT, EZH2. Interacts with cyclins A, B1, B3, D, or E. Triggers duplication of centrosomes and DNA. Acts at the G1-S transition to promote the E2F transcriptional program and the initiation of DNA synthesis, and modulates G2 progression; controls the timing of entry into mitosis/meiosis by controlling the subsequent activation of cyclin B/CDK1 by phosphorylation, and [...] (298 aa)*
	PNMT	*Phenylethanolamine N-methyltransferase; Converts noradrenaline to adrenaline (282 aa)*

AKT1	*V-akt murine thymoma viral oncogene homolog 1; AKT1 is one of 3 closely related serine/threonine- protein kinases (AKT1, AKT2 and AKT3) called the AKT kinase, and which regulate many processes including metabolism, proliferation, cell survival, growth and angiogenesis. This is mediated through serine and/or threonine phosphorylation of a range of downstream substrates. Over 100 substrate candidates have been reported so far, but for most of them, no isoform specificity has been reported. AKT is responsible of the regulation of glucose uptake by mediating insulin-induced translocation o [...] (480 aa)*
REN	*Renin; Renin is a highly specific endopeptidase, whose only known function is to generate angiotensin I from angiotensinogen in the plasma, initiating a cascade of reactions that produce an elevation of blood pressure and increased sodium retention by the kidney (406 aa)*
CCNA2	*Cyclin A2; Essential for the control of the cell cycle at the G1/S (start) and the G2/M (mitosis) transitions (432 aa)*
BHMT	*Betaine--homocysteine S-methyltransferase; Involved in the regulation of homocysteine metabolism. Converts betaine and homocysteine to dimethylglycine and methionine, respectively. This reaction is also required for the irreversible oxidation of choline (406 aa)*
CA2	*Carbonic anhydrase II; Essential for bone resorption and osteoclast differentiation (By similarity). Reversible hydration of carbon dioxide. Can hydrate cyanamide to urea. Involved in the regulation of fluid secretion into the anterior chamber of the eye. Contributes to intracellular pH regulation in the duodenal upper villous epithelium during proton-coupled peptide absorption. Stimulates the chloride-bicarbonate exchange activity of SLC26A6 (260 aa)*

AKR1B1	*Aldo-keto reductase family 1, member B1 (aldose reductase); Catalyzes the NADPH-dependent reduction of a wide variety of carbonyl-containing compounds to their corresponding alcohols with a broad range of catalytic efficiencies (316 aa)*
CCL5	*Chemokine (C-C motif) ligand 5; Chemoattractant for blood monocytes, memory T-helper cells and eosinophils. Causes the release of histamine from basophils and activates eosinophils. May activate several chemokine receptors including CCR1, CCR3, CCR4 and CCR5. One of the major HIV-suppressive factors produced by CD8+ T-cells. Recombinant RANTES protein induces a dose-dependent inhibition of different strains of HIV-1, HIV-2, and simian immunodeficiency virus (SIV). The processed form RANTES(3-68) acts as a natural chemotaxis inhibitor and is a more potent inhibitor of HIV-1- infection. [...] (91 aa)*
HPGDS	*Hematopoietic prostaglandin D synthase; Bifunctional enzyme which catalyzes both the conversion of PGH2 to PGD2, a prostaglandin involved in smooth muscle contraction/relaxation and a potent inhibitor of platelet aggregation, and the conjugation of glutathione with a wide range of aryl halides and organic isothiocyanates. Also exhibits low glutathione-peroxidase activity towards cumene hydroperoxide (199 aa)*
MMP3	*Matrix metallopeptidase 3 (stromelysin 1, progelatinase); Can degrade fibronectin, laminin, gelatins of type I, III, IV, and V; collagens III, IV, X, and IX, and cartilage proteoglycans. Activates procollagenase (477 aa)*

BTK	*Bruton agammaglobulinemia tyrosine kinase; Non-receptor tyrosine kinase indispensable for B lymphocyte development, differentiation and signaling. Binding of antigen to the B-cell antigen receptor (BCR) triggers signaling that ultimately leads to B-cell activation. After BCR engagement and activation at the plasma membrane, phosphorylates PLCG2 at several sites, igniting the downstream signaling pathway through calcium mobilization, followed by activation of the protein kinase C (PKC) family members. PLCG2 phosphorylation is performed in close cooperation with the adapter protein B-cel [...] (659 aa)*
F2	*Coagulation factor II (thrombin); Thrombin, which cleaves bonds after Arg and Lys, converts fibrinogen to fibrin and activates factors V, VII, VIII, XIII, and, in complex with thrombomodulin, protein C. Functions in blood homeostasis, inflammation and wound healing (622 aa)*
HRAS	*v-Ha-ras Harvey rat sarcoma viral oncogene homolog; Ras proteins bind GDP/GTP and possess intrinsic GTPase activity (189 aa)*
BACE1	*Beta-site APP-cleaving enzyme 1; Responsible for the proteolytic processing of the amyloid precursor protein (APP). Cleaves at the N-terminus of the A-beta peptide sequence, between residues 671 and 672 of APP, leads to the generation and extracellular release of beta-cleaved soluble APP, and a corresponding cell-associated C-terminal fragment which is later released by gamma-secretase (501 aa)*

NCOA1	*Nuclear receptor coactivator 1; Nuclear receptor coactivator that directly binds nuclear receptors and stimulates the transcriptional activities in a hormone-dependent fashion. Involved in the coactivation of different nuclear receptors, such as for steroids (PGR, GR and ER), retinoids (RXRs), thyroid hormone (TRs) and prostanoids (PPARs). Also involved in coactivation mediated by STAT3, STAT5A, STAT5B and STAT6 transcription factors. Displays histone acetyltransferase activity toward H3 and H4; the relevance of such activity remains however unclear. Plays a central role in creating mu [...] (1441 aa)*
PPP1CC	*Protein phosphatase 1, catalytic subunit, gamma isozyme; Protein phosphatase that associates with over 200 regulatory proteins to form highly specific holoenzymes which dephosphorylate hundreds of biological targets. Protein phosphatase 1 (PP1) is essential for cell division, and participates in the regulation of glycogen metabolism, muscle contractility and protein synthesis. Dephosphorylates RPS6KB1. Involved in regulation of ionic conductances and long-term synaptic plasticity. May play an important role in dephosphorylating substrates such as the postsynaptic density- associated Ca [...] (323 aa)*
HSP90AA1	*Heat shock protein 90kDa alpha (cytosolic), class A member 1; Molecular chaperone that promotes the maturation, structural maintenance and proper regulation of specific target proteins involved for instance in cell cycle control and signal transduction. Undergoes a functional cycle that is linked to its ATPase activity. This cycle probably induces conformational changes in the client proteins, thereby causing their activation. Interacts dynamically with various co-chaperones that modulate its substrate recognition, ATPase cycle and chaperone function. Binds bacterial lipopolysaccharide [...] (854 aa)*

	GSTA1	*Glutathione S-transferase alpha 1; Conjugation of reduced glutathione to a wide number of exogenous and endogenous hydrophobic electrophiles (222 aa)*
	PKIA	*Protein kinase (cAMP-dependent, catalytic) inhibitor alpha; Extremely potent competitive inhibitor of cAMP-dependent protein kinase activity, this protein interacts with the catalytic subunit of the enzyme after the cAMP-induced dissociation of its regulatory chains (76 aa)*
	FGG	*Fibrinogen gamma chain; Together with fibrinogen alpha (FGA) and fibrinogen beta (FGB), polymerizes to form an insoluble fibrin matrix. Has a major function in hemostasis as one of the primary components of blood clots. In addition, functions during the early stages of wound repair to stabilize the lesion and guide cell migration during re- epithelialization. Was originally thought to be essential for platelet aggregation, based on in vitro studies using anticoagulated blood. However, subsequent studies have shown that it is not absolutely required for thrombus formation in vivo. Enhan [...] (453 aa)*
	LCK	*Lymphocyte-specific protein tyrosine kinase; Non-receptor tyrosine-protein kinase that plays an essential role in the selection and maturation of developing T- cells in the thymus and in the function of mature T-cells. Plays a key role in T-cell antigen receptor (TCR)-linked signal transduction pathways. Constitutively associated with the cytoplasmic portions of the CD4 and CD8 surface receptors. Association of the TCR with a peptide antigen-bound MHC complex facilitates the interaction of CD4 and CD8 with MHC class II and class I molecules, respectively, thereby recruiting the associa [...] (509 aa)*

	PDPK1	*3-phosphoinositide dependent protein kinase-1; Serine/threonine kinase which acts as a master kinase, phosphorylating and activating a subgroup of the AGC family of protein kinases. Its targets include- protein kinase B (PKB/AKT1, PKB/AKT2, PKB/AKT3), p70 ribosomal protein S6 kinase (RPS6KB1), p90 ribosomal protein S6 kinase (RPS6KA1, RPS6KA2 and RPS6KA3), cyclic AMP-dependent protein kinase (PRKACA), protein kinase C (PRKCD and PRKCZ), serum and glucocorticoid-inducible kinase (SGK1, SGK2 and SGK3), p21-activated kinase-1 (PAK1), protein kinase PKN (PKN1 and PKN2). Plays a central rol [...] (556 aa)*
	PDE4D	*Phosphodiesterase 4D, cAMP-specific; Hydrolyzes the second messenger cAMP, which is a key regulator of many important physiological processes (809 aa)*
	SRC	*V-src sarcoma (Schmidt-Ruppin A-2) viral oncogene homolog (avian); Non-receptor protein tyrosine kinase which is activated following engagement of many different classes of cellular receptors including immune response receptors, integrins and other adhesion receptors, receptor protein tyrosine kinases, G protein-coupled receptors as well as cytokine receptors. Participates in signaling pathways that control a diverse spectrum of biological activities including gene transcription, immune response, cell adhesion, cell cycle progression, apoptosis, migration, and transformation. Due to f [...] (536 aa)*
	MME	*Membrane metallo-endopeptidase; Thermolysin-like specificity, but is almost confined on acting on polypeptides of up to 30 amino acids (PubMed-15283675, PubMed-8168535). Biologically important in the destruction of opioid peptides such as Met- and Leu-enkephalins by cleavage of a Gly-Phe bond (PubMed-17101991). Able to cleave angiotensin-1, angiotensin-2 and angiotensin 1-9 (PubMed-15283675).*

		Involved in the degradation of atrial natriuretic factor (ANF) (PubMed-2531377, PubMed-2972276). Displays UV-inducible elastase activity toward skin preelastic and elastic fibers (PubMed-20876573) (750 aa)
	CRABP2	*Cellular retinoic acid binding protein 2; Transports retinoic acid to the nucleus. Regulates the access of retinoic acid to the nuclear retinoic acid receptors (138 aa)*
	OAT	*Ornithine aminotransferase (439 aa)*
	PTPN1	*Protein tyrosine phosphatase, non-receptor type 1; Tyrosine-protein phosphatase which acts as a regulator of endoplasmic reticulum unfolded protein response. Mediates dephosphorylation of EIF2AK3/PERK; inactivating the protein kinase activity of EIF2AK3/PERK. May play an important role in CKII- and p60c-src-induced signal transduction cascades. May regulate the EFNA5-EPHA3 signaling pathway which modulates cell reorganization and cell-cell repulsion. May also regulate the hepatocyte growth factor receptor signaling pathway through dephosphorylation of MET (435 aa)*
	MMP9	*Matrix metallopeptidase 9 (gelatinase B, 92kDa gelatinase, 92kDa type IV collagenase); May play an essential role in local proteolysis of the extracellular matrix and in leukocyte migration. Could play a role in bone osteoclastic resorption. Cleaves KiSS1 at a Gly-|-Leu bond. Cleaves type IV and type V collagen into large C-terminal three quarter fragments and shorter N-terminal one quarter fragments. Degrades fibronectin but not laminin or Pz-peptide (707 aa)*
	AR	*Androgen receptor; Steroid hormone receptors are ligand-activated transcription factors that regulate eukaryotic gene expression and affect cellular proliferation and differentiation in target tissues. Transcription factor activity is modulated by bound*

		coactivator and corepressor proteins. Transcription activation is down-regulated by NR0B2. Activated, but not phosphorylated, by HIPK3 and ZIPK/DAPK3 (920 aa)
	PLA2G2A	*Phospholipase A2, group IIA (platelets, synovial fluid); Thought to participate in the regulation of the phospholipid metabolism in biomembranes including eicosanoid biosynthesis. Catalyzes the calcium-dependent hydrolysis of the 2- acyl groups in 3-sn-phosphoglycerides (144 aa)*
	TRDMT1	*tRNA aspartic acid methyltransferase 1; Specifically methylates cytosine 38 in the anticodon loop of tRNA(Asp) (391 aa)*
	AKR1C3	*Aldo-keto reductase family 1, member C3 (3-alpha hydroxysteroid dehydrogenase, type II); Catalyzes the conversion of aldehydes and ketones to alcohols. Catalyzes the reduction of prostaglandin (PG) D2, PGH2 and phenanthrenequinone (PQ) and the oxidation of 9-alpha,11-beta- PGF2 to PGD2. Functions as a bi-directional 3-alpha-, 17-beta- and 20-alpha HSD. Can interconvert active androgens, estrogens and progestins with their cognate inactive metabolites. Preferentially transforms androstenedione (4-dione) to testosterone (323 aa)*
	AKR1C2	*Aldo-keto reductase family 1, member C2 (dihydrodiol dehydrogenase 2; bile acid binding protein; 3-alpha hydroxysteroid dehydrogenase, type III); Works in concert with the 5-alpha/5-beta-steroid reductases to convert steroid hormones into the 3-alpha/5-alpha and 3-alpha/5-beta-tetrahydrosteroids. Catalyzes the inactivation of the most potent androgen 5-alpha-dihydrotestosterone (5-alpha- DHT) to 5-alpha-androstane-3-alpha,17-beta-diol (3-alpha-diol). Has a high bile-binding ability (323 aa)*

FKBP1A	*FK506 binding protein 1A, 12kDa; Keeps in an inactive conformation TGFBR1, the TGF-beta type I serine/threonine kinase receptor, preventing TGF-beta receptor activation in absence of ligand. Recruites SMAD7 to ACVR1B which prevents the association of SMAD2 and SMAD3 with the activin receptor complex, thereby blocking the activin signal. May modulate the RYR1 calcium channel activity. PPIases accelerate the folding of proteins. It catalyzes the cis-trans isomerization of proline imidic peptide bonds in oligopeptides (108 aa)*
GSTP1	*Glutathione S-transferase pi 1; Conjugation of reduced glutathione to a wide number of exogenous and endogenous hydrophobic electrophiles. Regulates negatively CDK5 activity via p25/p35 translocation to prevent neurodegeneration (210 aa)*
NCOA2	*Nuclear receptor coactivator 2; Transcriptional coactivator for steroid receptors and nuclear receptors. Coactivator of the steroid binding domain (AF- 2) but not of the modulating N-terminal domain (AF-1). Required with NCOA1 to control energy balance between white and brown adipose tissues. Critical regulator of glucose metabolism regulation, acts as RORA coactivator to specifically modulate G6PC expression. Involved in the positive regulation of the transcriptional activity of the glucocorticoid receptor NR3C1 by sumoylation enhancer RWDD3. Positively regulates the circadian clock b [...] (1464 aa)*
GPI	*Glucose-6-phosphate isomerase (569 aa)*
CASP1	*Caspase 1, apoptosis-related cysteine peptidase; Thiol protease that cleaves IL-1 beta between an Asp and an Ala, releasing the mature cytokine which is involved in a variety of inflammatory processes. Important for defense against pathogens. Cleaves and activates sterol*

regulatory element binding proteins (SREBPs). Can also promote apoptosis (404 aa)

2_ Listado de procesos en los que se encuentran involucradas las proteínas de consulta (51 proteinas humanas)

#pathway ID	pathway description	observed gene count
5205	Metabolic pathways	9
5215	Proteoglycans in cancer	8
4370	Pathways in cancer	7
4919	Prostate cancer	6
4611	Thyroid hormone signaling pathway	6
4664	Platelet activation	6
4915	Focal adhesion	6
4660	VEGF signaling pathway	5
480	Fc epsilon RI signaling pathway	5
4668	Estrogen signaling pathway	5
4510	T cell receptor signaling pathway	5
4621	TNF signaling pathway	5
5200	Insulin signaling pathway	5
4910	Hepatitis B	5
980	Rap1 signaling pathway	5
5161	PI3K-Akt signaling pathway	5

4917	Glutathione metabolism	4
5204	NOD-like receptor signaling pathway	4
4914	Metabolism of xenobiotics by cytochrome P450	4
4015	Prolactin signaling pathway	4
4722	Chemical carcinogenesis	4
4068	Progesterone-mediated oocyte maturation	4
4380	Neurotrophin signaling pathway	4
5213	FoxO signaling pathway	4
5160	Osteoclast differentiation	4
140	Hepatitis C	4
5223	Transcriptional misregulation in cancer	4
5221	Influenza A	4
590	Chemokine signaling pathway	4
982	Regulation of actin cytoskeleton	4
5120	Ras signaling pathway	4
4662	Endometrial cancer	3
5202	Steroid hormone biosynthesis	3
5164	Non-small cell lung cancer	3
4614	Acute myeloid leukemia	3
4062	Arachidonic acid metabolism	3
4012	Drug metabolism - cytochrome P450	3
4912	Epithelial cell signaling in Helicobacter pylori infection	3

4151	B cell receptor signaling pathway	3
1100	ErbB signaling pathway	3
4750	GnRH signaling pathway	3
4810	Inflammatory mediator regulation of TRP channels	3
5142	Chagas disease (American trypanosomiasis)	3
4014	Toll-like receptor signaling pathway	3
4620	Toxoplasmosis	3
5145	AMPK signaling pathway	3
4152	Dopaminergic synapse	3
5340	Tight junction	3
4728	Alcoholism	3
4530	Adrenergic signaling in cardiomyocytes	3
5219	Oxytocin signaling pathway	3
5034	Tuberculosis	3
4261	Viral carcinogenesis	3
4921	Epstein-Barr virus infection	3
5014	Endocytosis	3
5152	Renin-angiotensin system	2
5131	Primary immunodeficiency	2
4150	Bladder cancer	2
4623	Amyotrophic lateral sclerosis (ALS)	2
5203	Shigellosis	2

5214	mTOR signaling pathway	2
4720	Cytosolic DNA-sensing pathway	2
5169	Glioma	2
5211	Long-term potentiation	2
4144	Renal cell carcinoma	2
4610	Complement and coagulation cascades	2
5133	Pertussis	2
5218	Melanoma	2
5220	Chronic myeloid leukemia	2

3_Funcion molécular de las proteínas de consulta

ID	molecular function	count in gene set
GO.0003824	catalytic activity	38
GO.0016740	transferase activity	20
GO.0005515	protein binding	29
GO.0019899	enzyme binding	16
GO.0005102	receptor binding	14
GO.0004364	glutathione transferase activity	4
GO.0043167	ion binding	30
GO.0004672	protein kinase activity	9
GO.0043168	anion binding	18
GO.0016787	hydrolase activity	16

GO.0004175	endopeptidase activity	7
GO.0030235	nitric-oxide synthase regulator activity	2
GO.0004715	non-membrane spanning protein tyrosine kinase activity	3
GO.0019901	protein kinase binding	6
GO.0051117	ATPase binding	3